Summer 8-20-2021

Understanding the Adhesion Mechanism in Mycelium-Assisted Wood Bonding

Wenjing Sun
wenjing.sun@maine.edu

UNDERSTANDING THE ADHESION MECHANISM IN MYCELIUM-ASSISTED WOOD BONDING

By

Wenjing Sun

B.A. Beijing Forestry University, 2013

M.A. Beijing Forestry University, 2016

A DISSERTATION

Submitted in Partial Fulfillment of the

Requirements for the Degree of

Doctor of Philosophy

(in Forest Resources: Bioproducts Engineering)

The Graduate School

The University of Maine

August 2021

Advisory Committee:

Mehdi Tajvidi, Associate Professor of Renewable Nanomaterials, Advisor

Christopher G. Hunt, Research Chemist, USDA Forest Products Laboratory

Douglas J. Gardner, Professor of Forest Operations, Bioproducts, & Bioenergy

Barbara J. Cole, Professor of Chemistry

Jinwu Wang, Research Forest Products Technologist, USDA Forest Products Laboratory

UNDERSTANDING THE ADHESION MECHANISM IN MYCELIUM-ASSISTED WOOD BONDING

By Wenjing Sun

Dissertation Advisor: Dr. Mehdi Tajvidi

An Abstract of the Dissertation Presented
in Partial Fulfillment of the Requirements for the
Degree of Doctor of Philosophy
(in Forest Resources)
August 2021

The increasing environmental awareness has led to an increased interest in developing more sustainable materials as alternatives to petroleum-derived products. Among different nature-based products, fungal-mycelium-based bio-composites have gained considerable attention in various applications. Multiple materials with different densities and structures and potential applications can be fabricated by inoculating filamentous white-rot fungi in lignocellulosic materials and other substrates. Different from lower-density as-grown foam-like mycelium composites, higher-density mycelium-lignocellulosic panels have the potential to replace commercial particleboard and fiberboard bonded by petroleum-based resins. This kind of composite can be produced by directly adding heat and pressure to the low-density foams or by assembling mycelium-industry wastes before hot-pressing.

The main goal of this dissertation was to investigate the principal adhesion mechanisms involved in the production of hot-pressed mycelium bio-composites. The functionality of surface mycelium for wood bonding was thoroughly investigated by growing *Trametes versicolor* on yellow birch veneers. The presence of surface mycelium improved the interface between two wood layers and consequently enhanced bonding. The surface mycelium layer was also confirmed to be able to be utilized as a stand-alone adhesive to bond untreated wood. The exopolysaccharides and proteins located at the interface between aerial mycelium and the substrate were confirmed to play an essential role in adhesion. The bonding mechanism and functionality of mycelium were also investigated in both as-grown and hot-pressed bio-composite structures. For low-density as-grown foam structures, fungal mycelium only worked as a binder, the lignocellulosic substrate material played an essential role in sound absorption and thermal insulation properties, and the denser mycelium structure had a negative effect on these properties. In a higher-density hot-pressed panel system, fungal mycelium contributed to bonding and reinforced the bio-composite by filling the gaps.

Additionally, we also demonstrated that combining the advantages of nanocellulose research at UMaine into our novel mycelium bio-composite can provide further improvements in properties to manufacture formaldehyde-free hybrid composite panels. Finally, we discovered an all-natural mycelium surface with tunable wettability that can be switched several times from hydrophobic to hydrophilic status by a simple treatment. These surfaces can have potential applications in medical microfluidics and invisible pattern printing.

DEDICATION

To my mother.

ACKNOWLEDGEMENTS

I would like to thank my supervisor, Dr. Mehdi Tajvidi, for his support for all my thoughts and work and giving me the freedom to explore my interests.

Special thanks to Dr. Caitlin Howell for having me in her group, listening to me, providing me with access to her lab, and offering me all the guidance and advice.

Special thanks to Dr. Christopher G. Hunt for setting an example of a real scientist. I hope I can work harder to achieve your level of integrity.

I would also like to thank my other committee members, Dr. Douglas J. Gardner, Dr. Barbara J. Cole, and Dr. Jinwu Wang, for their great support and guidance on my dissertation work.

Thank you to everyone who has helped me with my research. Dr. Islam Hafez, Dr. Nima Amini, Dr. Shookofeh Ghasemi, Dr. Ali Tayeb and other LRN group members, Dr. Ling Li, Christopher London, Shane O'Neill, Cong Chen, Elliott Sanders, Justin Crouse, and other colleagues at School of Forest Resources. Dr. Seanna L. Annis, Kelly Edward, and Greg Kornelis at School of Biology and Ecology; Carlaile Nogueira, Dr. Douglas Bousfield, Dr. Dan Regan, and other Howell lab group members at Department of Chemical and Biomedical Engineering; Dr. William Gramlich, Peter Kelly, Dr. Grape Senkum and Ayan Dutta at Department of Chemistry; Dr. Balunkeswar Nayak and Dr. Praveen Sappati at the School of Food and Agriculture; Gavin Mclintyre from Ecovative Design LLC.; Amy Luce, Laurel Grosjean, and Dr. Indira Silwak from FBRI; John Vollmer and David Farley from the Jackson Lab.

I would also like to thank Dr. Tom Allen, Prof. Kathryn Slott, Jessica Browne, and Mireille La Gal for their support.

Special thanks to my father for always supporting me in pursuing my dreams, to my aunts and cousins for always taking care of my family and me throughout these years.

Special thanks to my friends Maggie Mansfield and Cong Chen for being with me throughout these years in Maine.

TABLE OF CONTENTS

LIST OF TABLES

LIST OF FIGURES

CHAPTER 1

INTRODUCTION

1.1. Research motivation

All-nature-based materials and bio-composites have gained considerable attentions in recent years attributed to the increasing concerns about environmental issues and human health. A surge of products based on novel resources and fabrication methods of bio-based material has resulted in many research projects in academia and start-up companies in industry. Lignocellulosic biomass, as a traditional natural material, has experienced a rejuvenation and new potential with the invention of fungal mycelium-based bio-composite products. The natural ability of partially degraded lignocellulosic components to bond together led to the first development of as-grown foams as novel packaging materials. The similarity of mycelium bonded foams and traditional wood-based panel composite motivated us to explore more potential of this novel system.

1.2. Research questions

Over the next chapters, we try to answer the following questions:

Can the mycelium-bonded lignocellulosic bio-composites be developed into all-natural panels?

Are there any similarities between the traditional bio-composites and pretreatment methods with the novel mycelium technology?

What is the function of fungal mycelia in the bio-composite system at different levels and how do they contribute to the bonding and other properties of the materials?

Are there any other potential applications that are well suited for the unique properties of mycelium and mycelium bonded bio-composites?

1.3. Research goal

The over-arching goal of this dissertation was to thoroughly study and understand the adhesion mechanism of mycelium assisted wood bonding at different levels of the structure and also provide guidance and potential approaches for future research and development.

1.4. Dissertation outline

In **Chapter 2**, we review the biological pretreatments used in hot-pressed lignocellulosic bio-composites production. We first compare the terms "lignocellulosic bio-composites" and "mycelium bio-composites" and reveal the similarity of these two categories of bio-composites. The raw materials and production process are described and compared in detail. The properties and affecting factors of the composites are summarized. The potential mechanisms, the knowledge gaps, and the commercial limitations of this kind of product are discussed.

Because of the complexity of the hot-pressed bio-composite system, we study the adhesion mechanism at three levels. In **Chapter 3**, we focus on the surface level and aim to understand the functionality of surface mycelium on wood bonding. We developed a simplified system to separate aerial hyphae and substrate by growing fungi on wood veneers. We compared the lap-shear strengths after hot-pressing to evaluate if the presence of surface mycelium can improve the interface between wood layers and consequently improve bonding.

In **Chapter 4**, we look further into the details of the wood-mycelium interface. We compared the influence of hot-pressing temperature and testing conditions. We also investigated the importance of water-soluble components for both wood bonding and mycelium bonding. We performed chemical analyses on multiple compounds and demonstrated the potential bonding mechanism.

We move back to the composite system in **Chapter 5** to confirm what we have found in **Chapters 2 and 3** and investigate other factors in the more complex 3D structure. We monitor the density of the mycelium in structure by growing samples for different periods. The essential properties for target applications were tested and compared. We studied the behavior of low-density as-grown foams and compared the difference of mycelium influences in the two systems.

After understanding the bonding mechanism of the system, we work on an improvement strategy by incorporating other natural materials. We developed and investigated a novel hybrid panel composite system based on wood, fungal mycelium, and cellulose nanofibrils (CNF) in **Chapter 6**. We

also present results and analyses pertaining to the development of unique lightweight composite systems for packaging and furniture applications.

Finally, in **Chapter 7**, we investigate the tunable wettability of surface mycelium. We demonstrate a simple method to alter the surface properties of a commercially available mycelium material that can be used to produce all-natural surfaces with reversible wettability.

CHAPTER 2

LITERATURE REVIEW: FUNGAL AND ENZYMATIC PRETREATMENTS IN HOT-PRESSED LIGNOCELLULOSIC BIO-COMPOSITES

2.1. Introduction

The use of nature-based materials instead of petroleum-derived products is a prospective solution for sustainability issues faced by industries and humankind. In the composites industry, lignocellulosic bio-composites and fungal mycelium bio-composites are both competent candidates. While the former (represented primarily by wood-based composites) features the most extended history and extensively available products (Hemmilä et al., 2017; Rowell, 1992), the latter is an emerging class of novel materials developed over the past ten years and has been achieving significant research and commercialization interest (Elsacker et al., 2020; Meyer et al., 2020).

2.1.1. Lignocellulosic bio-composites vs. mycelium bio-composites

Lignocellulosic bio-composites are conventionally in the form of panels and are manufactured from strands, flakes, particles, or fibers of wood or agricultural residues and are bonded together with a type of adhesive (Figure 2.1A). Woody biomass is the most traditionally used raw material in the lignocellulosic bio-composite industry, whereas non-wood fast-growing biomass feedstock has been more developed in response to the shortage of wood supply (Chaturvedi & Verma, 2013; Tye et al., 2016) and in response to regional availability. Differences in properties, function, and particle form yield categories such as insulation board, particleboard, fiberboard, oriented strandboard (OSB), and plywood (Suchsland & Woodson, 1987) (Figure 2.1). In 2019, over 355 million m^3 of these products were produced from forest resources, globally (FAO, 2020).

To bond reconstituted lignocellulosic biomass, adhesives are usually applied to the furnish and are cured under heat and pressure. The dominant adhesives in lignocellulosic bio-composite manufacturing are formaldehyde and isocyanate-based synthetic resins, which have drawn environmental and health questions and are typically not bio-based (EPA, 2017; Mantanis et al., 2018). There is a perceived consumer desire for completely bio-based alternatives, reflected in the commitment of IKEA, one of the world's largest

furniture retailers, to 40% natural raw materials for all their adhesives by 2025 and 80% by 2030 (Bruck, 2017). Many efforts have been devoted to replacing synthetic resins with natural-based adhesives (Ferdosian et al., 2017; He, 2017; Pizzi, 2006) or by developing binder-less lignocellulosic bio-composites (Hubbe et al., 2017; Pintiaux et al., 2015). Additional benefits may be achieved if lignocellulosic composites can be produced in a binderless manner as opposed to those made with bio-based adhesives. In the quest for adhesion promotion, pretreatments are often investigated to the raw materials to "activate" their surface physically or chemically (Pelaez-Samaniego et al., 2013; Saha et al., 2015; Widsten & Kandelbauer, 2008; Zhang et al., 2015). Conventional activation methods such as steam explosion, acid and alkali pretreatments, usually require large inputs of energy and cause pollution. For this reason, biological pretreatments are expected to be generally a milder, safer, and more environmentally friendly alternative (Maurya et al., 2015; Shirkavand et al., 2016). These processes typically require the "activation" of lignocellulosic raw materials by fungi or enzymes derived from fungi before hot-pressing.

The concept of "mycelium-based bio-composites" (Figure 2.1B), i.e., a product that is bonded by fungal mycelium, is quite new but has obtained significant research and industrial attention. The most well-studied and commercialized mycelium-based products are as-grown mycelium-based composites (Elsacker et al., 2020; Jones et al., 2020). Typically, the manufacturing starts with low-cost lignocellulosic biomass substrate. Then the mycelia of filamentous fungi are added to a mixture of the substrate and nutrients in a mold with a predetermined shape where the mycelium partially digests and adheres to the surface of the substrate particles. As they grow, the mycelium forms entangled networks and bind the substrate particles into a whole aggregation. Oven drying is often used to inactivate fungi growth and to produce the final product both in the industry and research labs (Elsacker et al., 2020). Fully processed composites typically have a density range of 0.06 to 0.30 g m^{-3} (Jones et al., 2020), depending on the substrate material.

More recently, a growing number of research projects have focused on developing mycelium-based bio-composites at higher density. One attempt was to add pressure during the growth step (Bajwa et al., 2017; Pelletier et al., 2017). Others mainly densified the composites by applying heat and pressure afterward (Appels et al., 2019; Liu et al., 2020; Liu et al., 2019; Sun et al., 2019).

It is not difficult to notice that the predominant substrate in this "novel mycelium bio-composite" is still lignocellulosic biomass. The weight percentage of fungal biomass in the system is usually very low (around 5% for 7 days growth of *Trametes (Coriolus) versicolor* on wheat grain, according to Jones et al. (2019)). Therefore, it is reasonable to categorize them together with the traditional definition of lignocellulosic bio-composites in the same class, especially for the hot-pressed products, as the mycelium development and enzyme secretion during fungi growth are the same as the fungal or enzymatic pretreatment in lignocellulosic bio-composite manufacturing.

2.1.2 The scope of this chapter

Multiple reviews focusing on binder-less lignocellulosic bio-composites have been published over the past 20 years (Hubbe et al., 2017; Nasir et al., 2019; Pintiaux et al., 2015; Zhang et al., 2015). Most of these publications include small sections on enzymatic activation of lignin as well. Widsten and Kandelbauer (2008) specifically summarized the adhesion improvement of lignocellulosic bio-composites by enzymatic pretreatment. The two main discussions were the oxidation of wood surface lignin before hot-pressing of fiberboard and using enzymatically pretreated lignin as adhesive in particleboard production. Since then, more research articles have been published, and explorations have been extended to binder-less particleboard and direct use of fungi for pretreatment.

For the "mycelium bio-composites," recent progress has been reviewed by several research groups in the past two years that cover manufacturing processes, material properties, applications, and life cycle assessment (Abhijith et al., 2018; Attias et al., 2020; Elsacker et al., 2020; Girometta et al., 2019; Jones et al., 2020). However, there is a lack of attention to the higher-density category (density above 0.30 g m^{-3}), and this category has not been connected and compared with biologically pretreated traditional lignocellulosic bio-composites.

In view of the intrinsic similarities of lignocellulosic and mycelium bio-composites, the objective of this chapter is to summarize literature pertaining to these two groups in the same category for the first time by focusing on hot-pressed higher-density bio-composites (Figure 2.1). The discussion will focus on

the changes in lignocellulosic biomass after fungal and enzymatic pretreatments and their possible links with the adhesion mechanisms.

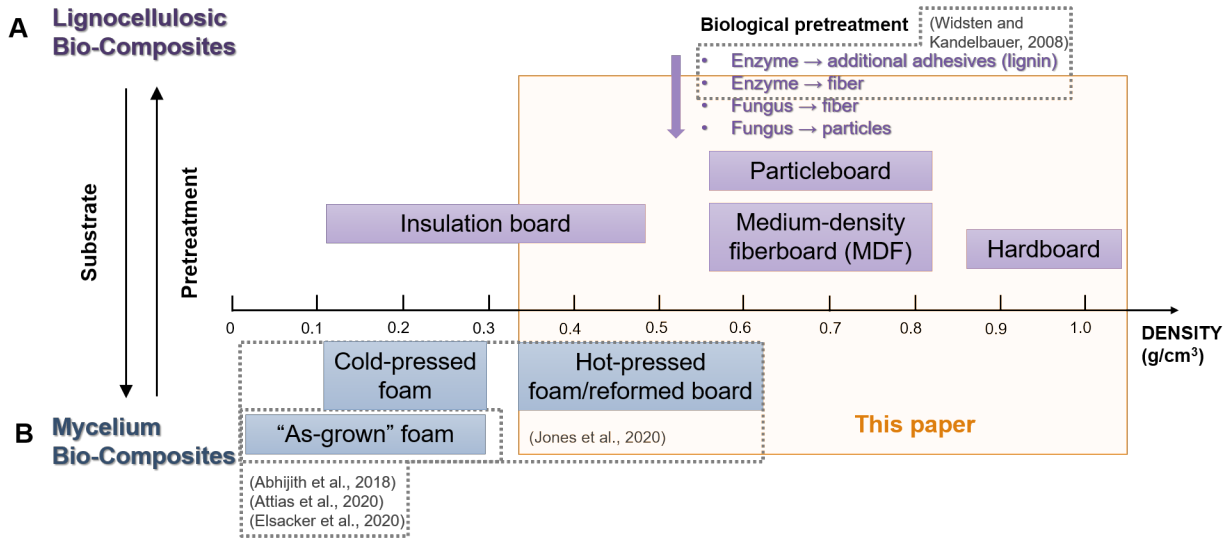

Figure 2.1. Classifications of common lignocellulosic (A) and mycelium (B) bio-composites, their relationships, and the scope of this paper.

2.2. Raw materials and production procedure

2.2.1. Lignocellulosic biomass

For hot-pressed bio-composites, it is better for the initial density of the biomass to be closer to the final product. Lower-density biomass would require more compression, which the manufacturers typically do not prefer; higher-density biomass would need less but would leave air in the structure (Hubbe et al., 2017). Woody biomass has an advantage over non-wood biomass as it is more abundant and year-round available (Suchsland & Woodson, 1987).

To take advantage of enzymes added to promote bonding, the surface chemistry of the biomass is important. In particular, the fibers for making fiberboard usually carry more water-extractable aromatic lignin on their surface because of the fiberizing process, which is more beneficial for the reactivity of the enzyme laccase (Suchsland & Woodson, 1987; Widsten, 2002). On the other hand, the composition and

complexity of the carbon sources greatly influence the growing behavior and properties of fungi (Ahmed et al., 2020; Antinori et al., 2020).

For the above reasons and many more different substrates may find optimal pairing with different fungi or enzymes for the most efficient activation and the most suitable applications. As shown in Table 2.1, generally, higher density woody substrates are more favored in producing medium-density fiberboard, while lower density agricultural plants are more used in low-density particleboard production.

Table 2.1. Summary of fungal/enzymatic pretreated hot-pressed lignocellulosic bio-composites studies

Biological pretreatment		**Substrate**		**Hot-pressing condition**				**Final Product**							
Fungi/Enzyme	**Type**	**Species**	**Time**	**Pre-processing, Moisture content**	**t, min**	**T, °C**	**Type**	**ρ, g/cm^3**	**Thickness, mm**	**MOR[1], MPa**	**MOE[2], MPa**	**IB[3], MPa**	**24h TS[4], %**	**24h WA[5] ,%**	**Reference**
Enzymatic	Laccase	Beech	1 h	Cold pressed (33 %MC)	5	180	Fiberboard	1.04	3	44.6	3360	1.55	57*	72	Felby et al. (1997)
Enzymatic	Laccase	Beech	1 h	Forced air dried, 40 °C, 18 h, 12 % MC	5	200	Fiberboard	0.90	3	41.7	4020	1.57	19*	72	Felby et al. (1997)
Enzymatic	Laccase	Mixed[6]	12 h	De-watered	5	190	Fiberboard	0.78	5.4	-	-	0.95	21*	-	Kharazipour et al. (1997)
Enzymatic	Laccase	Mixed[6]	12 h	Dried at 50 °C (20-25%MC	5	190	Fiberboard	0.77	6.0	-	-	0.59	22*	-	Kharazipour et al. (1997)
Enzymatic	Peroxidase	Mixed[6]	4h	De-watered	5	190	Fiberboard	0.8	5	41.7	4020	0.63	28*	-	Kharazipour et al. (1998)
Enzymatic	Laccase	Rape straw	-	Dry	-	-	Fiberboard	0.8	-	13*	-	-	50*	-	Unbehaun et al. (2000)
Enzymatic	*Trametes versicolor* medium	Rape straw	-	Dry	-	-	Fiberboard	0.8	-	20	-	-	50*	-	Unbehaun et al. (2000)
Enzymatic	Laccase	Beech	0.5 h	11-13%	3.4	200	Fiberboard	0.87	8	46.0	3950	0.93	46*	92	Felby et al. (2002)
Enzymatic	Laccase	Aspen	-	7%	5	170	Fiberboard	0.75	12	16.1	2170	1.02	33*	-	Widsten et al. (2003)
Enzymatic	Laccase	Birch	-	6%	4.7	190	Fiberboard	0.71	12	19.8	2730	0.86	39*	-	Widsten et al. (2003)
Enzymatic	Laccase	Spruce	-	7%	4.1	170	Fiberboard	0.91	12	23.5	3700	1.26	39*	-	Widsten et al. (2004)
Enzymatic	Laccase	Plantain plants	1h	Dried at 40 °C, 24h	8	200	Fiberboard	1.1	3	18.7	3600	-	30*	81	Álvarez et al. (2010)

Table 2.2 continued

Enzymatic	Laccase	Pine wood	20-30 min	Dried at 120°C, 10%	-	200	Fiberboard	0.8	10	20	-	0.39	65*	-	M. Euring et al. (2011)
Fungal	*Trametes hirsute*	Corn stalk	21 d	Fresh, wet	5	170	Fiberboard	0.39	3	2.6	413	-	-	-	Wu et al. (2011)
Fungal	N/A[7]	Coconut fibers	7 d	Dry	5	165	Fiberboard	-	-	10.9*	2784	-	-	-	Lokko (2016)
Fungal	*Trametes (Coriolus) versicolor*	TSR[7]	14 d	Fresh after incubation	8	185	Fiberboard	0.91	3	18.1	4300	-	-	-	Wu et al. (2016)
Enzymatic	Laccase	Mixed[8]	120 min	13%	15	170	Fiberboard	1	5	20.8	2944	0.25	-	-	Yang et al. (2017)
Enzymatic	Laccase + xylanase	Bamboo	2h	14 %	10	200	Particleboard	0.7	10	33.7	6100	0.77	-	-	Song et al. (2018)
Fungal	*Trametes multicolor*	Rapeseed straw	24 d	Fresh, wet	20	150	Particleboard	0.35	8.8	0.86*	80*	-	-	-	Appels et al. (2019)
Fungal	*Pleurotus ostreatus*	Cotton fibers	14 d	Fresh, wet	20	150	Particleboard	0.35	8.0	0.87*	34*	-	-	-	Appels et al. (2019)
Fungal	*Pleurotus ostreatus*	Rapeseed straw	14 d	Fresh, wet	20	150	Particleboard	0.39	9.5	0.62*	72*	-	-	-	Appels et al. (2019)
Fungal	*Ganoderma lucidum*	Cotton stalk	14 d	Dried at 65 °C, 10 h	7	200	Particleboard	0.6	12	4.6	680	0.18	-	-	Liu et al. (2019)
Fungal	*Ganoderma lucidum*	Rubberwood sawdust	N/A	Sun dried, blended into powder	20	160	Particleboard	1.2	-	-	-	2.5	3.1	-	Khoo et al. (2020)
Fungal	*Ganoderma lucidum*	cotton stalk	14 d	Dried at 65 °C, 10 h first; re-immerse in water; 30%	7	200	Particleboard	0.6	12	6.0	860	0.34	-	-	Liu et al. (2020)
Fungal	*Pleurotus ostreatus*	Rubberwood sawdust	45 d	Fresh after incubation	40	130	Particleboard	0.80	-	3.9	-	-	-	-	Shakir et al. (2020)
Fungal	*Trametes (Coriolus) versicolor*	Poplar	21 d	Fresh after incubation, 65%	10	170	Fiberboard	0.92	3	22.7	-	-	12	-	Wu et al. (2020)
Enzymatic	Laccase	Poplar	4 h	Fresh after incubation, 65%	10	170	Fiberboard	0.92	3	19.6	-	-	-	-	Wu et al. (2020)

The best property results and the corresponding conditions from different papers are presented in this table.

*: values that lower than the required values according to American National Standard values (minimum) of particleboard (ANSI A208.1-2016) and medium-density fiberboard (MDF) (ANSI A208.1-2016) for interior applications.

1 MOR: modulus of rupture (Typical used standards: ASTM D1037, ISO 16893, and GB/T 4897)

2 MOE: modulus of elasticity (Typical used standards: ASTM D1037, ISO 16893, and GB/T 4897)

3 IB: internal bond strength (Typical used standards: ASTM D1037, ISO 16893, and GB/T 4897)

4 TS: thickness swelling (Typical used standards: ASTM D1037, ISO 16893, and GB/T 4897)

5 WA: water absorption (Typical used standards: ASTM D1037, ISO 16893, and GB/T 4897)

6 Commercially produced wood fibers: 80% softwood (spruce and pine) and 20% hardwood (beech)

7 TSR: *Triarrhena sacchariflora* residue

8 80% wheat straw fibers and 20% bamboo fibers

2.2.2. Fungi and enzymes

Among different lignocellulosic-degrading microorganisms, white-rot fungi are often favored in pretreatments for lignocellulosic bio-composite manufacturing attributable to their three outstanding features. First, for the more traditional fiberboard and particleboard manufacturing, lignin oxidative enzymes that are secreted at the initial stage of white-rot fungi colonization are believed to be able to activate the surface by creating lignin radicals and benefit the bonding during hot-pressing (Figure 2.2) (de Paula et al., 2019; Narayanaswamy et al., 2013; Wesenberg et al., 2003). Simultaneously, white-rot fungi also have a tendency to grow elongated mycelium systems, which bind the substrates naturally and are particularly preferred for as-grown low-density mycelium bio-composites (Abhijith et al., 2018; Sauerwein et al., 2017). Finally, in contrast to brown rot, white rot does little damage to the mechanical integrity of the wood substrate at the early stage (Zabel & Morrell, 2020a).

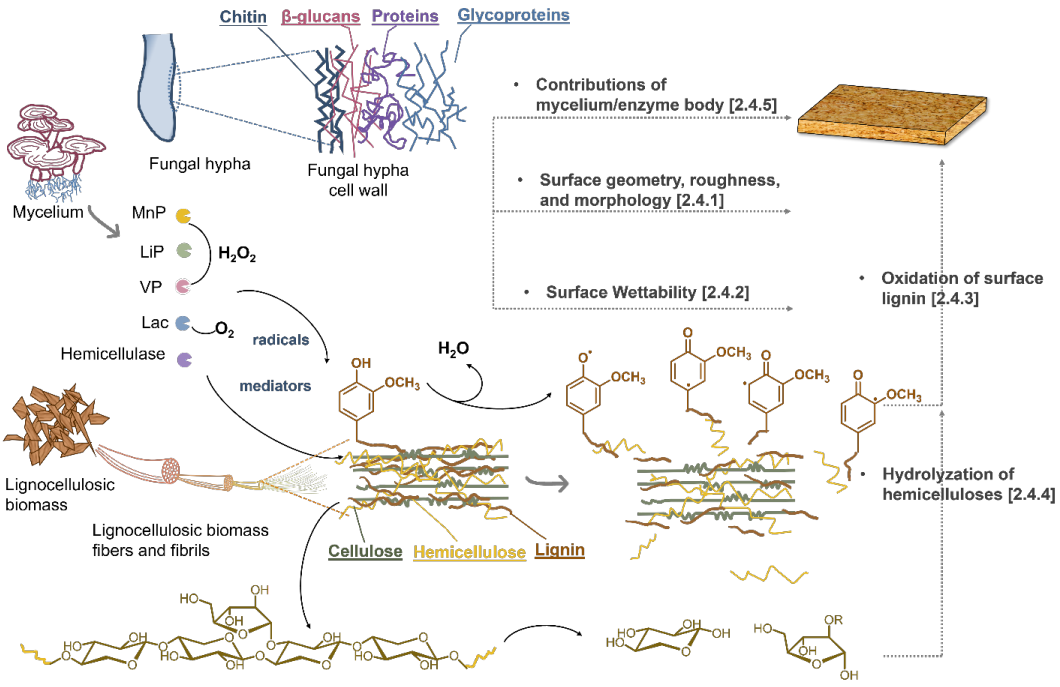

Figure 2.2. Schematic structure of lignocellulosic biomass and fungal hyphae cell walls, changes happening during fungal and enzymatic pretreatments and the possible corresponding mechanisms. MnP: manganese peroxidase; LiP lignin peroxidase; VP: versatile peroxidase ; Lac: laccase. The numbers in brackets correspond to the subsection headings in the chapter.

The selection of enzymes is much more straightforward than the selection of fungal species. Enzymes are believed to activate the surface of the biomass by breaking down molecules and generating more reaction sites such as radicals. There are four main lignin oxidative enzymes produced by white-rot fungi: laccase, manganese peroxidase (MnP), lignin peroxidase (LiP), and versatile peroxidase (VP) (Figure 2.2) (Asina et al., 2017; Janusz et al., 2017). Among these, laccase has the longest utilization history and application because it directly uses O_2 in the reaction process (Komal et al., 2018; Slagman et al., 2018). There are also hydrolytic enzymes in the white-rot degrading system, including cellulases and hemicellulases, which digest carbon sources for fungal growth and metabolism (Julia et al., 2016; Schimpf & Schulz, 2016). Because the cellulases would cause the loss of cellulose, which influences the mechanical properties of the final product (Sisti et al., 2018), only hemicellulases, such as xylanases, have achieved attention in previous research (Song et al., 2018).

When selecting the most suitable fungal species, more aspects need to be considered. To activate lignin and hemicellulose while maintaining the strength of the biomass particle, a selective white-rot fungus is preferable as it will degrade lignin and hemicellulose and leave cellulose unmodified to a large extent, as opposed to non-selective white-rot fungi, which degrade all major wood constituents at similar rates (Fackler. , et al., 2007; Watanabe et al., 2007). However, the definition of "selective fungi" is ambiguous and sometimes contradictory in the literature. For instance, *Trametes (Coriolus) versicolor* has been defined as both selective and non-selective fungus in different literature (Bhatt et al., 2016; Fackler et al., 2011; Nadir et al., 2019). It appears that the selectivity of different fungi varies with different lignocellulosic biomass and the pretreatment time (Wan & Li, 2012; Zhang et al., 2007). In other words, "non-selective fungi" are usually defined based on a long degradation period (weeks to months) in the traditional wood deterioration field. However, they also have a "selective" stage of only degrading hemicellulose and lignin at the very beginning of colonization. For this reason, "non-selective" fungi should not be entirely excluded. The selectivity ability is different in fungal strains and different when applied to different substrates. Wu et al. (2016) compared three lignocellulosic biomasses pretreated by five white-rot fungi and revealed that

only *Trametes (Coriolus) versicolor*-treated *Triarrhena sacchariflora* residue could further be produced into fiberboard with no apparent issues. Jones et al. (2019) compared the growth of *Trametes (Coriolus) versicolor* and *Polyporus brumalis* on different lignocellulosic substrates (wheat grains, wheat straw, rice hulls, and sugarcane bagasse) and reported that only wheat grains could result in sufficient growth. The other characteristic difference leading to more attention to white-rot fungi is the hyphal extension and growth density, which is mainly important for as-grown products. Jones, Bhat and John (2018) investigated the mycelium growth performance of various traditional and non-traditional fungal species and concluded that trimitic (containing three types of hyphae) and dimitic (containing two types of hyphae) species containing skeletal hyphae presented higher hyphal extension rates than other species. In this work, *Trametes (Coriolus) versicolor* and *Polyporus brumalis* were selected as the highest performing species for further applications attributable to their highest overall performance.

As shown in Table 2.1, only four types of enzymes and fungi have been investigated in the hot-pressed higher-density lignocellulosic boards, whereas in the bio-pretreatment for biofuel production (Narayanaswamy et al., 2013; Tian et al., 2012; Zhang et al., 2007) and ruminant feed ingredient (van Kuijk et al., 2015) fields, however, many more combinations have been explored. This body of work may provide some useful information for bio-composite production as well.

2.2.3. Production procedure

The production procedure of hot-pressed fungal or enzymatic pretreated lignocellulosic bio-composites is shown in Figure 2.3, using particleboard as an example. The basic procedures include three steps: 1) fungal or enzymatic incubation; 2) preparation for hot-pressing, and 3) the final hot-pressing.

2.3.3.1 Fungal and enzymatic incubation

As shown in Table 2.1, fungal incubation usually takes a much longer time than enzymatic incubation (days vs. hours) and requires an additional decontamination step for lignocellulosic biomass to prevent contamination (Elsacker et al., 2020). Ground mycelium tissues are mixed with the substrates, and the entire mixture is packed in containers or molds and incubated in a controlled environment (20 – 30 °C,

dark, humid, forced ventilation for larger volumes). To accelerate the colonization of fungi, a solution of nutrients may also be added to the mixture.

Although enzymes come from fungi, the ones used in research are usually purchased. The enzymes are usually in solutions and are either mixed with or sprayed onto the biomass. The incubation is carried out at a set pH and temperature, and lasts from 30 min to hours (Table 2.1).

2.3.3.2 Preparation for hot-pressing

The preparation step after incubation and before hot-pressing varies in different studies. For enzymatically pretreated substrates as well as some pretreated with fungi, the activated lignocellulosic biomass substrates are formed into mats directly, the water content is adjusted by filtration, squeezing, or low temperature drying (Figure 2.3). For other fungal incubation, the substrate is shaped before fungal growth so that after incubation, mycelia connect particles. Three possible routes may be applied after that: 1) directly hot-press the fresh auto-packed mixture; 2) heat treat the mixture to inactivate the fungi but keep the compressed mixture form and then hot-press or 3) inactivate the mixture, grind down the compressed mixture and repack in molds before hot-pressing. There are no studies that directly compare these different procedures in terms of the properties of produced bio-composites.

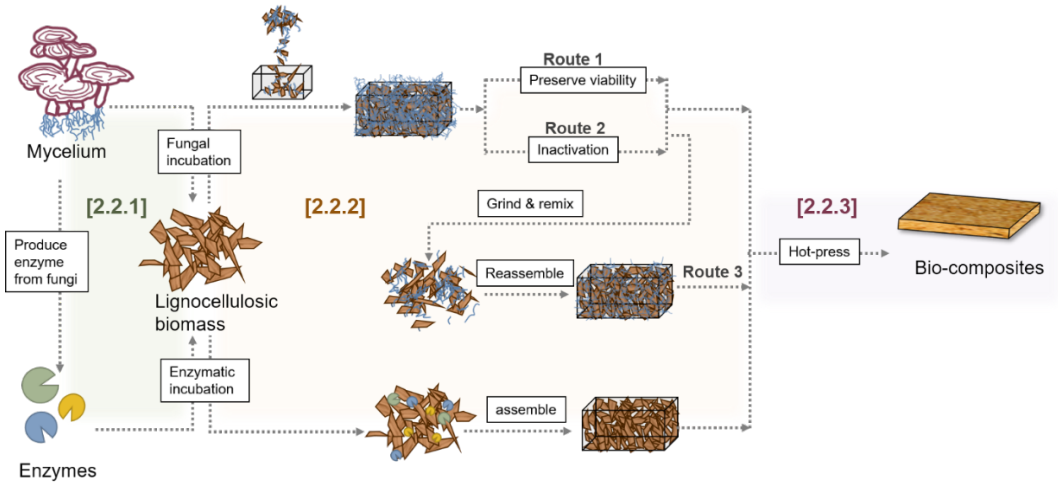

Figure 2.3. Production routes for fungal and enzymatically pretreated lignocellulosic bio-composites (using particleboard as an example). The numbers in brackets correspond to the subsection headings in the paper.

2.3.3.3 Hot-pressing

The purpose of the hot-pressing step is to densify the composite, create more adhesive bonds, and inactivate the enzymes or fungi in those cases where there is no pre-inactivation step. The hot-pressing temperature varies from 130 °C to 200 °C (The temperature in the center of the panel is usually not reported but it depends on the moisture/water content), as listed in Table 2.1. Two major different processes "wet process" and "dry process", differ in the moisture content of the mat as it enters the hot press. Typically, when the water content is above ~25% and has a significant role in bond formation and heat transfer, the term "wet process" is used. Wet processes are more favored in fungal pretreated substrates as the incubation itself requires high humidity, whereas dry processes are more developed as pilot scale in enzymatic pretreatments (Euring et al., 2013; Felby et al., 2002), as they do not require process water (Suchsland & Woodson, 1987), the energy requirement is far less (do not have to boil water), and the enzyme solution can be easily sprayed onto the substrate.

2.3. Composite Properties and affecting factors

Table 2.1 lists the characteristic properties of fiberboard and particleboard made from various lignocellulosic biomass through fungal or enzymatic pretreatment with no additional adhesive. The data is limited and is based on different substrates, conditions, and processing parameters, which makes it difficult to compare. Below we summarize some of the findings in the literature as they relate to the composite properties.

2.3.1 Mechanical properties

For the mechanical properties, the strength of bio-composites is usually given priority because of the typical applications (Pintiaux et al., 2015). This property was evaluated in most of the studies as modulus of rupture (MOR) from three-point bending tests. Figure 2.4 presents a comparison of the change of MOR with density and other typical parameters, including the temperature, the type of composites, and the substrate. Fiberboards are usually produced for higher-density applications and usually exhibit higher

strength. In contrast, lower-quality agricultural wastes are preferred in lower-density particleboard or insulation board and normally have lower strength.

Enzymatically pretreated bio-composites show higher strength, but it is mostly caused by the density difference: enzymes are more favored in pretreating higher-density fiberboards whereas fungi are more often used in lower-density particleboards (Table 2.1). Wu et al. (2020) treated poplar wood with both laccase and *Trametes (Coriolus) versicolor*; the fungus-treated products showed a higher MOR value (22.7 MPa vs. 19.6 MPa as shown in Table 2.1). As the efficiency of both fungus and enzyme treatment highly depends on a number of parameters (time, pH, temperature, relative humidity, etc.), it is hard to compare the results directly.

During the hot-pressing process, the higher temperature usually brings about higher MOR, which is attributed to the formation of more hydrogen and chemical bonds. Liu et al. (2019) compared *Ganoderma lucidum* pretreated cotton stalk bio-composites made at different hot-pressing temperatures (160, 180, and 200 °C) with controlled density and thickness. They showed that the interfacial bonding strength increased significantly with the increased temperature (230% increase in MOR from 160 °C to 200 °C). They also observed more repolymerization, esterification, and formation of hydrogen bonds from Fourier transform infrared (FTIR) spectra.

Enzymatic and fungal pretreatments are both wet-based, but the substrate may be pre-dried before pressing. The presence of moisture may lower the glass transition temperature (T_g) of the polymeric materials as water can act as a plasticizer (Jakes et al., 2019). These materials could soften and flow and increase the contact area to benefit bonding. Liu et al. (2020) reported that increasing the water content of the substrate by immersing in water before hot-pressing could increase the mechanical properties of the final product (1.5 times). They also reported that the plateau was around 30% water content. They explained that after 30%, the excessive water only remained in the cell lumen and had little effect on the properties of the fibers. It should be mentioned that the fiber saturation point (FSP) value was redefined by Engelund et al. in 2013 as about 40%. However, the extra 10% moisture content defines the water entering the cell wall but without breaking cell wall polymer hydrogen bonds (Engelund et al., 2012). Felby et al. (1997)

compared wet and dry processing methods with 33% and 12% water content, respectively. The average MOR of the dry-produced bio-composite revealed no significant difference than the wet-produced one.

Table 2.2 lists the minimum required values from the American National Standard of particleboard (ANSI A208.1-2016) and medium-density fiberboard (MDF) (ANSI A208.1-2016) for interior applications (ANSI, 2016a, 2016b). In addition to the MOR, modulus of elasticity (MOE), and internal bonding (IB) values are summarized in Table 2.1 and as seen, most of the produced fiberboards or particleboards could attain the standard value. For the ones with values lower than required (marked *), they either used hot-pressing temperatures lower than 180 °C (Appels et al., 2019) or ground and reassembled the fungus-pretreated substrate (Sun et al., 2019) which are believed to have negative effects on bonding. In the latter case, the disruption of the 3D structure of filamentous mycelium that has already held lignocellulosic particles together will deteriorate the mechanical performance of the bio-composite.

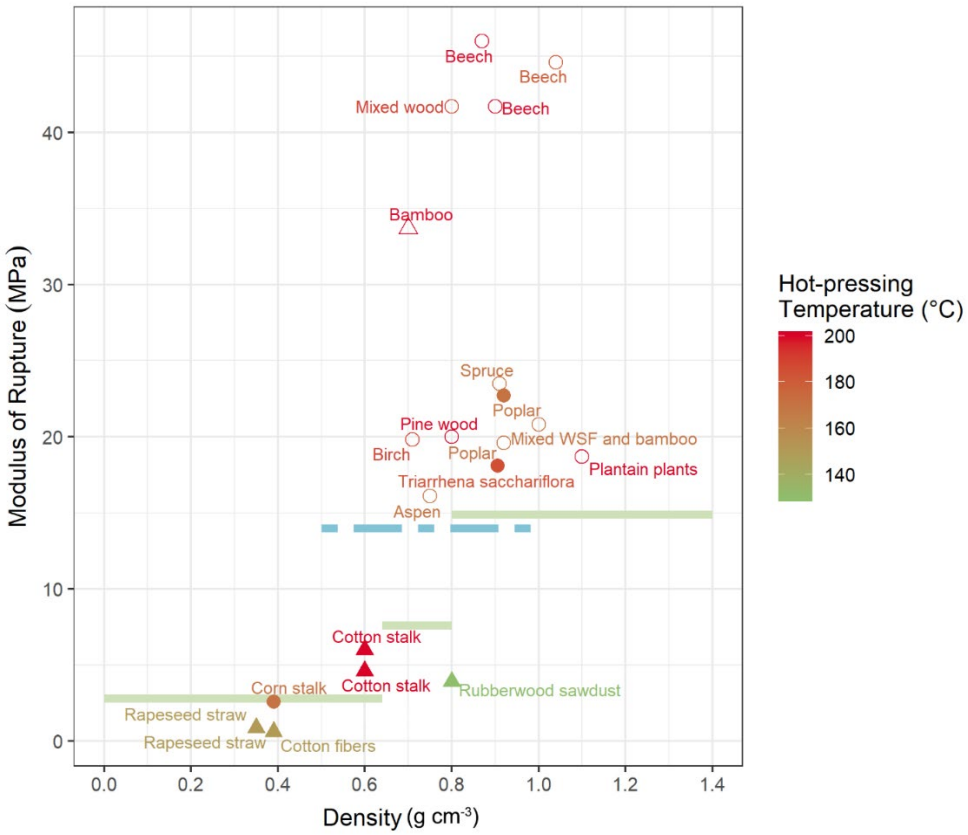

Figure 2.4. Density (g cm^{-3}) and modulus of rupture (MPa) of hot-pressed lignocellulosic bio-composites. Board type: ● ○ = fiberboard; ▲ Δ = particleboard. Pretreatment type: ○ Δ = Enzymatic; ●▲ = Fungal. All data come from Table 1; only the data that contain both density and MOR values are included. Solid line: ANSI standard MOR value for particleboard (Table 2.2); dashed line: ANSI standard MOR value for MDF (Table 2.2).

Table 2.3. American National Standard values (minimum) of particleboard (ANSI A208.1-2016) and medium-density fiberboard (MDF) (ANSI A208.1-2016) for interior applications

Product	**Density, g/cm^3**	**MOR, MPa**	**MOE, MPa**	**IB, MPa**	**TS, %**
Particleboard (H)	> 0.8	14.9	2160	0.81	N/A
Particleboard (M)	0.64 – 0.8	7.6	1380	0.31	N/A
Particleboard (L)	< 0.64	2.8	500	0.10	N/A
MDF	0.5 – 1.0	14	1400	0.30	10

*letters H, M and L indicate high density, medium density, and low-density panels, respectively.

2.3.2 Physical properties

While the mechanical properties of fungal and enzymatically pretreated bio-composites are nearly as good as the composites bonded by traditional adhesives, the physical properties are far from equivalent. Water absorption (WA) and thickness swelling (TS) are common measures of water resistance in panel products. As shown in Table 1, these parameters were only rarely reported, especially for the particleboard applications, probably because it is not required (Table 2.2). For fiberboards, although fungal and enzymatic pretreatment were reported to decrease the values, all reported 24h TS values are still much higher than the ANSI standard. One exception is from a recently published paper (Khoo et al., 2020) where the 24h TS of 160 °C hot-pressed fungal pretreated rubberwood sawdust was only 3.1%. This value is dramatically lower than the data obtained from other research groups. This low value might be a technical error as there are a few other technical errors in this particular paper including contact angle values.

2.3.3 Thermal stability

Thermal stability is highly depend on the substrate. The pretreatments are mild; the proportion of enzymes and fungal body is negligible in the entire mixture and there is little difference between thermal properties of the raw material and resulting composites.

Appels et al. (2019) reported that the colonized substrate thermally degraded faster than the uncolonized group. One possible reason is that fungal degradation makes the substrate more accessible for thermal degradation, but it also might be caused by the lower thermal stability of the mycelial body. Appels et al. (2019) also reported that there was no noticeable impact on degradation profiles of the produced bio-composite after hot-pressing at 150 °C. However, Liu et al. (2019) reported that hot-pressing at 160 °C and 180 °C caused a higher weight loss rate in thermogravimetric analysis (TGA), where heating and volatile release is similar to the first stage of thermal degradation, but this would be reversed when increasing the hot-pressing temperature to 200 °C. The authors hypothesized that the highest hot-pressing temperature might have already released the most unstable compounds.

2.3.4. Additives

To further improve the physical and mechanical properties of fungal and enzymatically pretreated bio-composites to compete with commercial formaldehyde-based adhesive-bonded products, different additives have been investigated. There are also attempts to add traditional formaldehyde-based adhesives (Nasir et al., 2014; Nasir et al., 2015; Zhu et al., 2017), which are not in the scope of this discussion.

2.3.4.1 Mediators

To promote enzymatic action, mediators are added in laccase systems. Mediators are small molecules which are oxidized by enzymes and act as electron carriers to oxidize other molecules. Mediators can increase the rate and number of chemical reactions in the biomass. The group of Euring et al. conducted several studies adding mediators including 4-hydroxybenzoic acid (HBA), 1-hydroxybenzotriazole (HBT) acetosyringone (AS), caffeic acid (CA) and vanillic alcohol (VAl) to medium-density fiberboard system (M. Euring et al., 2011; Markus Euring et al., 2011; Euring et al., 2013; Kirsch et al., 2016). All the mediators improved both physical (TS) and mechanical (MOR, MOE, and IB) properties of the bio-composite. HBA, CA, and VAl were considered better alternatives possibly because of their high redox potential.

2.3.4.2 Lignin derivatives

Based on the previously described laccase-mediator pretreatment system, Euring et al. (2016) upgraded the system by adding calcium-lignosulfonate to MDF. More phenoxy radicals were observed, which contributed to the bonding and further improved the mechanical properties. The produced bio-composites performed as well as those with 10% urea-formaldehyde bonded fiberboard.

2.3.4.3 Hydrophobic agents

Wax is typically added to commercial particleboard, OSB, and fiberboard to improve water resistance (Mantanis et al., 2017). Felby et al. (2002) added 1% liquid paraffin wax to the laccase treated fiber mixture, finding that a negative effect on bonding strength, and no improvement in dimensional stability. Because the amount of radicals generated by laccase was not changed, the authors correlate this observation with the reduced contacts and interactions among fibers caused by wax coating. Kirsch et al. (2016) made a similar attempt but changed the paraffin wax to hydrowax. They reported a noticeable

improvement comparing with previous work with no wax addition (Euring, 2008). Although these works were performed by the same research group, it is always difficult to compare numbers from different studies.

2.4. Effect of fungal/enzymatic pretreatment and links with adhesion

2.4.1. Surface geometry, roughness, and morphology

Mechanical interlocking and polymer interdiffusion theories are two of the main adhesion theories in lignocellulosic adhesive bonding for low viscosity adhesives such as urea-formaldehyde and phenol formaldehyde resins (Gardner et al., 2014). Lignocellulosic biomass carries a porous and irregular structure, which has air spaces between individual particles or fibers. The rougher surface provides more surface area for mechanical interlocking. A rougher surface also can expose a more porous structure on the surface for the diffusion of adhesives.

Because the cell wall of lignocellulosic biomass is an aggregate of microfibrils surrounded by the matrix of lignin and hemicellulose (Figure 2.1), breaking or removing the matrix would cause the exposure of more microfibrils and result in a rougher surface. At the same time, the growth of aerial hyphae on the surface also contributes to the change of the roughness by adding a microscale network on the original biomass surface (Wu et al., 2016). Enzyme treatments have been reported to have widely different effects on lignocellulose surfaces. When the incubation time is longer, the surface will become rough attributable to the significant loss of the surface layer. Zhu et al. (2017) treated poplar fibers with laccases for 11 days and found that the surface of the fibers became loose (compared by scanning electron microscopy (SEM) images). Rajak and Banerjee (2016) investigated the change of surface properties of Kans grass after laccase incubation. They found that the surface area (measured using Brunauer-Emmett-Teller (BET)), pore volume, and pore diameter (measured using differential scanning calorimetry (DSC)) all increased after the treatment, which could be explained by the opening of the outer layer of the matrix similar to the fungi treatment. Álvarez et al. (2010) treated leaf sheath fiber bundles with laccase for 24 h but were not able to find a noticeable change in fibrillation and integrity (in SEM). Nasir et al. (2015) treated rubberwood fibers with laccase for 30 min, and 60 min and found that laccase-treated fibers had a smoother surface compared

with the untreated fibers (in SEM). Similar observations are also reported by Kumar et al. (2009) and Nasir et al. (2014). It was believed that the loosely bonded lignin was removed by the enzyme, the aliphatic and aromatic ring molecules were also broken down, and the hydrolyzed lignin was re-precipitated onto the surface.

2.4.2. Surface wettability

Wettability describes the spreading and uniformity of the surface bonding agent. Lignocellulosic biomasses generally have high surface energy attributed to their chemical composition. For this reason, they require adhesives with polar molecules for better molecular interaction. However, the adhesives are better with lower viscosity for better spreading (Gardner et al., 2014; Hunt et al., 2018). In binder-less lignocellulosic bio-composite systems, the adhesion agents are considered to be heat-plasticized lignin and hemicelluloses (Hubbe et al., 2017). As these materials are already well-distributed on the surface of each particle or fiber, there are no issues of contacting and distribution. The hot-press process also promotes adhesion by plasticizing and compressing the surface components.

The aerial mycelia contains amphiphilic hydrophobin proteins, which make the aerial hyphae hydrophobic on the surface mediating the escape of hyphae from the aqueous environment into the air (Appels et al., 2018; Sammer et al., 2016), and have water contact angles higher than 120 °C (Antinori et al., 2020; Haneef et al., 2017).

Laccase incubation decreases the surface energy of lignocellulosic biomass substrates. Zhu et al. (2017) reported that the initial water contact angle of poplar fibers increased from 114° to 136° with 5-day to 11-day laccase treatment, respectively. Felby et al. (2004) investigated the change of surface energy components of beech fibers after laccase treatment. They reported reductions of 55% in hydrogen dipole (hydrogen bonds),77% Lewis acid-base interactions (covalent bonds), which indicates that the amount of Lewis acid-base interactions and hydrogen or dipole induced bonding in boards are lower compared to boards made from control untreated fibers.

2.4.3. Oxidation of surface lignin

One electron (radical) oxidation of lignin by enzyme systems secreted by white-rot fungus and covalent bonds formed by the lignin radicals during hot-press are the most accepted and well-studied mechanisms of adhesion in these composites. As introduced in Section 2.2.2, these enzymes are often heavily secreted during fungal colonization, attributable to the structure of the lignocellulosic cell wall. This selective stage is the critical period of direct fungal pretreatment. The main goal is to take full advantage of the lignin oxidation without damaging the cellulose.

As expected, secretion differs by fungal species, substrate, nutrient availability, culture conditions, age, etc. In work by Lekounougou et al. (2008)'s work treating beech with *Trametes (Coriolus) versicolor*, there was no peroxidase activity at all in the first ten days. In other words, they suggested that laccase was the only contributor to lignin degradation at the very first stage. However, when using the same fungus on poplar wood, Wu et al. (2020) reported that the activities of laccase and LiP are too low to be determined in the first 28 days, whereas the activity of MnP increased in the first 14 days then decreased in the following 14 days. This difference is also revealed in the correlations between the properties of the bio-composites produced. Some research reported direct positive correlations between the activity of a specific enzyme (laccase) and mechanical properties (Wu et al., 2011; Zhu et al., 2017), while Wu et al. (2020) revealed positive correlations between MnP and bending strength but with a 7-day lag.

Directly treating the substrate with specific lignin-degrading enzymes is more targeted than growing fungi and can avoid potential damage to carbohydrates. It is also easier to test adhesion mechanisms. The generation of more free radicals after enzymatic pretreatment of fibers was detected by electron paramagnetic resonance (EPR) spectroscopy (Felby et al., 2002; Felby et al., 1997). The fibers treated by higher dosages of enzymes showed a higher radical generation amount, and the bio-composite made from them had higher mechanical properties (Felby et al., 2002). The oxidation of surface lignin was confirmed by the increase of the surface O/C ratio, measured by X-ray photoelectron spectroscopy (XPS analysis) (Felby et al., 2004; Liu et al., 2020). Finally, gel permeation chromatography (GPC) revealed the increasing molecular weight of laccase pretreated lignin in the produced bio-composites compare with

unpretreated control sample, which confirmed the increasing polymerization during the hot-pressing process (Felby et al., 2002).

2.4.4. Hydrolysis of hemicelluloses

Another possible source of covalent bond formation is the degraded hemicelluloses produced by the action of white-rot fungi. Because hemicelluloses have naturally low thermostability, they are believed to decompose in the hot-pressing process of binder-less composite manufacturing and contribute to covalent bonds. Many studies have shown evidence of hydrolysis and thermal decomposition of hemicelluloses in binder-less bio-composites production (Brazdausks et al., 2015; Cristescu & Karlsson, 2013; Dolan et al., 2015). Hubbe et al. (2017) summarized the likely linking reactions involved in the degraded hemicelluloses and lignin fragments.

One possible explanation for the effectiveness of fungal pretreatment maybe due to the fact that lignin does not provide carbon and energy to the fungus in earlier stages of colonization (Lekounougou et al., 2008), but they also secrete hemicellulases. The surface hemicelluloses are hydrolyzed into smaller molecules, which decompose more easily providing reaction sites during hot-pressing (Mishra et al., 2017; Xie et al., 2017).

Wu et al. investigated the change of water-soluble hemicellulose in two of their published studies, treating corn stalk with *Trametes hirsuta* and *Triarrhena sacchariflor* with *Trametes (Coriolus) versicolor* (Wu et al., 2016; Wu et al., 2011). They found that the content of water-soluble polysaccharide first increased then decreased, corresponding well with the mechanical properties of the produced bio-composite. However, in their recently published research using *Trametes (Coriolus) versicolor*-pretreated poplar wood shavings, the ethanol-extracted polysaccharide content decreased throughout the 28-day incubation period which also has a positive relationship with the strength of the composite, while the reducing sugar in the filtrate first increased then decreased (Wu et al., 2020). There are a lot of things changing (surface chemistry, morphology, components from biomass and fungi etc.) during the period and decay time by fungi. Thus, it is not likely to find a direct relationship between the changes of polysaccharides and the composite properties.

2.4.5. Contributions of mycelium/enzyme body

When incubating fungi or enzymes on biomass, fungus and enzyme chemical components may also contribute to bonding and need to be considered. As shown in Figure 2.4, the typical basidiomycete white-rot fungal mycelium consists of two elemental layers. The inner layer is composed of chitin and branched β-(1,3) and β-(1,6) glucan, which work as the scaffold for the cell. The outer layer contains a protein layer, a glycoprotein layer, and a slime layer and that varies among the species (Gow et al., 2017; Steudler & Bley, 2015). Although there has not been direct exploration using the mycelium body as an adhesive in lignocellulosic bio-composites, there have been multiple reports on using bio-based proteins, carbohydrates, glycoprotein and protein/carbohydrates blends (Cheng & He, 2017). In fungal pretreatment of lignocellulosic substrates, fungal mycelium covers the surface, the protein and carbohydrates components in the outer layer of hyphae may contribute to the formation of bonds. Limited evidence was reported by Liu et al. (2019) on hot-pressed composites from mycelium-colonized cotton stalks. They found that there were new peaks appearing at 2978 cm^{-1} and 1086 cm^{-1} assigned to C-NH and C-O stretching, respectively, in the FTIR curve after hot-pressing at 200 °C, which they suggested the reactions between the mycelium and the cotton stalk particles. However, the reactions could also only happen within the fungal body and have no connection with the biomass. More evidence needs to be provided to confirm the bonding mechanism.

When using enzymes alone to pretreat biomass, the proportion of non-substrate material in the system is even lower than if a full fungal pretreatment had been used. It is unlikely that the bonding chemistry would be significantly altered. Felby et al. (1997) and Kirsch et al. (2016) confirmed this by comparing fiberboard made from untreated fibers and fibers pretreated with inactivated laccase (same addition levels as active laccase) and showed no significant difference in the physical and mechanical properties.

2.5. Knowledge gaps and commercial limitations

2.5.1. Knowledge gaps

2.5.1.1. Fungal pretreatment vs. enzymatic pretreatment

Generally, fungal pretreatment requires more incubation time, and results in a less targeted treatment, while enzymatic pretreatment, although more targeted, generally cost more due to the more complicated enzyme production processes. The question remains, then, whether such precision in lignocellulosic bio-composite manufacturing is in fact needed. If so, how much improvement in properties can be achieved? A detailed comparison of the pretreatment efficiency, cost of time, and energy would help to answer these questions.

2.5.1.2. Fresh vs. inactivated substrate

Radicals are generally not stable, but for enzyme generated lignin radicals, some could be stabilized in the substrate polymer and last for days (Perna et al., 2019; Shi et al., 2020). For enzymatic pretreatment, the hot-pressing usually proceeds right after pretreatment. When additional pre-drying is used , the content of radicals decreased but still had a considerable amount which presumably promote bonding (Felby et al., 2002). In the fungal pretreatment process, the situations are quite different. A certain number of reported experiments inactivated fungal growth by heat first, then proceeded with the hot-pressing. It is understandable that this process can make the production process more flexible and also reduce the hot-pressing time, but it is not clear how this step affects the bonding as the adhesion mechanism in fungal pretreatment system is more complicated and not well-understood. A direct comparison of the bio-composite made from fresh compressed and inactivated substrate would provide some information.

2.5.1.3. Fungal mycelium body vs. lignin radicals vs. degraded hemicellulose

As described in Section 4.5, the effects of the mycelium body have never been considered in hot-pressed biologically pretreated lignocellulosic bio-composite systems. Since most white-rot fungi used in the studies grow elongated surface mycelium at a very early stage, the question is if the mycelium contributes to or hinders bonding. Are there characteristics of mycelia that make them bond more effectively? If so, can we guide the fungi to express these characteristics when growing on our biomass

substrate? Just how much do various bonding agents contribute to dry (MOR, MOE, IB) and wet (TS, WA, creep, high humidity performance) properties? How can various bonding mechanisms be maximized? If the mycelium body has a generally positive effect on bonding, could there be a synergistic effect of mycelium body, lignin radicals, and hemicelluloses at a particular degradation stage? If the adhesion ability of surface mycelia themselves is strong enough, could we directly use the pure mycelium to mix with untreated lignocellulosic biomass substrates so that we could avoid the long incubation time? Thus, a thorough investigation of the functionality of surface mycelium will be beneficial.

2.5.2. Limitations for commercialization

Although some studies have proved the comparable mechanical properties of enzymatic and fungal pretreated bio-composites, there are common problems, such as the moisture resistance and performance at high relative humidity, and high compressing temperature that need to be addressed for industrial applications.

2.5.2.1. Moisture resistance

Moisture resistance of almost all the products described in the literature are extremely low and not suitable for humid conditions. This is not surprising because there is not enough covalent bond formation in these all bio-based systems, relative to traditional adhesives. The moisture resistance problems might not be a big issue for particleboard-related applications as the majority of commercialized particleboard are designed for interior usage. For MDF related applications, great improvement in the thickness swelling value is needed.

2.5.2.2. Processing temperature

High temperature (140-200 °C) is favorable in both of the enzymatic and fungal pretreatment systems. In “dry process” system and most of enzymatic pretreatment system, the high temperature aims to active the surface components. When the fungal incubated bio-composite is directly pressed, the higher temperature also facilitates the evaporation of water to reduce the needed time. The high processing temperature requires much more energy and limits the potential of commercialization. As most of the synthetic adhesives being used in the industry cure at much lower temperature (120-140 °C) for current

commercial panels (Mantanis et al., 2017), processing temperatures need to be reduced to be competitive or other energy savings could be considered in the larger life cycle analysis of the products.

2.5.2.3. Cost and time

There is no direct calculation regarding the manufacturing cost of enzymatic and fungal pretreated bio-composites. Because the raw materials are the same as the commercial products, the cost of enzymes and fungi are the main contributors to the raw material development. Fungi have a great advantage over enzymes as they do not require an additional extraction process and the commonly used white-rot fungal species are the same as the common commercial mushrooms. Mushroom spawns are easy to obtain and are also reusable. The long incubation time (days) is one of the biggest disadvantages of fungal pretreatment. Most of the species can be grown in ambient conditions, which only require energy for ventilation, but not heating.

2.5.2.4. Commercial products and potential improvement approaches

In the recent years, some compressed fungal mycelium – lignocellulosic bioproducts have been developed by companies. Ecovative Design LLC developed several fungal mycelium bonded particleboard-like bio-composites named MycoBoard™ (Ecovative, 2017) and mCore™ (Ecovative, 2018), successively in the past five years. In one technical report published in 2014, they reported the laminated MycoBoard™ achieved comparable mechanical properties as the MDF panels (Tudryn, 2014). However, no moisture-resistant related properties were reported and no related product is advertised in their website currently. MOGU S.r.l developed floor tiles using fungal mycelium bonded fiber waste as a core material. The floor tiles include a top coating layer (90% bio-based resin), a bio-polyurethane (PU) layer, the mycelium composite core, and a moisture barrier layer. With the added layers, the density is reported as 0.7 g cm^3 and the dimensional stability is 0.10% (MOGU, 2019). They also claimed that the bio-PU layer can be separated to enable the biodegradation of the core. Adding barrier layers is definitely a potential approach for commercialization of biological pretreatment bio-composites. The layers can be specially designed to create different functionalities to the composite.

2.6. Conclusions

Enzymatic and fungal pretreatment in lignocellulosic bio-composite manufacturing are technologies that have great potential to produce all-natural bio-composite materials for an array of applications. However, the complexities of the system require more investigations involving both the raw material and processing procedure, as well as testing the adhesion mechanisms and bonding theories. As a good number of transformations and reactions happen in both biodegradation and pressing processes, it is therefore quite challenging to focus on one possible mechanism and exclude others. In the meantime, different adhesion theories support or contradict one another. There might be a way to achieve a better knowledge of this complicated system by addressing the questions and limitations listed in Section 2.5. To produce commercial bio-composites with lower cost and better performances, there is a need to investigate the important factor for specific applications and adjust and design raw materials, pretreatment conditions, and additives accordingly.

CHAPTER 3

FUNCTIONALITY OF SURFACE MYCELIUM ON WOOD BONDING

3.1. Introduction

As summarized in **Chapter 2**, mycelium bio-composites are novel materials that provide the opportunity to achieve a bio-based circular economy and mycelium has become a popular novel biomaterial for multiple applications, including textiles, packaging, construction, and other applications (Elsacker et al., 2020; Girometta et al., 2019). Composite panels with higher density could be further generated by adding heat and pressure to those mycelium foams. These kinds of panels have components and structures similar to the traditional lignocellulosic-based particleboards and are being investigated as potential replacements for formaldehyde-based adhesive-bonded panels (Appels et al., 2019; Liu et al., 2019; Sun et al., 2019). Multiple bio-based adhesives have been explored and developed in lignocellulosic bio-composites manufacturing in the past few decades in response to the increasing environmental awareness. Proteins, carbohydrates, lignin, tannin, and other natural biopolymers have all been investigated as wood adhesives. Some of these adhesives even have had commercial success (Hemmilä et al., 2017). However, the adhesives market is large, with many products and needs, leaving opportunities for a variety of approaches. Hot-pressed mycelium-lignocellulosic bio-composites are an alternative path to 100% bio-based, eco-friendly bio-composites.

The bonding mechanism of hot-pressed mycelium bio-composite is not yet well understood. Because of the complexity of such systems, very limited evidence has been provided on the details of the role of surface mycelium on bonding in lignocellulosic bio-composites. The solid substrates are usually in small geometries (particles or fibers) and therefore it is hard to separate the surface mycelium from them, leading to problems in decoupling the effects of multiple variables. For the same reason, we have not found any reported research on developing pure fungal mycelium as a stand-alone adhesive.

In **Chapter 3**, we specifically investigated the wood bonding ability of fungal mycelia, and components that might be contributing or detracting from bond strength. We made the first attempt at quantifying the adhesive strength of a pure surface mycelium layer through a unique growing system. By

controlled growth of fungi on veneer, the surface mycelium could be easily separated. Using this system, we incubated white-rot fungi *Trametes versicolor* on yellow birch veneers for different time periods. The growth behavior of surface mycelium, the change of surface properties of veneers, and their influence on bonding strength were investigated in light of the contributions of various interfaces. The difference between the top and bottom surfaces of the mycelium layer was also discovered and compared.

3.2. Experimental Section

3.2.1. Materials

Yellow birch (*Betula alleghaniensis* Britt.) wood veneers with a thickness of 0.61 (±0.04) mm were kindly supplied by Columbia Forest Products LLC (Presque Isle, ME, USA). *Trametes versicolor* was supplied by Ecovative Design LLC (Green Island, NY, USA) and had been maintained on agar plates at 4 °C and was pre-incubated on malt extract agar (MEA) plates before the incubation process. Weldwood® carpenter's wood glue (polyvinyl acetate-based) (DAP Products Inc. Baltimore, MD) was purchased and used for the lap-shear experiments.

3.2.2. Mycelium incubation

The incubation methods were modified from the literature (Fackler, Schmutzer, et al., 2007; Fackler, Schwanninger, et al., 2007). Yellow birch veneer samples with the dimensions of 80 mm (length) × 80 mm (width) were steam sterilized at 121 °C for 60 min and soaked for about five seconds in 2% (w/v) corn steep liquor (CSL) (Sigma-Aldrich, Saint Louis, MO, USA) containing suspended fungal mycelium. One MEA plate overgrown by the fungus was mixed in 150 mL 2% (w/v) sterile CSL in a tissue grinder before they were transferred to Petri dishes containing MEA. Plastic canvas meshes were used as supports in between the veneer and agar. The Petri dishes were incubated at 28 °C, 80% relative humidity (RH) for up to 20 days.

3.2.3. Weight loss of wood veneers and weight gain of surface fungal mycelium

After different incubation periods, the surface mycelium was separated from the veneers. For earlier growth days, the mycelium was removed by using a stainless-steel ruler pushing to the side. At later stages of incubation and after the mycelium formed a mat, it was carefully peeled off with tweezers. Both the

veneer and the surface mycelium layer were dried in a sequence of elevated temperatures (40 °C, 24 h; 60 °C, 24 h; 103 °C, 24 h). The weight loss of wood veneers was calculated by the change of dry weight before and after incubation. The weight gain of fungal surface mycelium was the direct dry weight of the obtained surface mycelium from a full piece of veneer (80 × 80 mm). Weight loss/gain of five replicates were calculated for each group.

3.2.4. Stereomicroscopy

Bright-field images were captured using a Nikon Ni-E (Nikon, Japan) stereomicroscope with Nikon Plan Fluor 10× PH1 DL 0.3 NA and 40× PH2 DLL 0.75 NA. Z-stack images were acquired at 10 µm intervals from the first hyphae to 200 µm and processed using the Extended Depth of Field (EDF) plugin in the image analysis software Fiji (ImageJ 1.52p, National Institutes of Health, USA) (Schneider et al., 2012).

3.2.5. Hot-press and lap-shear samples preparation

The process of hot-press and lap-shear samples preparation is shown in Figure 3.1. After incubation, the wood veneers were cut into strips of 80 mm × 20 mm before hot pressing. The surface mycelium was either entirely removed or maintained in the lapping area (20 mm × 20 mm) for comparison. All lap-shear samples were hot-pressed at 180 °C for 5 min. The pressure was controlled at 2.78 MPa. Slight densification of wood veneers under this pressure could be expected but this was the lowest manageable pressure to apply using our hot press and it was kept constant for all experiments.

To exclude the change in wood surface and to compare the top and bottom position difference of the surface mycelium layer, a group of surface mycelium-bonded untreated veneers were also prepared. The removed mycelium layers were put in between two undegraded wood strips in different configurations (as depicted in Figure 3.1) and hot-pressed under the same conditions. Untreated autoclaved wood specimens and commercial wood glue (spread rate: 30 mg per glue-line) bonded specimens were also prepared for comparison. To minimize the influences from other processing steps, the undegraded veneers were also autoclaved and saturated by water for 24 h before hot-pressing.

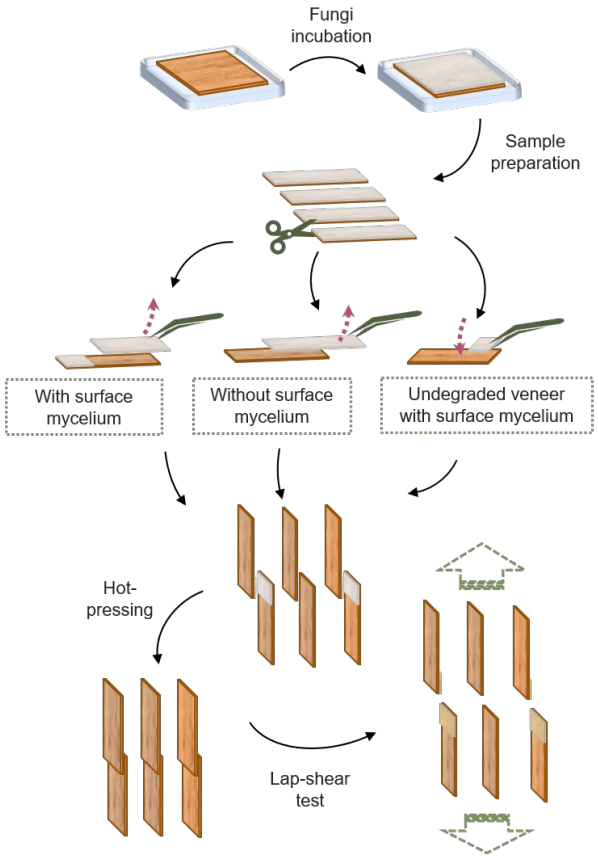

Figure 3.1. Schematic presentation of the procedure of hot-pressing and lap-shear sample preparation.

3.2.6. Lap-shear strength test

The lap-shear tests were carried out on an Instron 5966 (Instron, Norwood, MA, USA) with a 10 kN capacity load cell. The hot-pressed samples were conditioned at 23 ± 2°C and 50 ± 2% RH for 48 h (adequate to reach a constant mass). The crosshead speed was 0.5 mm/min, and the initial gauge length was 40 mm. Twelve replicates were tested for each group. Wet strength tests were carried out by soaking bonded specimens in distilled water at room temperature 20 ±1°C for 48 h and testing immediately.

3.2.7. Scanning electron microscopy (SEM)

The microstructures of the lap area of the samples and the top and bottom surfaces of the mycelium layer were analyzed using an Amray 1820 scanning electron microscope (SEM) (Amray Inc., New Bedford, MA, USA) at an accelerating voltage of 10 kV. The samples were placed on specimen mounts with double-

sided carbon tape and grounde on all edges with conductive silver paint and sputter coated with 3 nm of gold-palladium.

3.2.8. Thermogravimetric analysis (TGA)

Thermal stability evaluation was carried out under nitrogen gas on a TGA Q500 (TA Instruments, New Castle, DE, USA) with a high resolution (Hi-Res) option from room temperature to 600 °C. In the Hi-Res approach, the heating rate is dynamically and continuously modified, ranging from 0.001 °C min^{-1} to the maximum heating rate (20 °C min^{-1}) in response to changes in the decomposition rate of the sample. The resolution and sensitivity settings were 4.0 and 1.0 °C, respectively. The TGA results are shown as the variation of the sample mass (TG) and as a derivative weight loss (DTG) curve corresponding to the temperature.

3.2.9. Attenuated total reflection Fourier transform IR (ATR-FTIR)

ATR–FTIR spectra of the surfaces were obtained using a Spectrum Two IR spectrometer (Perkin Elmer, Waltham, MA, USA). All spectra were obtained in the range from 4000 to 600 cm^{-1} with 4 cm^{-1} resolution, accumulating 32 scans. The tested samples were all in room condition. To ensure the reproducibility of the obtained spectra, three replicate specimens were measured.

3.2.10. Water contact angle analysis

The contact angle analysis was carried out using a mobile contact angle analyzer (KRÜSS GmbH, MSA, Hamburg, Germany) and the corresponding software for this device. For each measurement, one 1µL drop of water was applied on a random area of the surface. Measurement was made on the same mycelium and wood samples used in the weight change testing. Six measurements were carried out per sample 2 seconds after the drop touched the surface.

3.2.11. Statistical analysis

The obtained lap-shear strength values were analyzed using a one-way analysis of variance (ANOVA) to determine statistical differences between the means. A Tukey's honestly significant difference (HSD) multiple comparison test was then performed to further assess the significance level of the mean

values for each treatment level. All comparisons were made at 95% confidence level. All the analyses were performed using RStudio (Version 1.2.5033).

3.3. Results and Discussion

3.3.1. Growth behavior of mycelium on wood surface

The development of aerial hyphae on the veneer surface is shown in the photos in Figure 3.2A and B and the microscopic images presented in Figure 3.3. Ground mycelial fragments were mixed with nutrients and dispersed on the surface of veneers on Day 0. There was no visible colonization on Day 0 and Day 2. The aerial hyphae started to be visible on Day 4. However, they were not very easy to be seen vertically (Figure 3.2A) but were more visible when viewed at an angle (Figure 3.2B). The microcolonies continued to expand, approach one another, and on Day 8, they nearly covered the entire surface. After that, the aerial hyphae started to grow thicker and formed a packed aerial layer until Day 18. Figure 3.2C shows the weight percent loss of veneer and weight gain of surface mycelium after different incubation days. With the colonization of fungi, the weight of removable surface mycelium increased dramatically from Day 6 to Day 8 and continued until Day 12. There was no significant difference ($p > 0.05$) from Day 12 to Day 18 in the weight of the grown surface mycelium, which indicates that the degradation and the growth of mycelium were most likely happening inside the wood substrate. On the contrary, there was no significant weight loss happening in wood veneers before Day 8. The negative percentages of weight loss come from the gained weight from the nutrient and mycelium (9.58 ± 2.38 mg on Day 0 and 21.44 ± 13.13 mg on Day 2, not shown in Figure 3.2). Starting from Day 6 until Day 18, there was a continuous wood weight loss, indicating the progressive degradation of wood substrate, corresponding well with the weight gain of the surface mycelium.

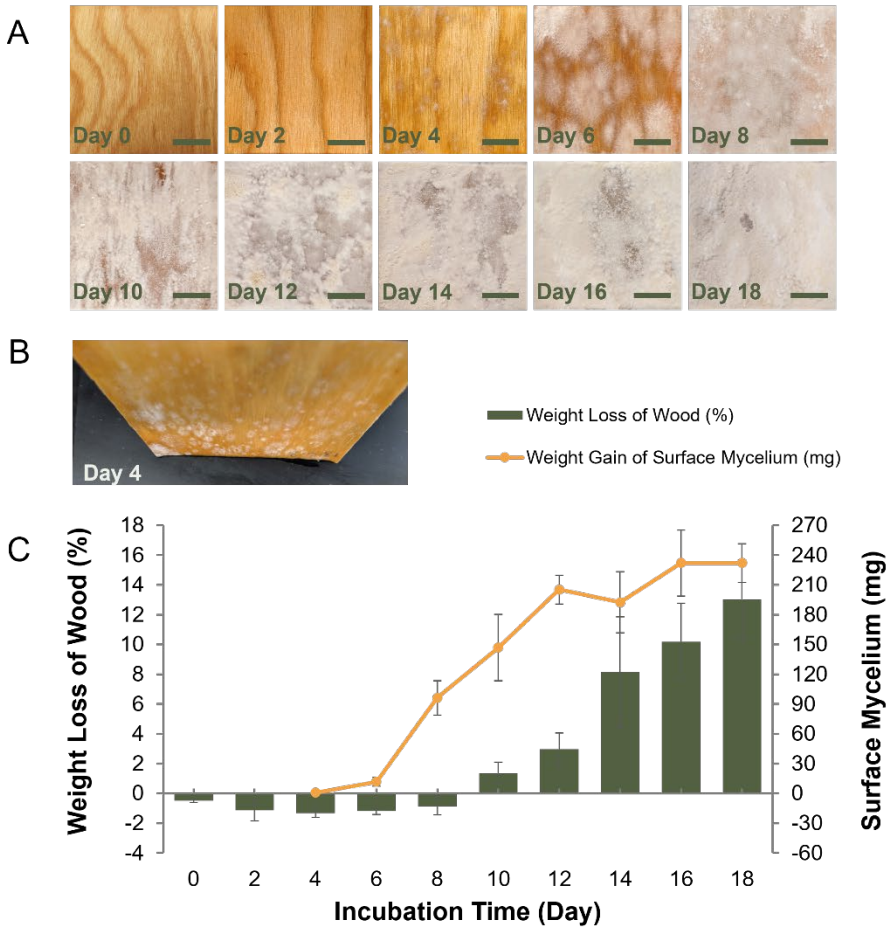

Figure 3.2. (A): The development of surface mycelium on yellow birch veneer over 18 growing days (scale bar: 2 cm); (B) the surface of Day 4 sample in a different viewing angle; (C): the weight loss of wood (%) and weight gain of surface hyphae (mg).

Stereomicroscopic images of the growth of surface mycelium on veneers after different incubation days are shown in Figure 3.3. Figure 3.3A, E, I, and M depict the extended z-stack focus stacking image to better present the surface changes. Figure 3.3 B-D, F-H, J-L and N-P reveal the images taken at different depths. Although ground mycelial fragments loaded on the veneer surface already existed on Day 0, they were almost not visible in the microscopy images (Figure 3.3 A-D). On Day 4, the surface mycelium layer was quite thin, and the texture of the wood surface was visible in the microscopic images (Figure 3.3E-H).

When the surface mycelium layer was thick enough (Day 8 and Day 12), only branched hyphae could be captured in the applied depth.

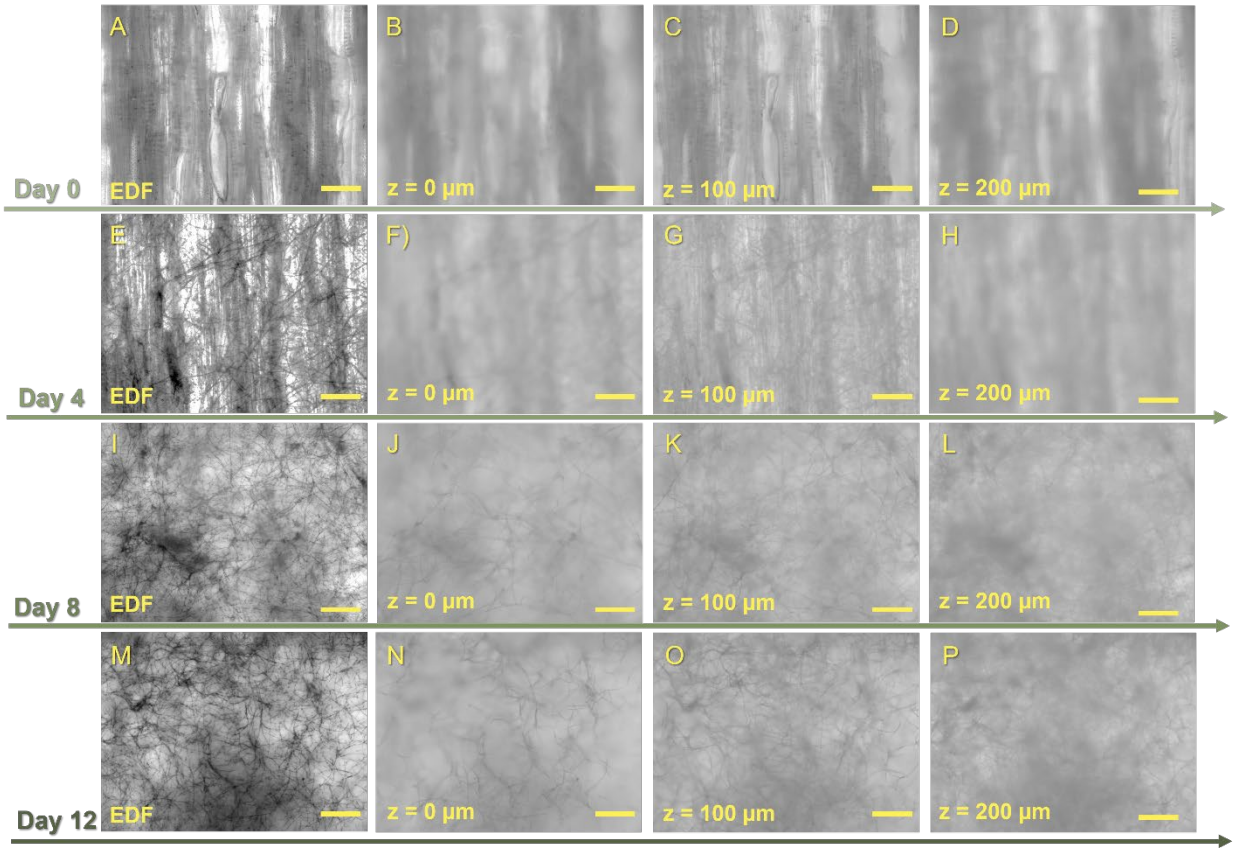

Figure 3.3. Stereomicroscopic images of the growth of surface mycelium on yellow birch veneers after different incubation days. (A)(E)(I)(M): Extended focus Z-stacking images; (B-D)(F-H)(J-L)(N-P): images at different depths. Scale bar: 200 µm.

3.3.2. Changes in wood surface and thermal properties

The colonization of the surface mycelium also altered the surface properties of the yellow birch veneer. Figure 3.4A shows an EDF microscopy image of a 20-day incubated veneer after surface mycelium has been removed. It is obvious that there were almost no mycelia on the surface comparing with Figure 3.3E, I and M. After four days of incubation, the water contact angle increased from less than 100° to 125±3° and then stayed relatively constant (no statistically significant change), as shown in Figure 3.4B. It is known that the outer layer of aerial hyphae contains a kind of hydrophobin protein that makes the

mycelium surface hydrophobic (Appels et al., 2018; Sammer et al., 2016) and helps fungi to escape from the aqueous environment and grow in air. Therefore, the initial increase in the water contact angle can be attributed to the coverage of the surface by aerial hyphae where the increased mass of mycelium at longer times does not affect wettability any further. On the surface after mycelium removal, the water contact angles dropped to 84 - 95°, and there was no significant difference ($p > 0.05$) among the different incubation times. We also compared the contact angle of undegraded wood veneers and autoclaved undegraded wood veneers (not shown) for reference. The contact angle of autoclaved veneer was 93±11°, which was not significantly different ($p > 0.05$) from the degraded wood surfaces after removing the mycelium layer, indicating that fungal degradation did not have a significant effect on the surface wettability of wood. In contrast, the untreated wood veneer had a contact angle of 73±10°, which was significantly lower than that of autoclaved sample and corresponded well to the reported values in the literature for the same species (Landry & Blanchet, 2012). An increased contact angle after autoclaving could possibly relate to the reorganization of the lignocellulosic polymeric components of wood surface attributable to the plasticization of lignin (Hakkou et al., 2005).

Figure 3.4C and D show the TG and DTG curves of the veneers without surface mycelia after different incubation days. For wood samples, the TG curve usually show a three-step degradation: from start to around 220 °C as water and volatile extractives leave the sample; 220 °C to 360 °C as hemicelluloses, amorphous cellulose and some lignin are mainly degraded, and 360 °C to the final temperature as lignin and cellulose degrade (Figure 3.4C) (Grønli et al., 2002; Hostikka & Matala, 2017; Zhai et al., 2016). When using a conventional fixed heating rate TGA, the degradation of hemicelluloses is usually shown as a left shoulder in the DTG curve, whereas the dynamic mode separated it as an individual peak (Figure 3.4D). As the fungi degraded wood components into smaller molecules, the thermal stability decreased correspondingly, which is shown in the DTG curves as the degradation peaks moving to lower temperature and also becoming broader along with the degradation time. The added nutrient also caused a similar trend when comparing the DTG curves of autoclaved wood and Day 0 wood, but is not as extreme as in the case of the extended degradation days.

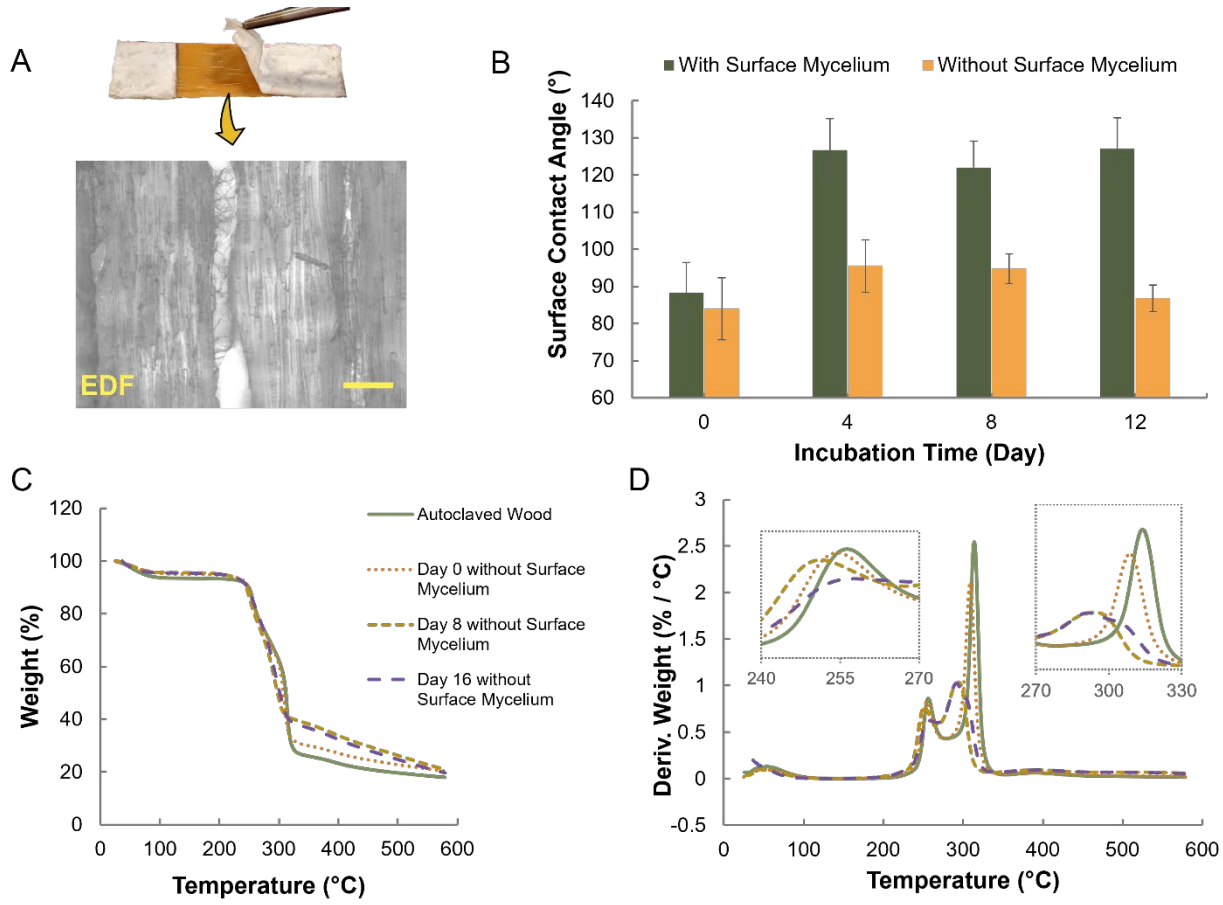

Figure 3.4. (A): Extended focus Z-stacking stereomicroscopic images of veneer surface after removing surface mycelium (Day 20), Scale bar = 200 µm; (B): Surface water contact angle of the veneers with and without surface mycelium after incubation; (C) and (D): TG (C) and DTG (D) curves of veneers without surface mycelium after incubation. (Day 0 without surface mycelium indicates autoclaved wood immersed in ground agar and CSL mixture with no mycelial fragments.)

3.3.3. Bonding properties

Figure 3.5A shows the lap-shear strengths of the three groups of veneers after various incubation times. The incubation times are different for the three groups with or without surface mycelium because before Day 12, a continuous mycelium mat was not fully produced or was too thin to be removed without damage. For the group of "with surface mycelium," the lap-shear strength generally showed a similar trend as the surface coverage of mycelium shown in Figure 3.2A. On Day 0 when there was only a small amount

of nutrients and mycelium were loaded on the wood surface, the lap-shear strength was as low as the bonded autoclaved undegraded wood (0.29 ± 0.09 MPa vs. 0.23 ± 0.06 MPa). The lap-shear strengths increased with the coverage of the mycelium on the surface. After the mycelium covered the whole surface, the increase of the mycelium mat thickness did not further improve bonding. The "without surface mycelium" group did not show a consistent trend and the strength values generally remained stable with no statistically significant change regardless of apparent maximums and minimums. This observation might relate to the change in the wood components, and functional groups at different degradation stages (Álvarez et al., 2010; Wu et al., 2020), or for some other unknown reasons. In practice, it is impossible to separate the surface mycelium from the small substrates of particles and fibers if the mycelium is grown on lignocellulosic particles or fibers and therefore, a combination in which mycelium body is present is more technically feasible. Although the details of this change are not in the scope of this paper, when comparing the "with" or "without mycelium" groups, it is evident that the additional growth of the surface mycelium layer had more contribution to bonding than the possible changes in the wood surface, as bonding undegraded wood with mycelium always gave equal or better results than bonding degraded wood without mycelium (Figure 3.5A). It could be concluded that both the surface mycelium and the change on the wood surface could promote bonding between wood surfaces, and the effect of surface mycelium is higher than the wood surface changes.

Microscopic images of the lap areas after failure provide more information regarding failure modes. When looking at the lap area after the lap-shear test, the two groups that contained two layers of surface mycelium broke at the interface between the surface mycelia. This suggests that the adhesion between two layers of surface mycelia is weaker than the adhesion between mycelium and wood. Compared with the images of the surface before hot-pressing (Figure 3.5B), the color of the mycelium layer changed from white to slightly transparent (Figure 3.5C), consistent with compression of the hyphal mat (Figure 3.5D, E). Underneath the flattened surface fibers, there was a much denser structure with more connected fibers and small holes, which probably originated from the bottom part of the surface mycelium layer or caused by compression.

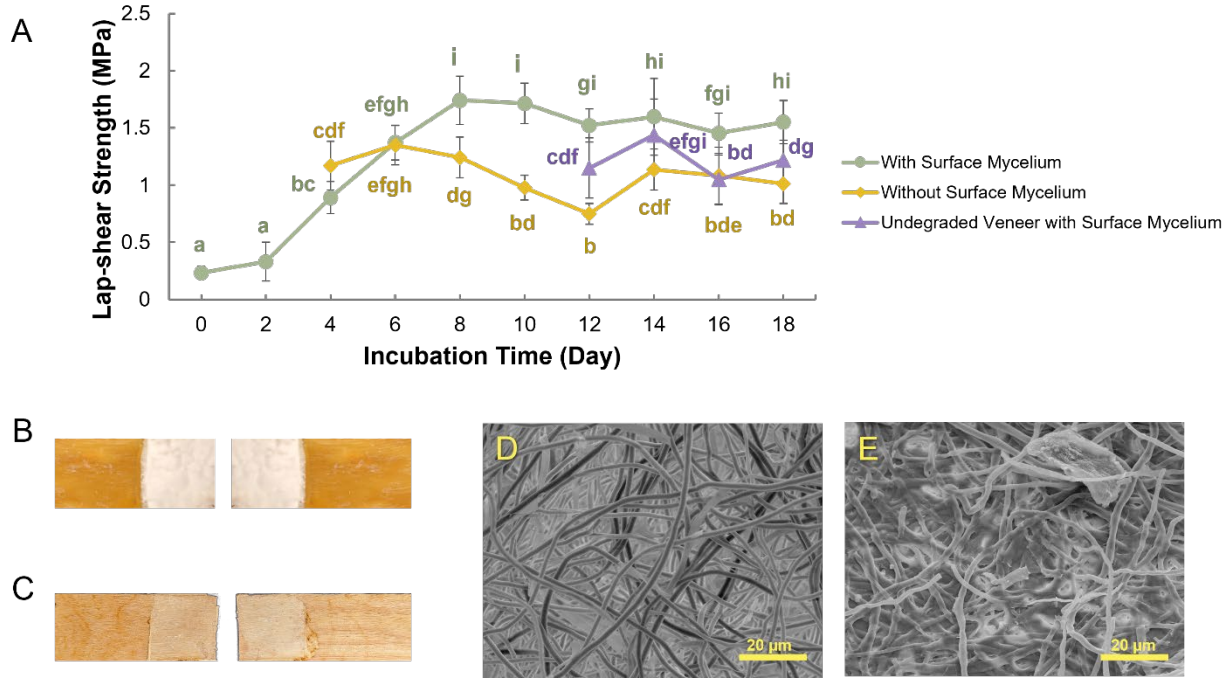

Figure 3.5. (A): Lap-shear strength of wood veneers after different incubation days with or without surface mycelium, and undegraded wood with applied surface mycelium, data points with common letters are not significantly different at 95% confidence level ($p > 0.05$); (B)(C): Lap area of "with surface mycelium" group before hot-pressing (B) and after the lap-shear test (C); (D)(E): SEM images of lap area of "with surface mycelium" group before hot-pressing (D) and after the lap-shear test (E) (Scale bar: 20 µm).

3.3.4. Top vs. bottom mycelium surface

To understand the different factors influencing the bonding of the two mycelium surfaces, we arranged them in different lay-ups in terms of surfaces contacting each other and repeated the same hot-pressing and lap-shear tests. As shown in Figure 3.6A, when growing on the surface of veneer, the mycelium surface that was exposed to air was termed top surface (T), while the surface that was attached to wood was called bottom surface (B). The mycelium layers were removed from the wood they grew on and were placed in between two undegraded veneers for lap-shear sample preparation. The four combinations are BTTB, TBBT, BTBT and BT, respectively (Figure 3.6A). For the first three groups, two layers of surface mycelium were used, while for BT, there was only one layer. The lap-shear strength of

each group is shown in Figure 3.6A. The BTTB combination achieved the highest lap-shear strength of about 1.11 MPa, whereas the other three groups showed only about half of the strength (0.56 to 0.62 MPa). When looking at failure modes shown in Figure 6B, the BTTB lay-up showed mycelium cohesive failure; TBBT, BTBT and BT showed mycelium-wood adhesive failure, all from the top surface of the mycelium layer. Based on the failure modes, it can be concluded that the adhesion of the bottom surface of the mycelium layer is stronger than the top surface, both with wood and with mycelium itself. For the strongest BTTB group, it was hard to tell if the failure had occurred between the two top surfaces or within the matrix of mycelium body. In either case, it was stronger than the bond between the mycelium top surface and wood, but weaker than the bond between mycelium bottom and wood.

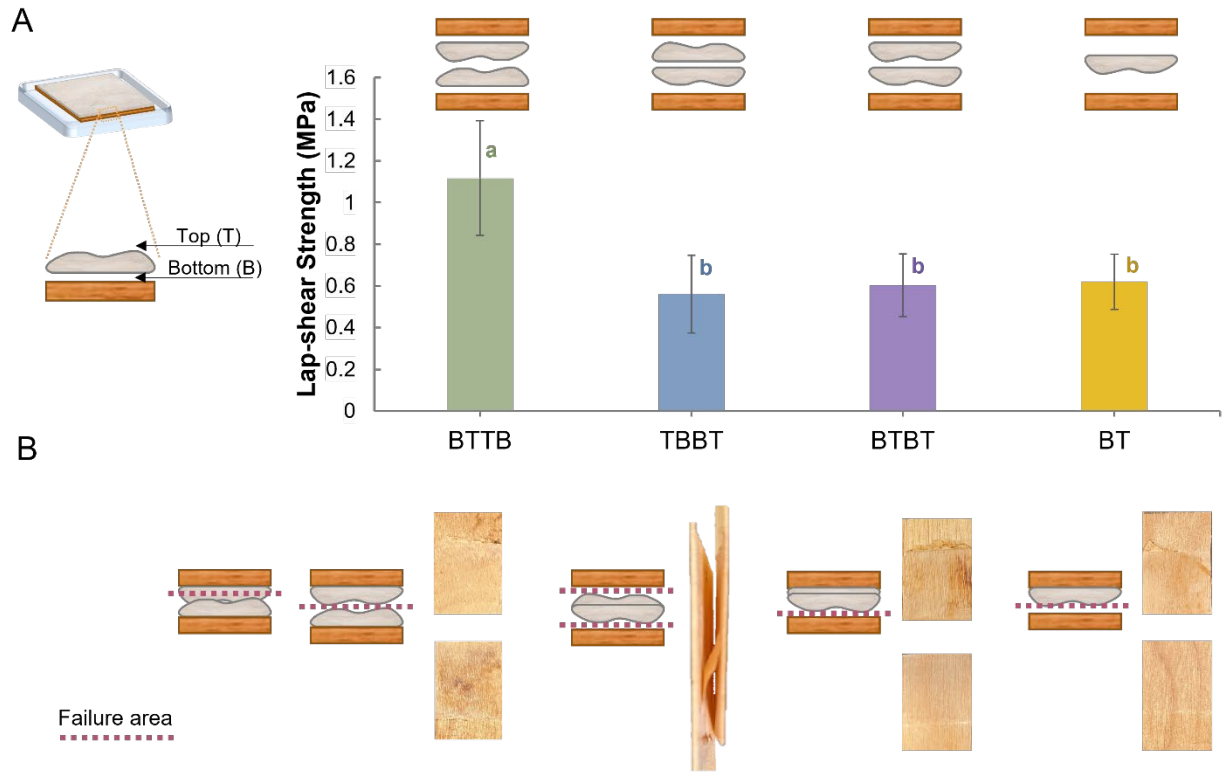

Figure 3.6. (A): Lap-shear strengths of the different surface contact of mycelium layers bonded undegraded veneers and the corresponding sketches, columns with common letters are not significantly different at 95% confidence level ($p > 0.05$). (B): Photos of the failure mode of each group and the corresponding sketches.

In view of the different behavior of the top and bottom surface of the removed surface mycelium layer, further characterizations were performed to compare them in detail. As shown in the stereomicroscopic images in Figure 3.7A and B, both the top and bottom surfaces show entangled filamentous structures but at very different scales. The top surface is fluffier with less visible hyphae in the EDF light microscopy image (Figure 3.7A), whereas the bottom surface is quite dense (Figure 3.7B). In higher magnification images taken by SEM, the individual hyphae on the top surface are distinguishable with a diameter of 2.0 ± 0.5 μm (Figure 3.7C). At the same time, the bottom surface shows a flat, sheet-like structure (Figure 3.7D). Under higher magnification, individual hyphae could be identified within the sheet-like structure (Figure 3.7E). Similar hyphal fusion and pseudo-laminar sheet formation of *T. versicolor* were reported in previous research (Jones et al., 2019).

When comparing the FTIR curves of the top and bottom surfaces of the mycelium layer, there are also distinct differences, which we believe indicate differences in chemical composition. The spectra of the bottom surface show a higher peak in the region of 3600 - 3000 cm^{-1}, which corresponds to the O-H and N-H stretching (Figure 3.7G). More differences are shown in the region between 1800 cm^{-1} and 600 cm^{-1}. The two main peaks at around 1640 cm^{-1} and 1545 cm^{-1} correspond to amide I (C=O stretch) and II (N-H bend and C-H stretch) vibrations in proteins (Lecellier et al., 2014; Naumann, 2009; Nooshkam & Madadlou, 2016), which showed much higher intensities for the bottom surface compared with the top surface. This indicates that there were probably more proteins that existed on the bottom surface. Notably, the peak at 1540 cm^{-1} was almost invisible on the spectra of the top surface but on the bottom surface, was intense and broad and had a shoulder at about 1530 cm^{-1}. The region from 1470 cm^{-1} to 1240 cm^{-1}, known as amide III band, is complex and affected by C-N from chitin and C-O from polysaccharides (Girometta et al., 2020). More peaks showed up in this region on the bottom surface than the top surface, providing more evidence to the hypothesis that more protein exists on the bottom. The absorbance between 1200 cm^{-1} and 960 cm^{-1} is attributed to polysaccharides in general (Girometta et al., 2020). The peak at 1073 cm^{-1}, probably due to the presence of O-substituted glucose residues (Duvnjak et al., 2016), is more intense in the spectra of the bottom surface; and the peaks at 970 cm^{-1}, 933 cm^{-1}, and 893 cm^{-1}, corresponding to C-C stretching in

molecular backbone (Girometta et al., 2020), only showed up in the spectra of the bottom surface, indicating that there are also more varieties of sugars exposed.

It should also be mentioned that as mycelium samples were dried directly without washing, the potentially remaining nutrition liquid (CSL) may also have contributed to the film-structure formation during the drying process. There are also some hyphae structures within the film-structure as shown in higher magnification in Figure 7F. Different from the hyphae from the top surface, there are more thread-like and tube-like structures, on the bottom (Haneef et al., 2017). The FTIR spectra of CSL is also included in Figure 7G. CSL contains a large variety of nutrients and is enriched with carbon, nitrogen and vitamins (Hofer et al., 2018; Xiao et al., 2012). The FTIR spectra of CSL showed very different peaks compared with either mycelium top or bottom surface. We believe that this evidence, and the general assumption that fungi consume CSL very quickly during colonization, means that IR spectra are not significantly affected by the CSL.

As shown in Figure 7H the bottom surface of the mycelium layer was more significantly hydrophilic (contact angle 79 ± 3°) compared with the top surface (contact angle 123 ± 5°). This explains why the bottom surface that was attached to wood interacted better with wood surfaces, which also have relatively high surface energy.

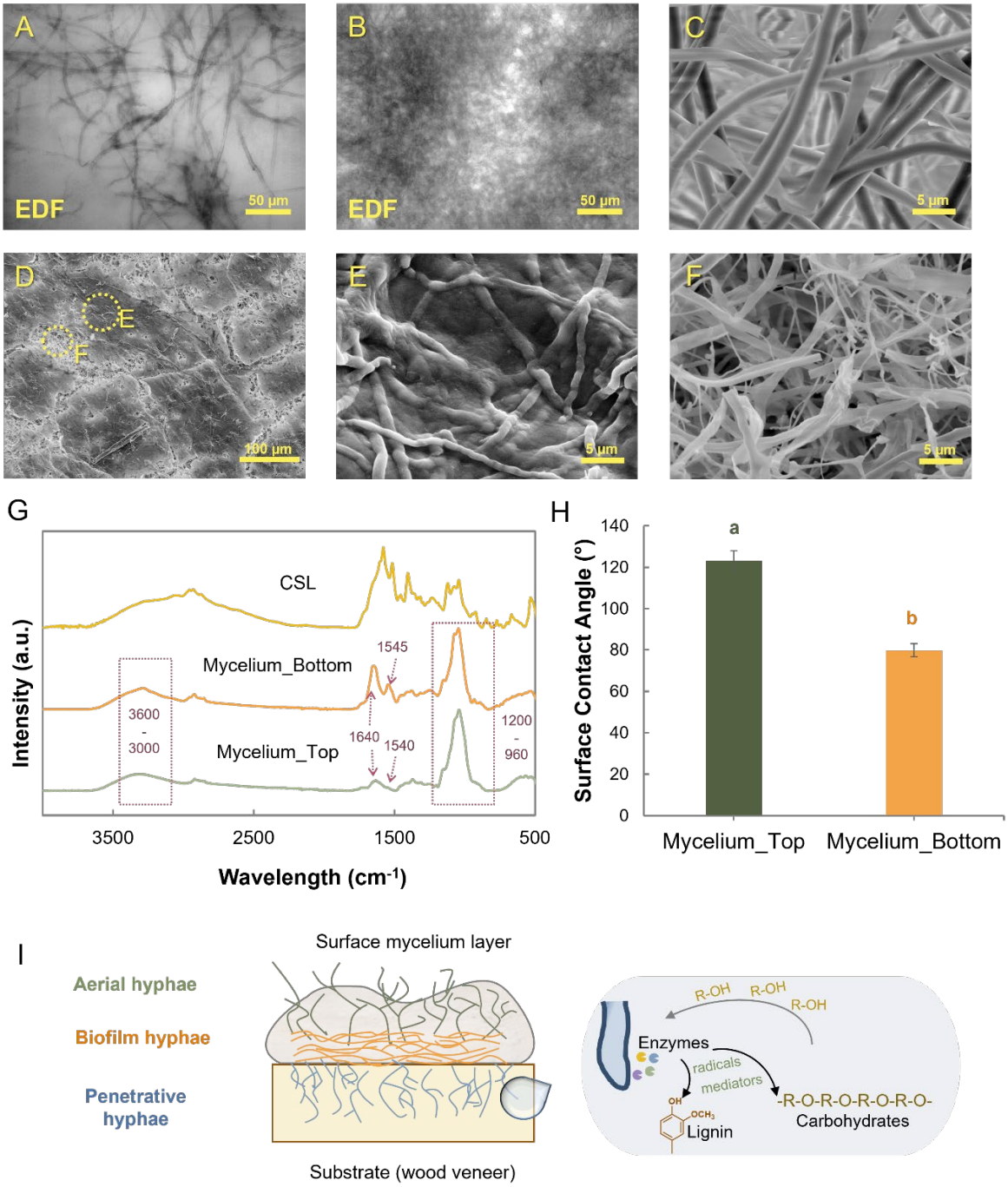

Figure 3.7. (A)(B): Extended focus Z-stacking images of the top (A) and bottom (B) surface; (C)(D)(E)(F): SEM images of the top (C) and bottom (D)(E)(F) surface; (G) ATR-FTIR spectra of CSL, top and bottom sides of surface mycelium; (H): Water contact angle of top and bottom sides of surface mycelium; (I): Schematic classification of hyphae and hyphal colonization of wood (gaining deep access through rays and branching through fibers).

According to Sugai-Guérios et al. (2015), there are three basic types of hyphae in the solid-state fermentation system: the aerial hyphae, the biofilm hyphae, and the penetrative hyphae as shown in the sketch in Figure 7I Sugai-Guérios et al. (2015). As there were no hyphae visible on the wood surface after removing the surface mycelium layer (Figure 3.4A), the bottom mycelium layer must include the biofilm hyphae. Therefore, the top and bottom surfaces reveal the properties of aerial and biofilm hyphae, respectively. The biofilm hyphae hold more moisture and are shown as densely packed structures whereas the aerial hyphae are directly in contact with the gas phase and hold air in their porous structure Sugai-Guérios et al. (2015). At the initial stages of white-rot fungal metabolism, enzymes are first released by the biofilm hyphae to the substrate through the diffusion medium, which is water. The enzymes secrete reactive oxygen species (ROS) and ROS precursors which react with wood components, and the degraded fragments such as monosaccharides are transported back to the hyphae through diffusion (Zabel & Morrell, 2020b) (Figure 3.7I). Therefore, when removing the surface mycelium layer, the secreted proteins and the fragments of degraded substrate components can remain on the bottom surface and contribute to bonding through diffusion, hydrogen bonding and potential covalent bonding after heat treatment. In addition, the surface itself is modified: lignin is depolymerized and free volume in the cell wall increased by component removal, potentially improving bonding by allowing more polymer interdiffusion and interaction at the surface (Bari et al., 2016; Herrera et al., 2015). The chemical difference between the top and bottom may also relate to the difference in the main component of hyphae at difference location (top and bottom), which could not be separated here.

Because the bonds always fail on the top side of the mycelium layer, the exact bond strength between the bottom surface of mycelium layer and veneer surface is not possible to measure in the current experimental set-up. It should be highlighted that although the adhesion ability of the top surface is weaker than the bottom surface, it is still a competitive candidate for wood bonding. We tested commercial wood glue for comparison, the lap-shear strength was 1.72 (±0.54) MPa, which showed no significant difference ($p > 0.05$) from the lap-shear strength of the sampled made with mycelium on degraded wood (Day 8) and slightly higher than the one formed with mycelium on untreated wood. Moreover, after water soaking, the

commercial wood glue-bonded samples completely fell apart, whereas although the mycelium adhesive also lost the majority of its strength (the lap-shear strength dropped to 0.27 ±0.10 MPa), the two pieces of wood held together. Thus, mycelium growth could be at the minimum a potentially efficient pretreatment method for producing all-natural bio-composites such as packaging materials, insulation board, particleboard and fiberboard. Moreover, as the surface layer of mycelium is very easy to remove and apply to untreated wood, they could also be considered as a novel stand-alone adhesive.

The mycelium used in the current research is directly produced from harvest with no grinding, extraction or combination with other crosslinkers. Multiple approaches could be followed to further improve its bonding strength and water resistance. For the wood pretreatment purpose, mixing the growing system continuously may stop the development of aerial hyphae, only biofilm hyphae would exist at the interfaces (Sugai-Guérios et al., 2015) and the adhesion could be improved. For the stand-alone adhesive purposes, surface mycelium could be produced in large-scale in bioreactors with more control of the nutrient supply and air flow (Bajoul Kakahi et al., 2019). As the mycelium composition and surface properties are highly influenced by the nutrient source, the attaching surface and the growing environment (Antinori et al., 2020; Haneef et al., 2017), it could be worthwhile to increase the active functional groups on the surface through controlling the substrate. Alternatively, very limited fungal species (36 according to Elsacker et. al (Elsacker et al., 2020)) have been investigated in mycelium-based composite production and they are restricted to Basidiomycota phylum because of their ability to grow large mycelium networks. However, in our current work, we discovered that the density and thickness of the surface mycelium layer is not crucial in bonding after hot-pressing. In this case, more species of fungi could be investigated with the purpose of finding a more active and functional interface.

3.4. Conclusions

The colonization of white-rot fungi *Trametes versicolor* on yellow birch veneers provided promising bonding on wood. The adhesion strength achieved was higher than that potentially caused by the physical or chemical changes of wood surface only. The best pretreatment time was found to be eight days; at this time the mycelium covered the entire surface with no apparent weight loss of wood and provided the

best bonding performance. Our results showed that the surface mycelium layer could also be utilized as a stand-alone adhesive to bond untreated wood. The bottom surface of the mycelium was found to be denser, flatter, more hydrophilic, and provided stronger bonding than the top surface. This work demonstrates the importance of surface mycelium interfaces in wood bonding and provides useful information for the development of bio-based materials, such as fungal-pretreated lignocellulosic bio-composites and novel mycelium-based adhesives.

CHAPTER 4

ADHESION CONTRIBUTIONS AT THE INTERFACE BETWEEN MYCELIA AND WOOD

4.1. Introduction

In **Chapter 3**, we demonstrated the importance of the mycelium-wood interface in the bonding of wood veneer. The mycelium-wood interface connects two surfaces, the bottom surface of mycelium and the top surface of wood veneer. The adhesion potential of the bottom surface of the mycelium layer can support the single mycelium layer to be a stand-alone adhesive to bond untreated wood. Meanwhile, the changed wood surface can also provide impressive bonding to the wood veneer themselves without any mycelia.

As briefly discussed in **Chapter 3**, the components located at the interface are thought to include the enzymes secreted by fungi, the degraded wood components such as monosaccharides, and depolymerized lignin. And they can contribute to the bonding of both wood and mycelium through diffusion, hydrogen bonding, and potential covalent bonding after heat treatment. However, those theories were not firmly confirmed, and there are also some remaining questions. When separating surface mycelium from wood veneer surface, how much of the "adhesion components" attach to the mycelium bottom surface and how much remain on the veneer surface, and how do they contribute to the bonding of stand-alone mycelium and stand-alone wood? What are the adhesion mechanisms involved in different systems, and what are their contributions? How does the change in the pressing temperature influence the bonding performance? And how stable is adhesion in wet conditions?

In **Chapter 4**, we aim to answer these questions by further investigating the adhesion mechanism of the mycelium-wood interface. We started by testing more of our three bonding systems: "degraded veneer without surface mycelium", "degraded veneer with surface mycelium", and "untreated veneer with surface mycelium". We investigated the effect of hot-pressing temperature on both the dry and wet lap-shear strength the wood veneer samples. We further examined the importance of water-soluble components in these systems by washing the separated veneer and mycelium by water and evaluating changes in their behavior. We also identified the chemicals that had been washed off from veneer and mycelium and the

changes in the surfaces. Finally, we could demonstrate a full description of the adhesion mechanism at the interface between mycelium and wood.

4.2. Experimental Section

4.2.1. Materials

Yellow birch (*Betula alleghaniensis* Britt.) wood veneers with a thickness of 0.61 (±0.04) mm were kindly supplied by Columbia Forest Products LLC (Presque Isle, ME). *Trametes versicolor* was supplied by Ecovative Design LLC (Green Island, NY) and had been maintained on agar plates at 4 °C and was pre-incubated on malt extract agar (MEA) plates before the incubation process.

4.2.2. Mycelium Incubation

The incubation methods were modified from the literature (Fackler, Schwanninger, et al., 2007). Yellow birch veneer samples with the dimensions of 80 mm (length) × 80 mm (width) were steam sterilized at 121 °C for 60 min and soaked for about five seconds in 2% (w/v) corn steep liquor (CSL) (Sigma-Aldrich, Saint Louis, MO) containing suspended fungal mycelium. One MEA plate overgrown by the fungus was mixed in 150 mL 2% (w/v) sterile CSL in a BagMixer (Interscience, St Nom, France) for 3 min before they were transferred to Petri dishes containing MEA. Plastic canvas meshes were used as supports in between the veneer and agar. The Petri dishes were incubated at 28 °C, 80% relative humidity (RH) for 15 days.

4.2.3. Hot-press and lap-shear samples preparation

After incubation, the wood veneers were cut into strips of 40 mm × 20 mm before hot pressing. The surface mycelium was either entirely removed or maintained in the bonding area (20 mm × 10 mm), or applied in between two undegraded strips in the same configuration as the original degraded samples. For the water-washed veneer and mycelium samples, the separated veneer and mycelium pieces were put in a bag filled with deionized water (100mL per piece). The sealed bags were taped on a plate shaker and were shaken at the full speed for 2h. The washed samples were directly used for hot-pressing and the supernatant was freeze-dried for further analysis. The lap-shear samples were hot-pressed for 5 min. Different hot-pressing temperatures (120, 160 and 180 °C) were applied to different groups. The pressure was controlled at 2.78 MPa. Slight densification of wood veneers under this pressure could be expected but

this was the lowest manageable pressure to apply using our hot press and it was kept constant for all experiments. To minimize the influences from other processing steps, the undegraded veneers were also autoclaved and saturated by water for 24 h before hot-pressing. The freeze-dried supernatant was diluted in water and applied to the wood veneers as a binder (50 wt.%, 10 mg cm^{-2} per glueline) for comparison.

4.2.4. Lap-shear strength test

The lap-shear tests were carried out on an Instron 5942 (Instron, Norwood, MA, USA) with a 500 N capacity load cell. The hot-pressed samples were conditioned at 23 ± 2°C and 50 ± 2% RH for 48 h (adequate to reach a constant mass). The crosshead speed was 0.5 mm/min, and the initial gauge length was 40 mm. Twelve replicates were tested for each group. Wet strength tests were carried out by soaking bonded samples in distilled water at room temperature 23 ±1°C for 48 h and testing immediately.

4.2.5. X-ray photoelectron spectroscopy (XPS)

The XPS analysis was conducted with a hemispherical energy analyzer (SPECS PHOIBOS HSA 3000 Plus). The X-ray radiation was induced by an aluminum anode. For each group, two replicates were measured.

4.2.6. FTIR

ATR–FTIR spectra of the surfaces were obtained using a Spectrum Two IR spectrometer (Perkin Elmer, Waltham, MA). All spectra were obtained in the range from 4000 to 600 cm^{-1} with 4 cm^{-1} resolution, accumulating 64 scans. The tested samples were all at room conditions. To ensure the reproducibility of the obtained spectra, three replicate specimens were measured.

4.2.7 Protein concentration

The protein concentration of freeze-dried supernatants was determined using a modified Lowry protein assay kit (Pierce Biotechnology, IL). The proteins were precipitated with acetone and redissolved in water to remove potential interfering substances.

4.2.8. NMR

Freeze-dried samples for NMR were prepared by dissolving about 30 mg samples in 0.65 mL DMSO-*d6* and were sonicated for 1h. ^{1}H NMR and ^{13}C NMR were obtained on a Bruker Avance NEO 500 MHz spectrometer. 512 scans were conducted for ^{1}H NMR and 2048 scans were conducted for ^{13}C NMR analysis.

4.3. Results and Discussion

4.3.1. Adhesion performance

Figure 4.1 shows the adhesion performance of the three major groups: "degraded veneer without surface mycelium" (D), "degraded veneer with surface mycelium" (DM), and "untreated veneer with surface mycelium" (UM) where the degradation times are all 15 days. Generally, the dry lap-shear strength (Figure 4.1A and C) followed the trend that we have shown in **Chapter 3**. The DM group showed the highest strength in all three temperatures examined. Group D and UM also showed competitive lap-shear strengths, which exhibited little or no difference with the group DM at 120 °C and 180 °C temperatures. There was no significant difference between the D and UM group in any of the three temperatures, indicating that stand-alone degraded veneer and stand-alone mycelium sheet had similar adhesion potential. However, they behaved very differently after water washing. As shown in Figure 4.1A and C, after water washing (WD group), the D group does not lose any of its dry lap-shear strength (Figure 4.1A); all three temperatures' results exhibit no significant difference compared to the unwashed group. As for the UM group however, after washing (WUM group), the surface mycelium layer lost most of its bonding strength for all three press temperatures examined. This indicates that the water-soluble components that had been washed off were essential for mycelium bonding but not necessary for wood bonding.

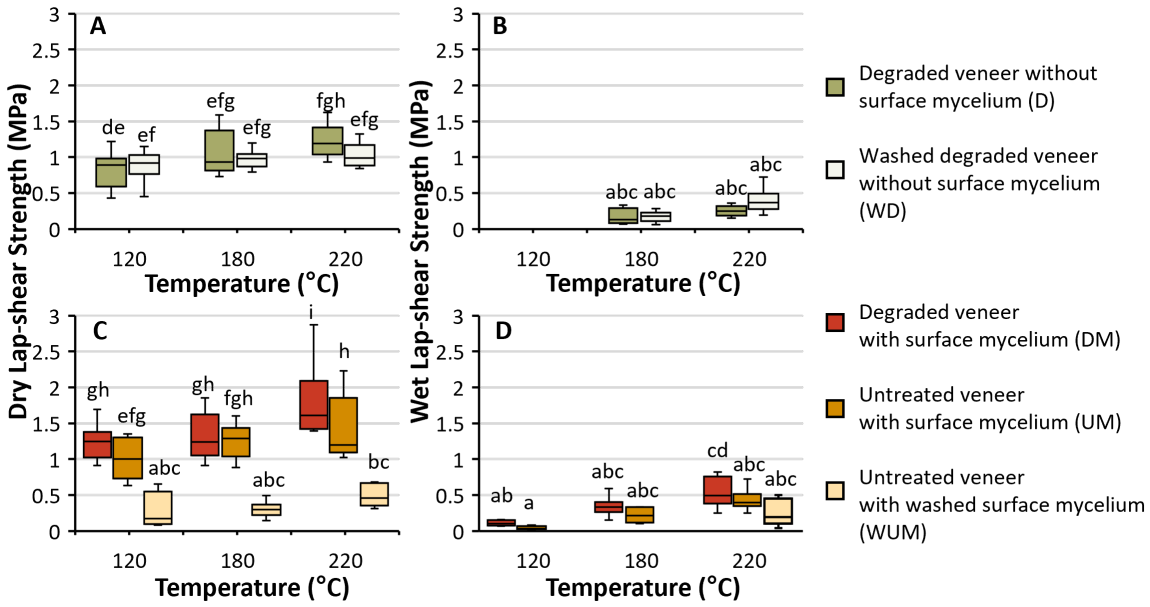

Figure 4.1. Lap-shear strengths of different samples after different temperature hot-pressing tested under variable conditions. (A) unwashed and washed degraded veneer, dry strength; (B) unwashed and washed degraded veneer, wet strength; (C) degraded veneer with surface mycelium, untreated veneer with unwashed or washed surface mycelium, dry strength; (D) degraded veneer with surface mycelium, untreated veneer with unwashed or washed surface mycelium, wet strength.

Figure 4.1 B and D show the wet lap-shear strength of different groups after being soaked in water for 48h. Water-resistance properties are essential for exterior applications and can provide useful information on the adhesion mechanism. As expected, all the groups lost more than 70% of their lap-shear bonding strength. For 120 °C pressed D and WD groups, all the samples delaminated after soaking in water for 48 h, therefore no data could be obtained. There was no significant difference on the strength value between 180 °C and 220 °C pressed WD groups and they were all lower than 0.5 MPa (Figure 4.1B). The wet lap-shear strength of the DM and UM groups behaved similarly, only DM group that was pressed at 220 °C showed a value significantly higher than the other groups (0.54 MPa) (Figure 4.1 D).

From a practical point of view, it seems that there is no need to apply a higher temperature for better bonding. As for all three systems, only increasing the hot-pressing temperature from 120 °C to 220 °C

could achieve some but still very little improvement in the lap-shear strength. And the wet strength for all the temperatures was very low which will limit the applications for the products that purely based on these bonding systems. These observations are different from what we summarised in **Chapter 2**, Table 2.1 and Figure 2.4, where higher temperature generally showed higher MOR values for the composites system. However, none of the studies listed in **Chapter 2** compared the temperature in the same experimental set-up, the trend might just be caused by other experiment factors such as the composite type, the pressure and time used, or substrate species.

As for the adhesion mechanism examination, the weak wet strength indicates that there are not enough covalent bonds in the adhesion system. The bonding may come from water-sensitive hydrogen bonds and Van der Waals interactions (Gardner et al., 2014). Increasing the pressing temperature may degrade more surface components to small molecules and accelerate the softening and flowing of them to improve the diffusion and mechanical interlocking (Hubbe et al., 2017) but this was not very efficient in our experimental set-up.

4.3.2. Wood veneer analysis

In this section, we investigated the change of veneer surface after degradation, washing and different temperature treatments, to further explain what we found in Section 4.3.1 and reveal the adhesion mechanisms.

Figure 4.2 shows the physical changes of wood veneer fungal degradation. Thickness compression after hot-pressing decreased for the degraded samples, indicating that the undegraded samples were more softened and the wood cell walls collapsed more under temperature and pressure. This suggests that the mechanical interlocking is not the main contributor for the increase of bonding of veneers after fungal degradation as in that case, a higher compression would have been expected.

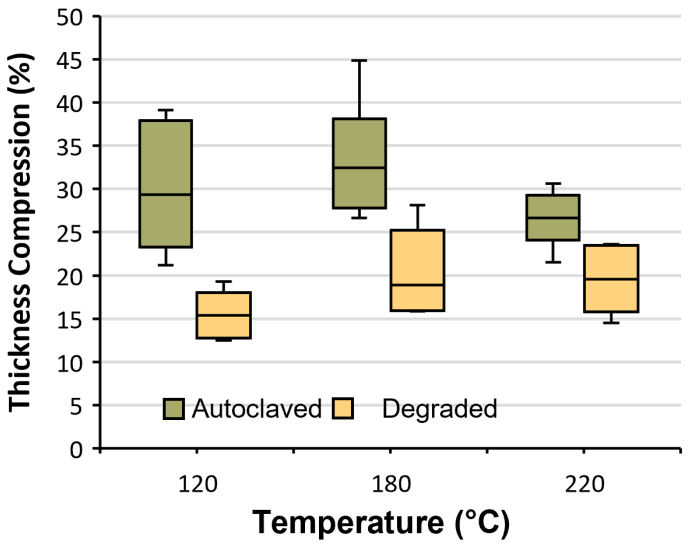

Figure 4.2. Thickness compression of veneers after compression at different temperatures

The chemical changes of the veneer surfaces are shown in Figure 4.3. The fingerprint area of FTIR spectra (Figure 4.3A) shows no major changes after degradation and washing, indicating that the chemical components remained similar on the surface or could not be detected using FTIR. With the increasing hot-press temperature, the two peaks at 1594 cm^{-1} and 1640 cm^{-1}, representing the aromatic rings of lignin, became closer and merged together at 220 °C. This may be attributed to the increase in relative lignin content attributable to the degradation of hemicellulose (Belleville et al., 2013). Differently, the peaks between 1460 and 1470 cm^{-1}, attributed to aliphatic CH bending of lignin, were separated into two peaks after heat treatment. This may reveal the lignin changes as a result of condensation and/or formation of CH_2 bridges between lignin fragments (Belleville et al., 2013). The peak at 1250 cm^{-1} was also increased in intensity and separated into two peaks, indicating new linkages on the asymmetric C-O-C stretching band for lignin (Delmotte et al., 2008). The appearance of the peak at 781 cm^{-1} also reveals the production of new unknown compounds after high temperature treatment (Rana et al., 2009).

XPS was also applied on the veneer surfaces after different treatments (Figure 4.3BCD) to study the surface chemistry changes. As shown in Figure 4.3B and C, the relative O/C and N/C ratios were increased after degradation and decreased after hot-pressing. The increase after degradation indicates the

oxidation of veneer surface and the secreted proteins from fungi (Xu et al., 2013). The decrease of O/C ratio with the heating temperature (Figure 4.3B) could be attributed to hemicellulose degradation and lignin rearrangement during the heat treatment as the O/C ratio of hemicellulose is much higher than that of lignin (Wang et al., 2015). Figure 4.3C shows the percentage of different carbon types. Carbon I corresponds to carbon atoms bonded only by carbon or hydrogen atoms (C-H, or C-C); Carbon II corresponds to carbon atoms bonded to one single non-carbonyl oxygen atom (C-O); and Carbon III peak corresponds to carbon atoms bonded to a carbonyl or two non-carbonyl oxygen atoms (C=O or O-C-O) (Sinn et al., 2001; Wang et al., 2015). The degradation of wood veneer caused the decrease of Carbon I and the increase of Carbon III (Figure 4.3C), confirming the oxidation caused by fungal degradation. Carbon I further decreased after heat treatment, which may be attributed to the reactions of fragmentation and oxidation because of the high temperature. The increase of Carbon II at 200 °C may due to the degradation of amorphous polysaccharides and the general increase of Carbon II is due to the formation of carbonyl structures (Belleville et al., 2018).

FTIR and XPS spectra differences between different groups suggested chemical transformations occurred on wood surface and the formation of new chemical bonds after the degradation by hot-pressing, which may contribute to the bonding.

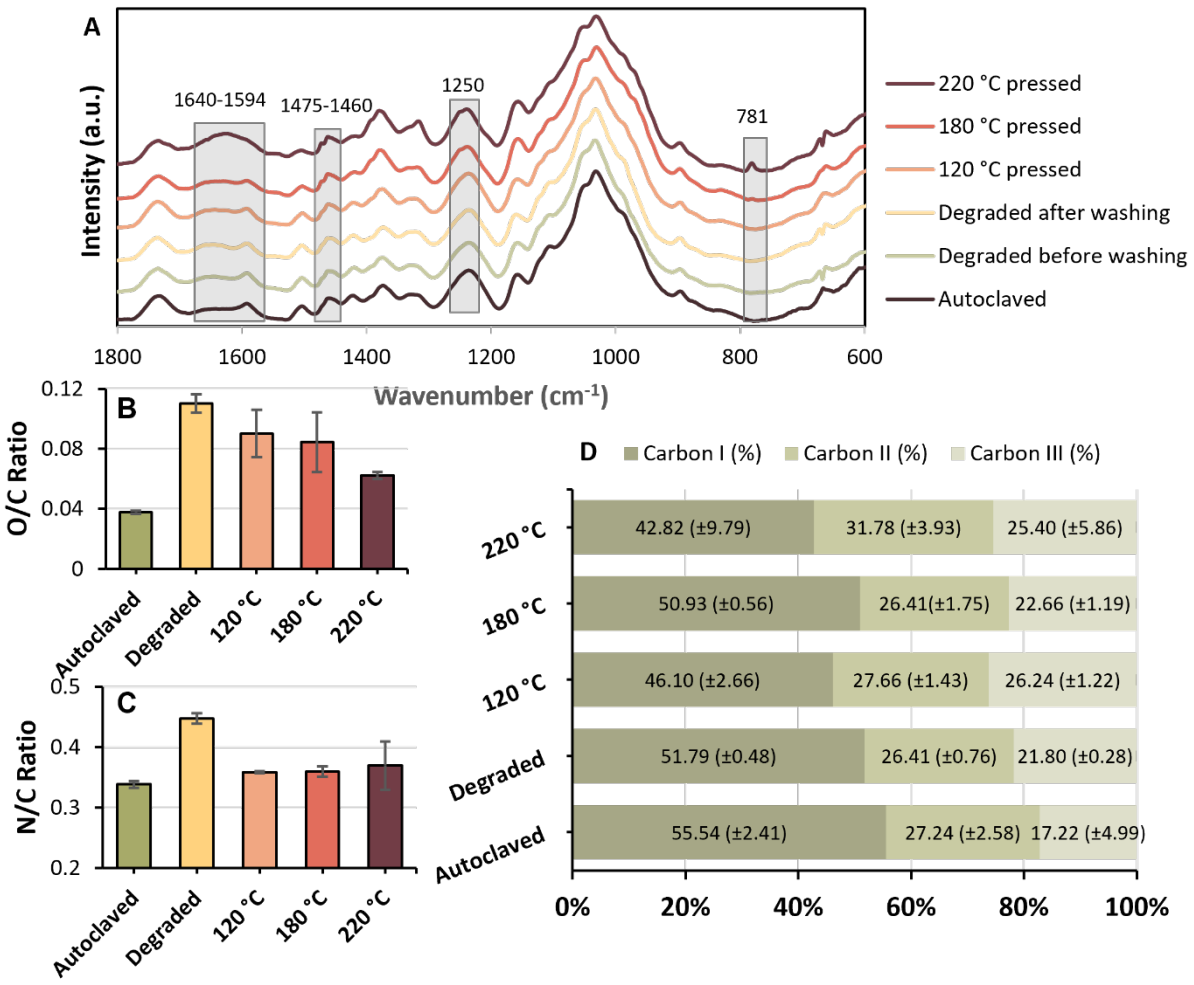

Figure 4.3. Chemical changes of wood veneers after degradation, washing and hot-pressing. (A) Thickness compression of veneers after compression at different temperature; (B) FTIR; (C) O/C ratio; (D) N/C ratio; (E) Carbon I, II, III ratios.

4.3.3. Supernatant analysis

One interesting observation in Section 4.3.2 was that the water-soluble components washed off from the surface mycelium layer played an essential role in bonding untreated wood veneers. In this section, we further explore their chemistry and potential bonding mechanisms. Figure 4.4A shows the dry lap-shear strength of autoclaved wood veneers bonded with supernatants and hot-pressed at 120 °C. When using degraded veneer supernatant (Figure 4.4A) to bond untreated veneer, the obtained lap-shear strength is similar to the strength of bonded unwashed and washed degraded veneers (Figure 4.1A). The typical FTIR

peaks at 1730, 1604, 1509, 1381, and 1250 cm^{-1}, indicate veneer surface compositions including hemicellulose and lignin fractions (Figure 4.4B). Differently, the mycelium supernatant showed a much higher lap-shear bonding strength (Figure 4.4A), 2.22 MPa. It is significantly higher than the values of all groups pressed at 120 °C (Figure 4.1A and C) and confirms the importance of water-soluble components in the bonding system of surface mycelium layer. It is worth to be mentioned that the components that had been washed off were not only located at the bottom surface of mycelium, but also at any thickness level of the mycelium sheet. In Chapter 3, we already showed that the top surface of the mycelium layer provides less bonding strength than the bottom surface, we could attribute this positive influence to the bottom and other locations of the mycelium. The FTIR curve of mycelium supernatant (Figure 4.4B) shows similar peaks to veneer supernatant with some differences. The missing peak at 1730 cm^{-1} which correspond to the carbonyl group, indicates that the degraded xylan fractions majorly remained in the wood veneers. The peak at around 1620 cm^{-1} (amide I: C=O, C-N) is broader and there are two more peaks appearing at 1545 cm^{-1} (amide II: C-N, C-H) and 1317 cm^{-1} (amide III: CO-NH) compared with the veneer supernatant, which indicates that more protein exists in the mycelium supernatant. The protein concentration shown in Figure 4.4C confirms this observation, where mycelium supernatant had 7% more protein concentration than wood supernatant.

After heat treatment, there are no significant changes in the FTIR curve of the veneer supernatant, as shown in Figure 4.4B, whereas the mycelium supernatant shows some changes. The mycelium supernatant shows a broad peak at the region around 1620 cm^{-1}, which corresponds to amide II of the proteins. After heat treatment, it downshifts to the wavelength of 1610 cm^{-1} as a sharp peak, which along with the increased intensity of amide III peak at 1317 cm^{-1} may indicate protein denaturation and conformation change due to heat treatment (Ioannou & Varotsis, 2017). There is also some evidence of Maillard related reactions between proteins and carbohydrates after heat treatment of the mycelium supernatant. The newly appeared peak at 1660 cm^{-1} has been assigned to the C=N stretching vibration, indicating Schiff's base products (Pérez et al., 2010; Zha et al., 2019). The appearance of an additional frequency shoulder at 1715 cm^{-1}, corresponding to a carbonyl (C=O) group, may originate from the

Amadori products (glycated residues) (Ioannou, 2017). The features between 1360 and 1460 cm^{-1} are broader after heat treatment, probably corresponding to C-N=C bond of imine (Ioannou, 2017; Zhao et al., 2020).

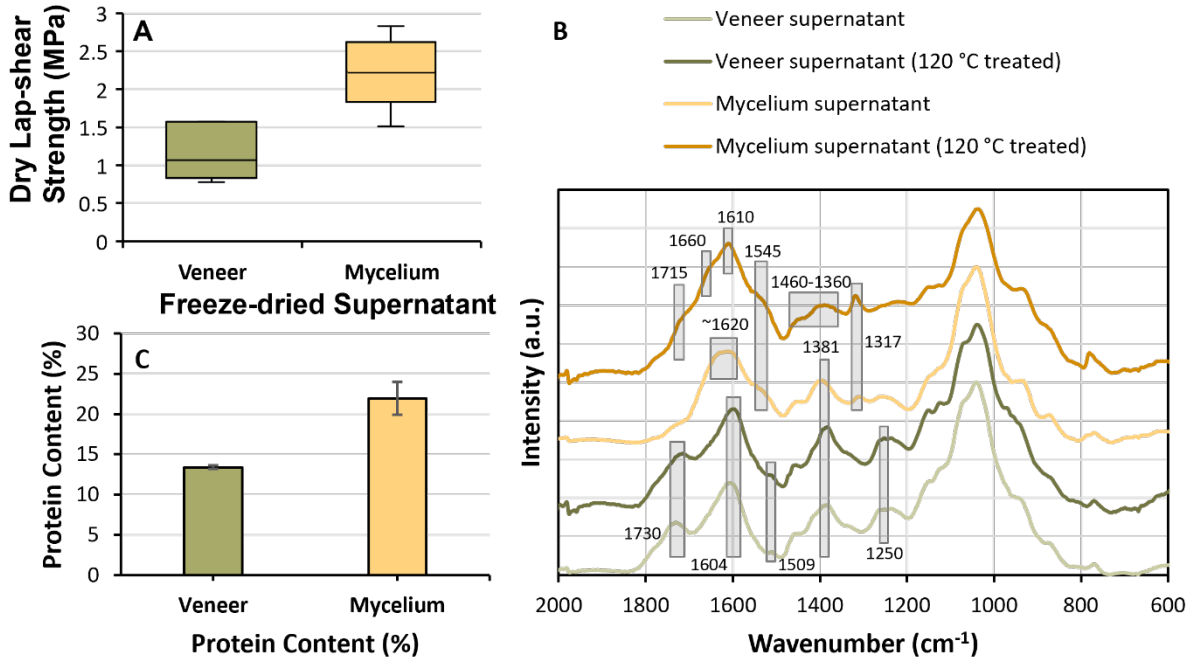

Figure 4.4. Performance and characterization of freeze-dried supernatants from veneer and mycelium: (A) Dry lap-shear strength; (B) FTIR; (C) protein content.

To further confirm the results from FTIR analysis, we also performed ^{1}H NMR and ^{13}C NMR on the freeze-dried mycelium supernatant before and after heat treatment (Figure 4.5). As shown in the ^{1}H NMR spectra (Figure 4.5A), the signals corresponding to reducing ends at 4.3 and 4.9 ppm (Chen et al., 2017; Vachoud et al., 2001) disappear after heat-treatment, indicating the complete substitution of reducing ends of carbohydrates. The new signal at 8.2 ppm corresponding to HC=N (Pramod et al., 2015), appearing in ^{1}H NMR spectra after heat treatment, provides evidence for the formation of Schiff's base. In the ^{13}C NMR spectra shown in Figure 4.5B, the peak at 202.4 and 93.7 ppm, corresponding to C=O in ketones and C1 of sugar reducing residue (Gorshkova et al., 1993; Li et al., 2016; Peleg et al., 1989), disappears after heat treatment, confirming the substitution of reducing ends.

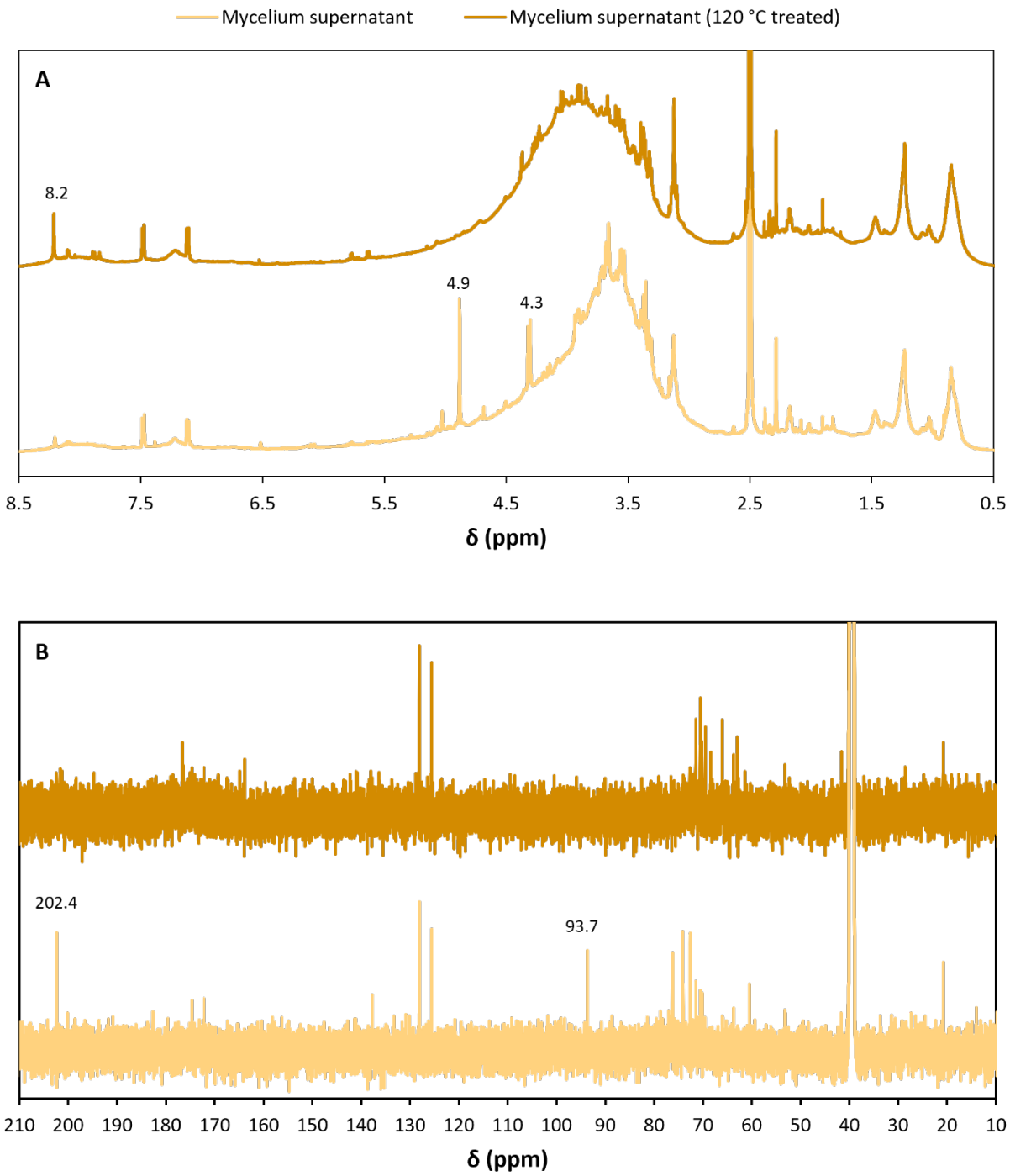

Figure 4.5. NMR spectra of freeze-dried supernatants before and after heat treatment: (A) ^{1}H NMR; (B) ^{13}C NMR

4.4. Conclusions

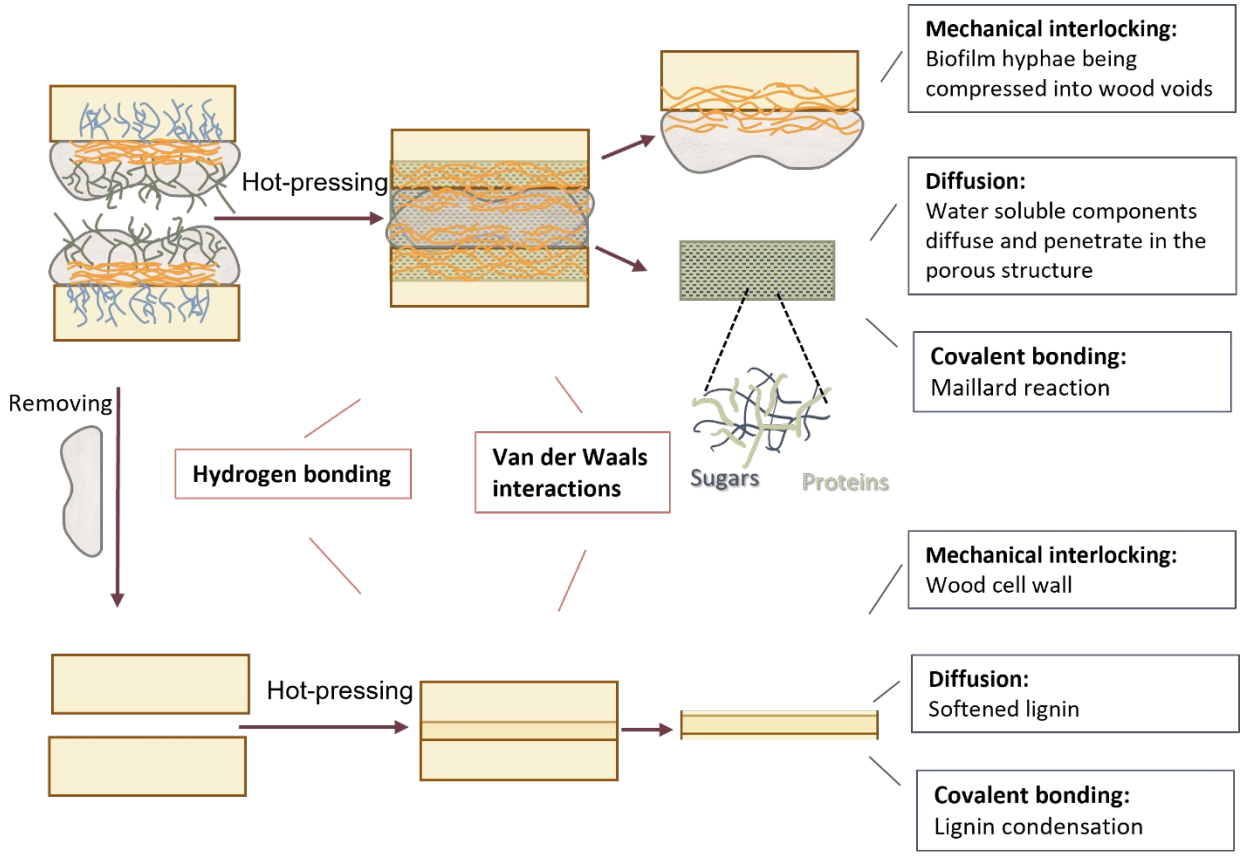

Figure 4.6. Schematic figure showing adhesion mechanism involved in wood-wood bonding and wood-mycelium bonding in view of current adhesion theories

Both the stand-alone degraded wood veneer and surface mycelium can provide similar bonding after hot-pressing at different temperatures. A temperature of 120 °C during pressing is sufficient as higher pressing temperatures only provide very limited adhesion improvement. The essential adhesion factor for mycelium bonding is the water-soluble components which contain both carbohydrates and proteins. Both wood-wood bonding and wood-mycelium bonding include some mechanical interlocking, diffusion and covalent bonds as shown in detail in Figure 4.6. However, the low wet strength in both system reveals that the major bonding mechanism is hydrogen bonds and Van der Waals interactions due to the redistribution of surface components.

CHAPTER 5

FUNCTIONALITY OF MYCELIUM IN COMPOSITE SYSTEMS

5.1. Introduction

Chapters 3 and 4 investigated the adhesion mechanism of fungal-pretreated wood at the surface and interface level, respectively. The functionality of the surface mycelium and the interface elements were well defined separately. However, when it comes to the composite system, the system becomes more complicated and there might be more factors involved, which could affect the performance of the whole bio-composite. This complexity also causes difficulty in examining and linking the product properties to the essential components and the structure of the system.

As the main component of the hybrid system, the lignocellulosic biomass defines the majority of the properties. However, as an "additive" to the system, filamentous fungi possess multiple identities. Their colonization binds the individual substrate elements together. Meanwhile, they also modify the chemical and physical nature of the biomass by digesting their components. Their own physical body, known as mycelium, also distributes throughout the system, which could be considered an additional type of substrate (Carlile, 1995; Lew, 2011).

Our review of available literature shows that despite efforts to understand the contribution of mycelium and lignocellulosic substrate materials on the structure and properties of both the foam and panel-like composite systems, a systematic evaluation to elucidate governing factors is currently missing. Thus, in this Chapter, we aimed to understand further the principles that determine the performance for both as-grown mycelium-based foams and hot-pressed panels. To achieve this, we first evaluated this dynamically changing system in detail by focusing on one substrate and one fungal species. Then, we monitored the physical and chemical structure of the composites by incubating fungi for different periods. Finally, by testing and comparing the essential properties of these composites, we attempted to link the changing system to its changing properties and establish a principle regarding their performance in different applications.

5.2. Experimental Section

5.2.1. Materials

Yellow birch (*Betula alleghaniensis* Britt.) wood veneers with a thickness of 0.62 (±0.04) mm were kindly supplied by Columbia Forest Products LLC (Presque Isle, ME). *Trametes versicolor* was supplied by Ecovative Design LLC (Green Island, NY) and had been maintained on agar plates at 4 °C and was preincubated (28 °C, 80% relative humidity (RH)) on malt extract agar (MEA) plates before the incubation process.

5.2.2. Mycelium incubation

Wood veneers were ground into particles and sieved to a size between 0.5 to 2.0 mm. A sample of 225g wood particles was poured into a filter patch bag and steam-sterilized at 121 °C for 60 min. One MEA plate of a 7-day preincubated fungal mycelium was mixed in 300 mL of 2% (w/v) sterile corn steep liquor (CSL) (Sigma-Aldrich, Saint Louis, MO) in a BagMixer (Interscience, St Nom, France) for 3 min after which the materials were transferred to the filter bag and were mixed with wood particles. The filter bags were incubated at 28 °C, 80% RH for 8 days, then the mixture was transferred to a stand mixer with a paddle mixing blade and was mixed at speed 2 (KitchenAid, Benton Harbor, MI, approximately 60 rpm) for 2 min. After mixing, the mixture was separated and packed in square Petri dishes (80 mm × 80 mm × 14 mm) 50 g (dry weight: 19.8 (±1.3) g) per dish. The Petri dishes were incubated at 28 °C, 80% RH for up to 30 days.

5.2.3. Post-processing process

After specific incubation periods, half of samples were oven-dried for 48 h at 50 °C to produce as-grown foams. The other half of the samples were hot-pressed (Carver, INC., Wabash, IN) at 180 °C for 8 min with a thickness control of 4 mm to produce high-density panels. The foams and panels were cut into different sizes using a laser cutter (Full Spectrum Laser LLC, NV) for further analyses. For chemical analysis, part of the foam samples was also milled into fine powders using a coffee grinder.

5.2.4. Density and porosity

The bulk density (ρ_b) of the composites was determined by measuring the mass of the samples conditioned at 20 °C and 50%RH divided by their geometric volume. The nominal size of the samples was 25 mm × 25 mm × 13 mm for the foams and 25 mm × 25 mm × 4 mm for the panels. Six replicates were used in each group.

The true density (ρ_t) of the composites was measured with an AccuPyc II pyconometer (Micromeritics, GA) after drying the samples at 103 °C for 24 h. The porosity value was calculated using the following equation:

$$\text{Porosity} = \left(1 - \frac{\rho_b}{\rho_t}\right) \times 100 \qquad (1)$$

5.2.5. ATR-FTIR

ATR–FTIR spectra of the surfaces were obtained using a Spectrum Two IR spectrometer (Perkin Elmer, Waltham, MA, USA). All spectra were obtained in the range from 4000 to 600 cm^{-1} with 4 cm^{-1} resolution, accumulating 64 scans. The tested samples were all in room condition. To ensure the reproducibility of the obtained spectra, three replicate specimens were measured.

5.2.6. TGA

Thermal stability evaluation was carried out under nitrogen gas on a TGA Q500 (TA Instruments, New Castle, DE) with a high resolution (Hi-Res) option from room temperature to 600 °C in nitrogen atmosphere. In the Hi-Res approach, the heating rate is dynamically and continuously modified, ranging from 0.001 °C min-1 to the maximum heating rate (20 °C min-1) in response to changes in the decomposition rate of the sample. The resolution and sensitivity settings were 4.0 and 1.0 °C, respectively. The TGA results are shown as the variation of the sample mass (TG) and as a derivative weight loss (DTG) curve corresponding to the temperature.

5.2.7. Stereomicroscopy

Bright-field images were captured using a Nikon Ni-E (Nikon Instruments Inc., Melville, NY) stereomicroscope with Nikon Plan Fluor 4×/0.13 objective lens. The interior surfaces of both foams and

panels were observed by the microscope. The foams were broken to expose the interior surface, and for the panels, failure areas were examined after the internal bonding strength tests were done. Z-stack images were acquired at 30 µm intervals from top to 1500 µm and processed using the extended depth of field (EDF) plugin in the NIS-Elements software.

5.2.8. Moisture/water uptake and thickness swelling

The moisture and water uptake and thickness swelling of the different composites were measured according to ASTM D1037-12 with modifications. For moisture uptake, the samples were conditioned in a humidity chamber at 20 (±2) °C and 50 (±2) % RH or 80 (±2) % RH. For water uptake and thickness swelling analysis, the samples were immersed in distilled water in room temperature (20 (±1) °C) and the weights and thicknesses were measured after 2h, 24h, 48h, and 96h. The moisture/water uptake and thickness swelling values were determined from the weight or thickness difference in relation to initial weight or thickness. The dimensions of the samples were 25 mm × 25 mm × 13 mm for the foams and 25 mm × 25 mm × 4 mm for the panels. Twelve replicates were used in each group.

5.2.9. Mechanical properties

For the foams, the compressive strength was measured according to ASTM C165-17 (ASTM, 2017a). For the panels, the modulus of rupture (MOR), the modulus of elasticity (MOE) and the internal bond strength (IB) were determined according to ASTM D1037-12 (ASTM, 2012). All mechanical tests were performed with an Instron 5942 universal testing machine (Instron, Norwood, MA) with a 500 N load cell capacity. For the compression testing, foam samples measuring 25 mm × 25 mm × 13 mm were used. Each piece was compressed up to 40% deformation at a rate of 1mm min^{-1}. For shape-recovery measurements, after the samples were compressed to 40%, the load was released, and the thickness recovery was measured immediately and after 24h. For the three-point bending test, the panel samples measuring 25 mm × 80 mm × 4 mm were tested using a span of 70 mm and a cross-head speed of 3 mm min^{-1}. For the internal bonding strength tests, the 20 mm diameter circular specimens were used, and the cross-head speed was 0.4 mm min^{-1}. Between 12 and 18 replicates were tested in each group. All samples were conditioned at 20 (±2) °C and 50 (±2) % RH before the mechanical analysis.

5.2.10. Thermal conductivity

The thermal conductivity of the foams was measured using a TA Fox 50 heat flow meter (TA Instruments, New Castle, DE) according to ASTM C518-17 (ASTM, 2017b). The tests were conducted at temperature gradients of 10 °C to 30 °C and 20 °C to 40 °C where the reported result was the average of the two gradients. Six replicates were tested for each group. All samples were conditioned at 20 (±2) °C and 50 (±2) % RH before the thermal conductivity measurement.

5.2.11. Acoustic properties

The sound absorption measurements were conducted using an impedance tube BSWA-III-C021-03-0027-IMP (BSWA Technology, Beijing, China) according to ASTM E1050-19 (ASTM, 2019). Foam samples with a diameter of 30 mm were tested in triplicates. The sound absorption coefficients were reported covering the frequency range from 1000 to 6000 Hz.

5.2.12. Statistical analysis

The obtained testing values were analyzed using a one-way analysis of variance (ANOVA) to determine statistical differences among the means. A Tukey's honestly significant difference (HSD) multiple comparison test was then performed to further assess the significance level of the mean values for each treatment level. All comparisons were made at 95% confidence level. All the analyses were performed using RStudio (Version 1.2.5033).

5.3. Results and Discussion

5.3.1. Growth of mycelia on the substrate

The development of fungal mycelium in between the substrate particles is shown in the series of photos in Figure 5.1A. The white mycelium tissue is easy to distinguish from the brownish wood particles. The growth of fungal hyphae gradually expanded within the wood particles and by Day 12 was uniformly distributed. From Day 12 to Day 18, the aerial mycelium grew thicker and denser and revealed more white color on the surface. There was no apparent visual difference between Day 18, Day 24, and Day 30. Unlike the significant difference in hyphae density between the core and the surface of the final composite reported by other research groups (Jones, Bhat, Kandare, et al., 2018; Shakir et al., 2020), in our growing system,

the substrate was fully packed and attached to the Petri dish, and the size of the particles was relatively large to ensure minimal oxygen availability difference between the surface and the core. The cross-section picture shown in Figure 5.2 reveals that the growth of mycelium was uniform across the whole composite, and the photo of the surface can represent the whole structure.

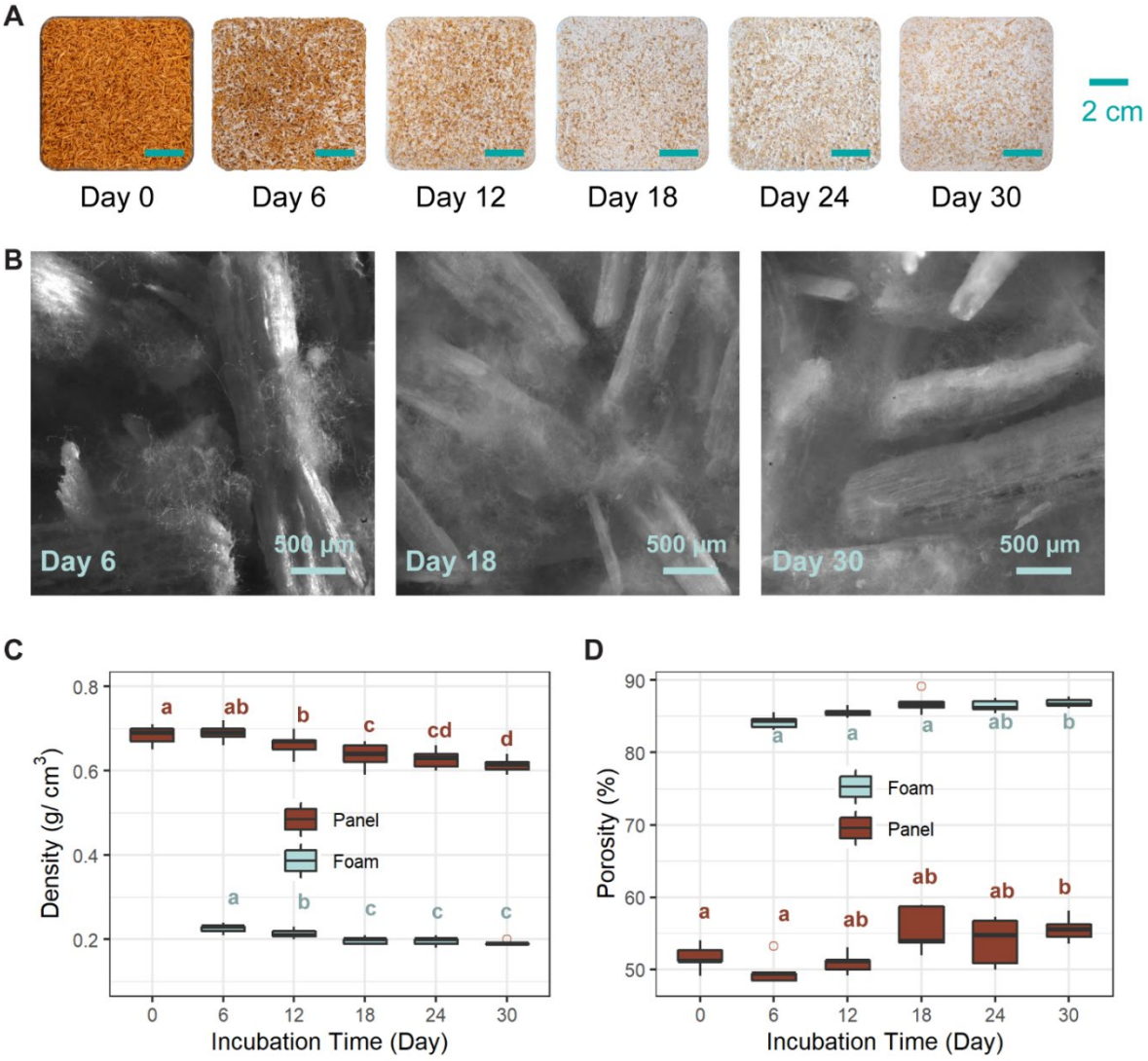

Figure 5.1. Changes in the appearance and properties of the incubation system after different incubation times: (A) development of fungal mycelium in the substrate; (B) EDF images of the internal surfaces of as-grown foam; (C) density changes of as-grown foams and compressed panels; (D) porosity change of as-grown foams and compressed panels. Within each group, common letters indicate no significant difference at 95% confidence level.

Figure 5.2. Cross section figure of Fresh Day 18 Composites.

Figure 5.1C and D show the changes of density and porosity of the direct oven-dried foam and hot-pressed panels. The density of both foams and panels generally decreased with the continuous colonization of fungi. However, there was no significant difference among Day 18, 24, and 30, which corresponded well with the visual changes in Figure 5.1A. While colonizing the substrate, fungi utilize the substrate as a food source and gain energy from the respiration of organic compounds (Zabel & Morrell, 2020b). Therefore, the unchanged density after Day 18 directly relates to the unchanged weight as the difference among the volumetric shrinkage of samples incubated for different days was negligible (data not shown).

Two factors influence the weight change of the composite. The loss of the substrate and the increase of fungal mycelium body. To further reveal the fungal behavior at different growing days, we compared the chemical features of the composite using ATR-FTIR and TGA analysis. Figure 5.2A shows the FTIR curves of samples after different degradation days. It is clear that the changing trend of peaks continues throughout 30 days. The curves were normalized by the highest peak at 1032 cm^{-1}, corresponding to the C-O stretching in cellulose I and cellulose II (Belleville et al., 2013). Under this normalization, the peaks at 1504, 1319, 1231 cm^{-1}, corresponding to C=C stretching of the aromatic ring (S), CH_2 wagging in cellulose I and cellulose II, and C-O stretching in lignin and xylan (Bari et al., 2020), respectively, decreased over the incubation days. The consistent trend indicates that the degradation is still going on from Day 18 to Day 30. The ratio of the intensity of lignin-associated bands with carbohydrate bands is presented in Table 5.1.

The decreasing ratio indicates the selective nature of the fungus at this early stage of degradation as lignin was removed more than the structural carbohydrates. The decrease in the lignin/carbohydrate ratio is less for the 1722 cm^{-1} band when compared to other carbohydrate bands, indicating that the fungus preferably decayed the hemicellulose fraction over cellulose (Mohebby, 2005; Pandey & Pitman, 2003).

Table 5.1. The ratio of the intensity of lignin associated band 1504 cm^{-1} to carbohydrate bands for the composite degraded by *T.versicolor* for different days.

Group	**Reference Peaks (cm^{-1})**			
	1504/1722	1504/1369	1504/1156	1504/896
Control	0.64 (0.02)	0.57 (0.02)	0.41 (0.03)	0.58 (0.08)
Day 0	0.80 (0.05)	0.60 (0.01)	0.43 (0.01)	0.65 (0.08)
Day 6	0.63 (0.03)	0.43 (0.03)	0.30 (0.04)	0.59 (0.12)
Day 12	0.63 (0.03)	0.37 (0.02)	0.27 (0.01)	0.70 (0.25)
Day 18	0.62 (0.02)	0.35 (0.07)	0.25 (0.04)	0.60 (0.14)
Day 24	0.61 (0.01)	0.35 (0.01)	0.24 (0.01)	0.54 (0.09)
Day 30	0.60 (0.03)	0.35 (0.01)	0.24 (0.02)	0.54 (0.11)

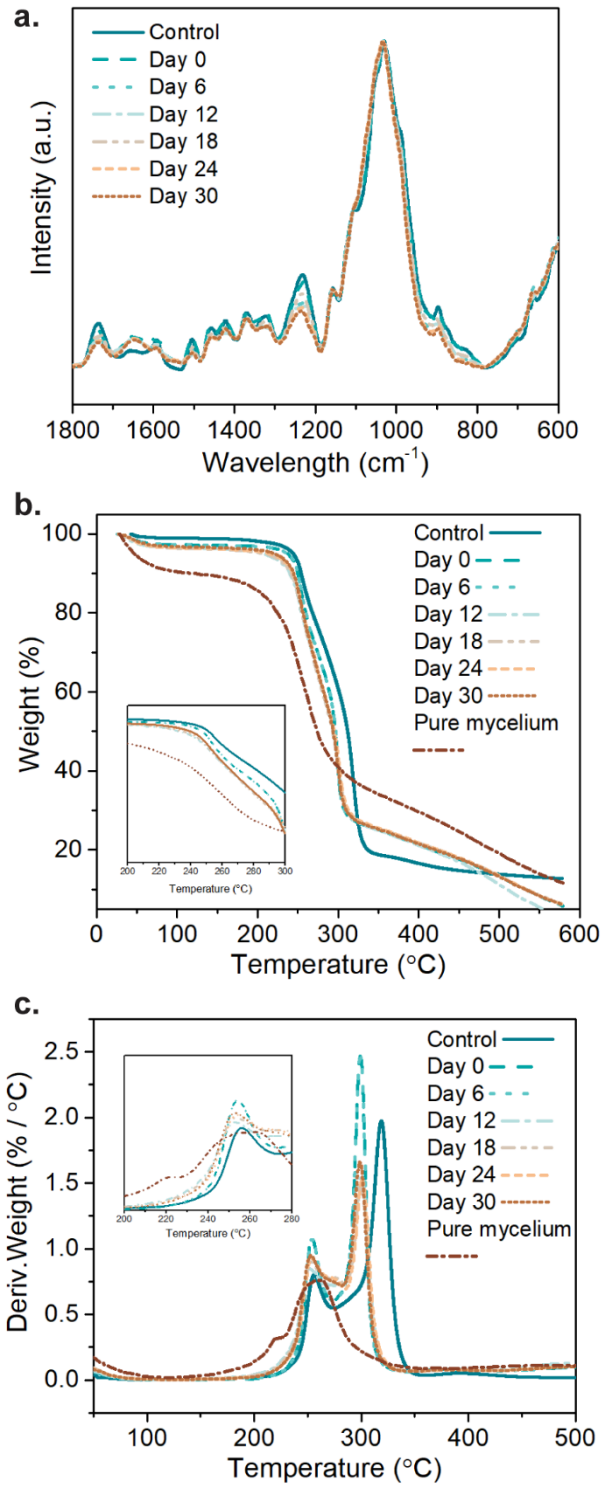

Figure 5.3. Chemical changes of the composite after different growing days as determined from: (A) FTIR; (B) TG and (C) DTG

Figure 5.3B and 5.3C show the TG and DTG curves of the samples after different incubation days using Hi-Res approach to better separate overlapped peaks (Sun et al., 2019). Undegraded wood had the highest thermal stability with the highest onset temperature (220 °C). The two peaks regarding maximum degradation appeared at 256.3 and 318.5 °C (Table 5.2), respectively. As fungi degraded wood components into smaller molecules, the thermal stability decreased correspondingly. Day 0 and Day 6 samples showed almost identical TG and DTG curves with lower onset and peak temperatures. Starting from Day 12, the peaks continued to shift to lower temperatures and became broader, and a third peak appeared at about 270 °C. The additional peak might have come from the further degraded wood components and the added fungal mycelium. As the pure mycelium showed the lowest thermal stability, it started to degrade at 153.3 °C and had three peaks at 220.2, 245.5, and 263.7, respectively. The results from TGA analysis revealed a similar trend to the observations found in Figure 5.1. It appears that the colonization of fungi separated the composites into two major groups; Day 0 and 6 showed similar physical and chemical features; where Day 18, 24, and 30 were grouped together. Day 12 was more like a transition state between the two groups.

Table 5.2. Onset and peak temperatures of thermal degradation of composites from DTG data (Figure 5.3C).

Group	**[a]T_{on} (°C)**	**[b]T_{P1} (°C)**	**[b]T_{P2} (°C)**	**[b]T_{P3} (°C)**
Control	217.8	256.2	N/A	318.5
Day 0	217.0	254.5	N/A	299.3
Day 6	213.5	253.8	N/A	298.6
Day 12	183.0	251.9	N/A	300.6
Day 18	180.4	252.5	257.2	299.4
Day 24	177.0	254.0	272.0	301.0
Day 30	170.0	253.5	272.5	299.0
Pure mycelium	153.3	220.2	245.5	263.7

[a]The onset temperature T_{on} was estimated by the intersection of the tangent lines.
[b]The degradation temperature T_{P1}, T_{P2} and T_{P3} refer to the different peak temperatures observed on the DTG curves and are related to the different thermal degradation steps for each material.

5.3.2. Essential properties of as-grown foams

As-grown mycelium-lignocellulosic foams were specifically developed for packaging, thermal insulation, and acoustic absorption applications in most recent studies, some important mechanical and physical properties related to these foams are shown in Figures 5.4 and 5.5.

The generic stress-strain response (Figure 5.4A) of the as-grown composite foams under uniaxial compression revealed that at less than about 10% strain, the stress-strain curve showed a linear behavior, where the stress increased linearly with deformation. After 20% strain, the stress-strain curve showed a gradual stiffening and further a rapid stiffening response. This behavior is similar to what Islam et al. reported for mycelium-agriculture waste composites (Islam et al., 2018). When comparing the compressive modulus obtained in the linear region (Figure 5.4B), even though the mycelium matrix significantly increased based on the observations in Figure 5.1A and 5.1B, there was no significant difference between the different growing days in terms of stiffness. According to Islam et al. , the linear region is primarily controlled by the mycelium matrix (Islam et al., 2018), which could not explain the phenomenon revealed in our setup. The possible explanation is that the linear region of the wood particles overlaps with that of the mycelium. Therefore, the amount of mycelium does not influence the compressive modulus of the system. Similarly, there was no significant difference in compressive strength at 10% and 25% strain (Figure 5.4C). Although the density of the composites decreased at longer incubation days, the compressive modulus and strength remained unchanged. The thickness of the foam recovered more than 80% immediately after load release and could reach 90% after 24h for samples incubated more than 12 days after 40% strain compression (Figure 5.4D).

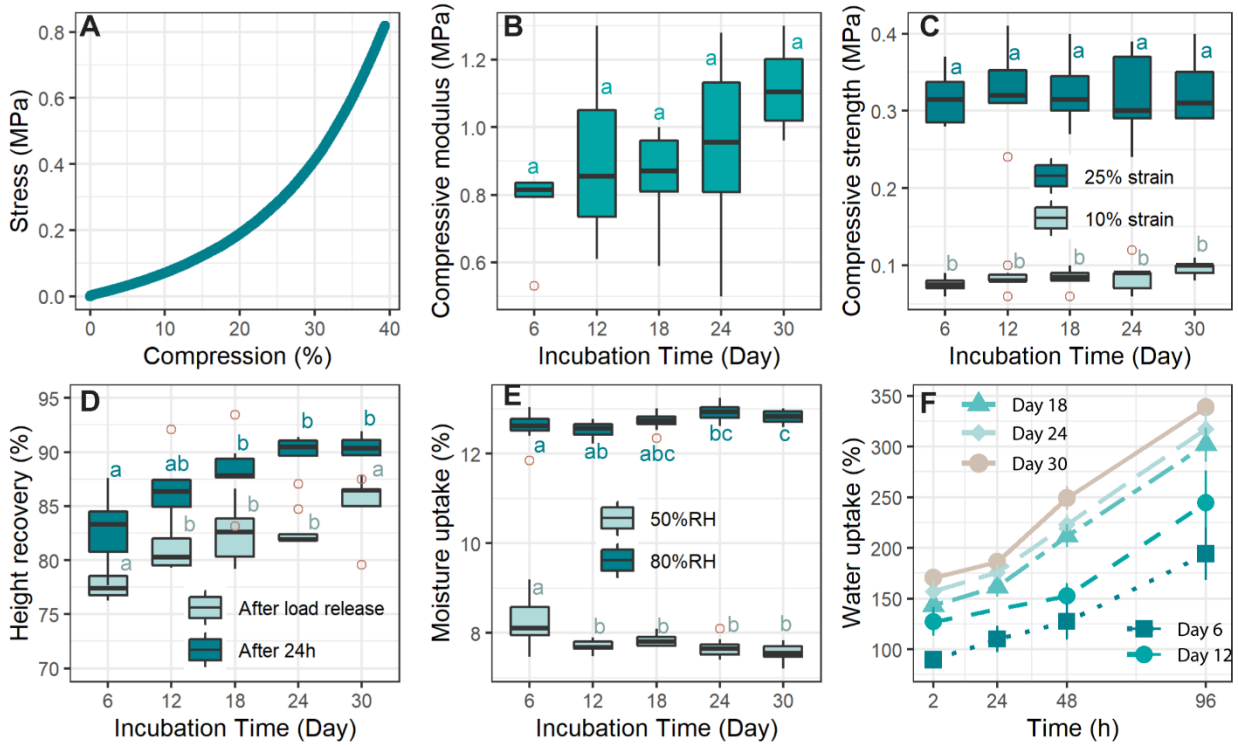

Figure 5.4. Essential properties of as-grown composite foams: (A) representative stress-strain curve; (B) compressive modulus taken from the elastic region (< 5% strain); (C) compressive strength at 10% and 25% strain (D) percentage of thickness recovery after compression immediately and after 24h; (E) moisture absorption after conditioning at 50% RH and 80%RH; (F) water uptake.

The degradation by the fungi can also cause changes in the equilibrium moisture content at some degradation stage, which may cause changes in the other properties and bring about deterioration issues. The moisture uptake values of the foams generally showed small or no significant changes among different groups (Figure 5.4E). Considering the mycelium continued to develop throughout the growing period, their influences needed to be considered. As listed in Table 5.3, the moisture uptake of pure mycelium was 11.5 (± 1.2) % at 50% RH and 19.5 (± 2.3%) at 80% RH, which was higher than corresponding values for the as-grown foams. This may be compensated by the selective removal of wood components at the early stages of decay. Differently, when fully immersed in water, more water can be retained in the structure after longer incubation days (Figure 5.4F). One reason for the increase in water uptake is the increase in porosity, which allows more water to occupy the porous structure. Most of the fungi initially penetrate through the

pits. The removal of the pit membrane also accelerates the movement of fluids (Zabel & Morrell, 2020a). Moreover, the increasing mass of the mycelium matrix occupied more space in between the particles, retaining more water in the structure attributable to capillary forces (Tuller et al., 1999).

Table 5.3. Properties of pure mycelium.

Property	**Value (SD)**
Density (g cm^{-3})	0.04 (0.01)
Porosity (%)	97.3 (1.3)
Moisture uptake at 50%RH (%)	11.5 (1.4)
Moisture uptake at 80%RH (%)	19.5 (2.3)

Figure 5.5a shows that the thermal conductivity of the foam composites decreased with the longer incubation days. It is reasonable, as for porous materials, thermal conductivity correlates strongly with the material density. The lower the density, the higher quantity of dry air, which has an extremely low thermal conductivity and corresponds to the lower thermal conductivity of the foam. The 30 days of degradation only caused a density reduction of about 10% and a thermal conductivity deduction of less than 10%, indicates that fungal degradation is not an efficient approach to achieve composites with low thermal conductivity. It is more efficient to choose a substrate with naturally low thermal conductivity or modify the construction method to lower the density of the foam structure.

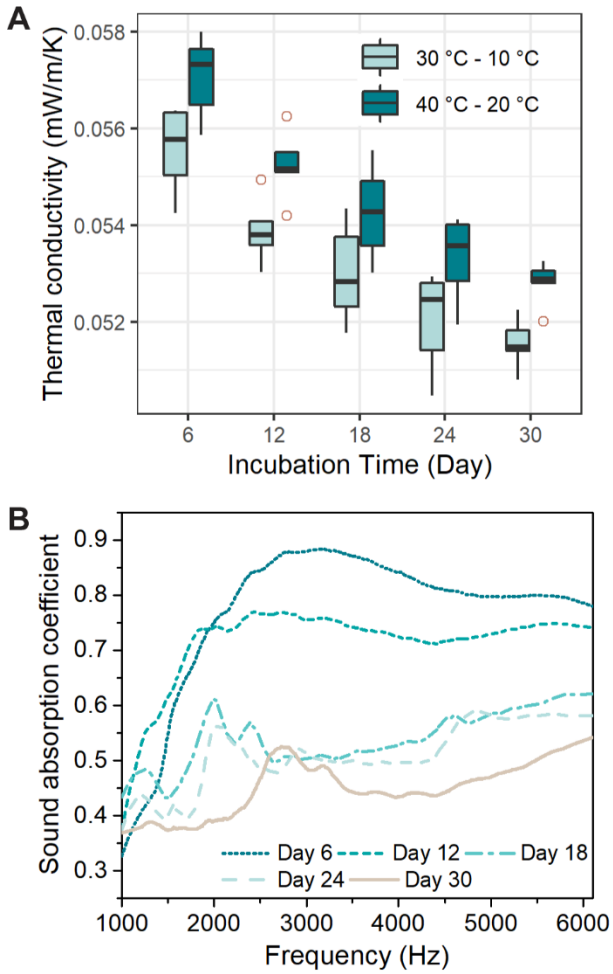

Figure 5.5. Thermal conductivity and sound absorption properties of as-grown foams: (A) thermal conductivity; (B) sound absorption coefficient.

Figure 4b shows the sound absorption coefficient of the composites after different incubation days at the range of 1000 – 6000 Hz. For all samples, the highest peak values of the curves were all above 0.5. Interestingly, the sample that experienced the lowest incubation time showed the best sound absorption property. It can be observed that the sound absorption coefficient increased with the frequency of the sound. The maximum absorption coefficient was found to be 0.87 for the sound frequency of 2800 Hz, then the values reduced with the frequency but were all above 0.8. With the increase of incubation time, the sound absorption property deceased. The Day 12 sample showed a similar trend as Day 6 sample with a lower peak (0.76). Day 18, 24, and 30 samples showed a much lower coefficient in the majority of the frequencies

above 1500 Hz. The highest values were 0.61, 0.56, and 0.53, respectively. Multiple small peaks also appeared at different regions that were different from Day 6 and Day 12, which only had one major peak. From Figure 5.1C and D, the density of Day 18, 24, and 30 samples were smaller than Day 0 and Day 6 samples, and the porosity values were opposite; properties that are beneficial for sound absorption.

The contradicting sound absorption coefficient results may have been caused by the structural changes at the microscopic level, such as tortuosity, airflow resistivity, viscous, and thermal characteristic lengths (Yang et al., 2020). At the beginning of the incubation, when the mycelium did not fully colonize the large spaces in between wood particles, the larger pores can provide more air vibration in the sample. The growth of mycelium narrowed down the air channels at the inter-particle scale and consequently reduced the pore diameter gradient and mean pore size and thus caused a lower air viscosity ramp during the movement of sound energy (Basu et al., 2021). At the same time, it has been previously found that both mycelium bonded composites and pure mycelium foams showed improvement of sound absorption at lower frequency range (Pelletier et al., 2013; Pelletier et al., 2019). We also found a similar trend in Day 12, 18, and 24 samples, but it was combined with the massive reduction of sound absorption property at a higher frequency range. To achieve a higher sound absorption coverage at all frequencies, one approach could be a hybrid system composed of different materials.

5.3.3. Essential properties of hot-pressed panels

The essential physical and mechanical properties of hot-pressed panels made from wood particles and mycelium are shown in Figure 5.6. Both MOR and MOE reveal a similar trend (Figure 5.6A and 5.6B). The Day 0 sample showed very low values; Day 6 and Day 12 samples showed improved MOR and MOE around 3 MPa and 700 MPa, respectively; Day 18 samples achieved a higher value of MOR and MOE of about 5 MPa and 900 MPa. Further incubation did not cause further improvement in the mechanical properties. The degradation does not cause any negative effect either. This trend is not as obvious in the IB test results. The IB value is consistent from Day 6 to Day 30, around 3 MPa. According to ANSI A208.1-2016 standard (ANSI, 2016b), half of our processed particleboards (Day 18, 24, and 30) fall into low-density range (< 0.64 g cm^{-3}). As shown in Figure 5.6 (add value line in the figure), their mechanical

properties are incredibly higher than the standard value and also very close to the standard value for medium-density particleboard. With a slight increase of density or other processes such as adding face and back layers, they offer a great potential to be utilized in medium-density panels for specific applications such as furniture and construction.

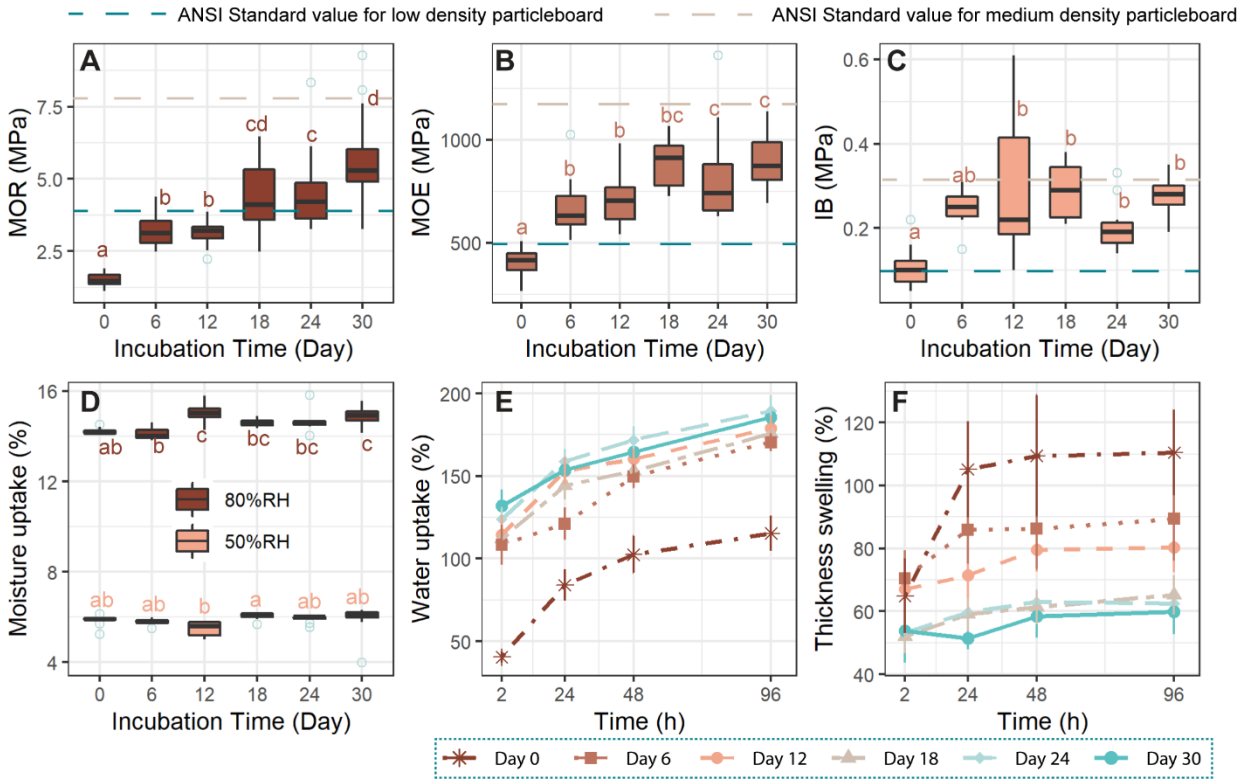

Figure 5.6. Essential properties of hot-pressed composite panels: (A) MOR; (B) MOE; (C) IB; (D) moisture absorption after conditioning at 50% RH and 80%RH; (E) water uptake; (F) thickness swelling.

Moisture absorption, water uptake, and thickness swelling properties of the panels are shown in Figure 5.6 D, E, and F. Similar to the foams, the moisture absorption values remained relatively unchanged among different groups, but with more mycelium growing, more water was absorbed in the panels. The hot-pressing process compressed the panels and closed up space for water to penetrate resulting in less water uptake for the panels than the foams at the same testing point. The thickness swelling values of the panels show an opposite trend, the longer growing days, the lower thickness swelling. This confirms better

bonding after hot-pressing; as the particles moved closer to each other after pressing, they did not move away much when water was absorbed.

Theoretically, mycelium incubation can reduce the wood quality and density. White-rot can cause 13-14% and 4% loss on MOR and MOE of hardwood, respectively, when there was only 2% weight loss (Wilcox, 1978). Interestingly, the decreased wood quality and density did not cause negative effects in the mechanical properties of the panels. The improvement of inter-particle adhesion may compensate the quality change of wood and the reduction of wood particle density can improve bonding by providing a higher compaction ratio. The broken surface of the panels after IB test are shown in Figure 5.7. On Day 0 (Figure 5.7A), when there was almost no mycelium growing, the surface texture of the wood particles is clear, and there were a lot of unoccupied spaces in between the individual wood particles. With the mycelium growing, more and more voids were filled up with entangled mycelium (Figure 5.7B, C, D). The mycelium fully covered the interface on Day 18 (Figure 5.7E) so that the texture of the wood surface can be barely seen. The microscopy images correspond well with the mechanical property results, showing that fungal hyphae worked as a filler and positively affected the system; the connected mycelium network also may provide support for the system. Meanwhile, our previous work on the functionality of surface mycelium on wood bonding has shown that the chemical components (fungal biofilm and degraded small molecules of wood components) located at the mycelium and wood substrate interface are one of the critical factors for the degraded wood and surface mycelium bonding system (Sun et al., 2020). This mechanism may also be a factor in the composite system and provide inter-particle bonding.

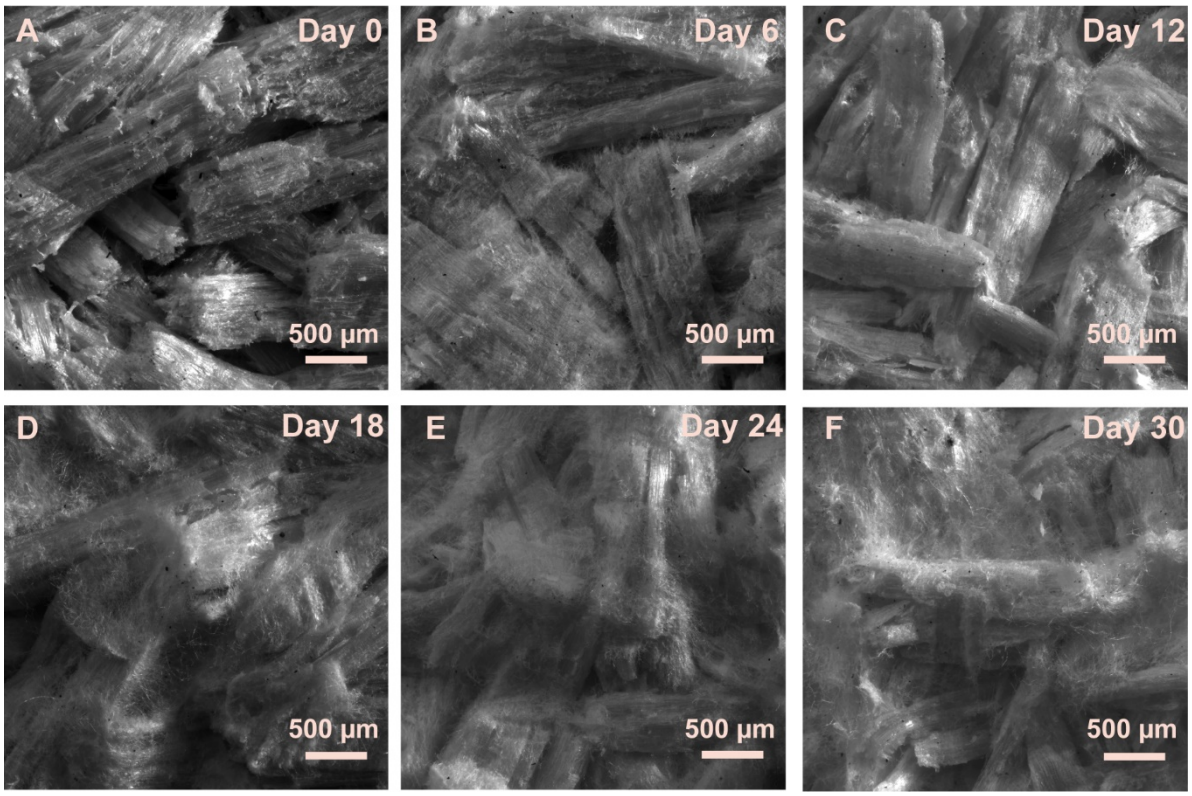

Figure 5.7. EDF images of the internal surfaces of hot-pressed panels after IB test (A) Day 0; (B) Day 6; (C) Day 12; (D) Day 18; (E) Day 24; (F) Day 30.

To confirm the reinforcing functionality of the mycelium network and the bonding chemistry at the mycelium-wood interface, we used Day 18 samples and designed the following tests. In this experiment, we used a mixer to break up the mycelium network before packing the Petri dishes. We used oven drying to "pre-cure" the potential interface adhesives. After mixing, we reassembled the particles in the same Petri dish; with the difference that the 3D mycelium structure was disrupted. Water was added to the pre-dried materials to ensure the samples have the same moisture content before hot-pressing as the as-grown samples. Figure 5.8A and B shows the MOR and MOE values of the four groups. The mechanical properties decreased both after mixing and after pre-drying. The mixing step destroyed the connections between the wood particles through the mycelium so that the voids in between wood particles showed up again (Figure 5.8A, B). The drying process inactivated the adhesive chemicals located at the interface between wood and mycelium. Although the "dried" group maintained the mycelium connections, its MOR and MOE still

decreased to a similar level as the "fresh mixed" group (Figure 5.8A, B). For the group ("Dried mixed) that suffered both mixing and drying process, the mechanical properties were the lowest. These observations confirm the contribution of these two essential factors. It is also worth mentioning that, although the mechanical properties of "fresh mixed" and "dried" groups were significantly lower than the "fresh" group, they are still much higher than the ANSI standard value (ANSI, 2016b). Multiple starting materials can be processed in specific ways to reach different application requirements.

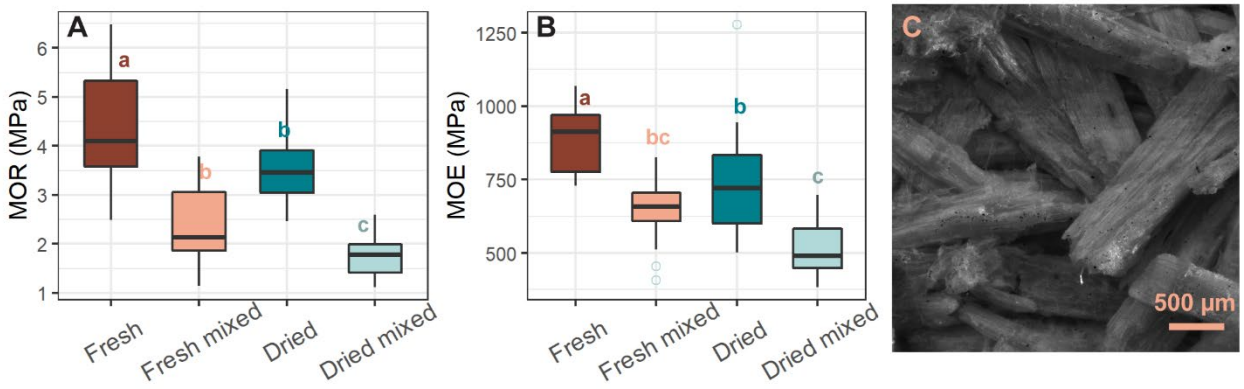

Figure 5.8. Essential properties of Day 18 hot-pressed panels with several pretreatments before hot-pressing: (A) MOR; (B) MOE; (C) EDF image of the internal surfaces of hot-pressed panels after IB test: Day 18 "Fresh mixed" group.

5.4. Conclusions

In the bio-composite structure, the fungal mycelia behave differently in different composite forms. For low-density as-grown foam structures, fungal mycelium only worked as a binder, the lignocellulosic substrate material played an essential role in sound absorption and thermal insulation properties, and the denser mycelium structure had a negative effect on them. In a higher-density hot-pressed panel system, fungal mycelium contributed to bonding, also reinforced the bio-composite by filling the gaps. For future mycelium-lignocellulosic based bio-composite development, it can be recommended to design and produce the materials through monitoring the substrates, growing time, and processing method tailored for their required applications.

CHAPTER 6

IMPROVEMENT STRATEGIES: INCORPORATION OF CELLULOSE NANOFIBRILS

6.1. Introduction

Apart from fungal mycelium, cellulose nanofibrils (CNF) have been demonstrated as a binder in conventional and novel composite systems most recently. CNF has extremely high surface area and can bond wood particles and fibers through hydrogen bonding and mechanical interlocking, providing structural integrity to the composites (Amini et al., 2017; Arévalo & Peijs, 2016; Leng et al., 2017; Tajvidi et al., 2016; Theng et al., 2015).

In **Chapter 6**, we introduce a panel system that incorporates wood particles treated with fungus where additional bonding is provided by CNF. We aimed to investigate the physical properties of a 100% bio-based particleboard-like hybrid composite by combining the binding capacity of CNF and mycelium together. The adhesion mechanism of mycelium bonding was also further confirmed by testing two material systems as shown in Figure 6.1. In Group 1, pure mycelium was grown in nutrient substrate and was mixed with pure wood particles after thermal inactivation. The mixture was used as basic material for hybrid composite manufacturing. In Group 2, the mycelium was directly grown on wood particles and the partially decayed wood particles were inactivated as well and then used as basic material for the other set of experiments. The production procedures were simple forming, cold-pressing, and hot-pressing. The morphology of the materials, the physical and mechanical properties of composites with different material combinations, and densities were also investigated.

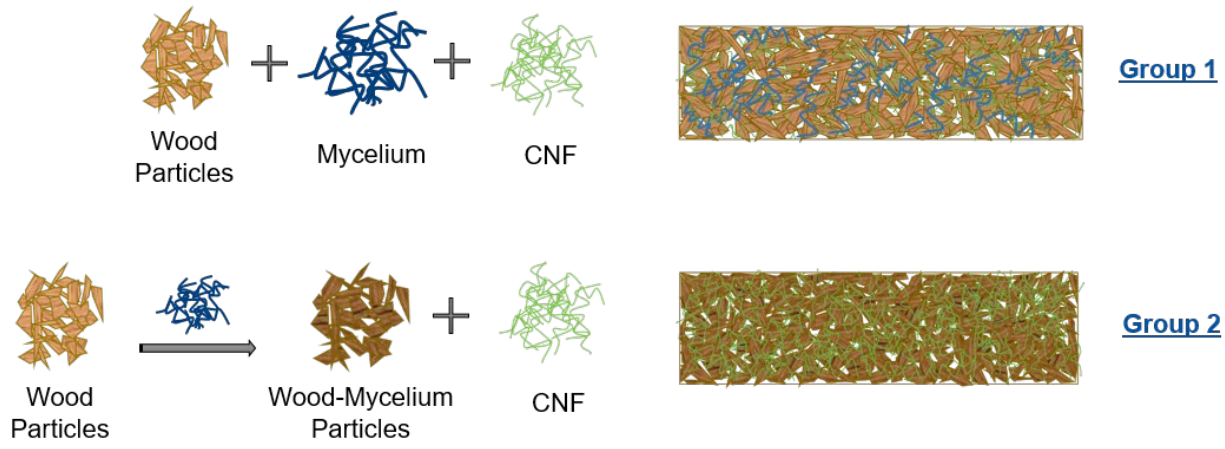

Figure 6.1. Schematic representation of the materials and composite production.

6.2. Experimental Section

6.2.1. Materials

The wood particles were a commercially available mixture of spruce, pine, and fir (SPF) particleboard particles, provided by Ecovative Design LLC (Green Island, NY). The pure white-rot basidiomycete mycelium tissue was grown in a solid-state fermentation process at the Ecovative Design facility in Green Island, NY, USA. The tissue was grown aerially in a proprietary incubation environment such that it grew up and out of the substrate with a loft height of 75 mm. The tissue was then harvested and dried at 43° C to deactivate the fungus. The wood-mycelium particles (WM) were produced by growing the same fungus on SPF softwood particles using the same procedure as growing the pure mycelium.

Cellulose nanofibrils (CNF) were the product of the University of Maine's Process Development Center (PDC). Characteristics of the CNF used in this study are provided elsewhere (Ghasemi et al., 2017; Johnson et al., 2016; Nazari et al., 2016). Briefly speaking, bleached softwood kraft pulp fibers were circulated through a refiner until the fines content was over 90% as determined by laser diffraction as fibers smaller than 200 microns. The original concentration of CNF was 3% wt.

6.2.2. Hybrid composite manufacturing

Two different forms of wood and mycelium mixture were used as a basic combination for hybrid composite manufacturing. The first is directly mixing wood particles and pure mycelium; the second is

using wood-mycelium particles produced from growing mycelium on wood particles. These two basic mixtures were combined with CNF in different percentages as shown in Table 6.1. The particle sizes of the wood materials used in both groups were 1.40-3.50 mm screened through a vibrating sieve. The target density was 0.6 $g \cdot cm^{-3}$, with thickness of 9.4 mm, controlled by stops in the hot press.

To further investigate the utilization of wood-mycelium particles and CNFs system in lightweight structures, additional composites with different densities and CNF contents were manufactured. Details are shown in Table 2. For all groups, five replicate panels were manufactured.

Table 6.1. The experimental design of hybrid composite manufacture (Group 1: wood particles + mycelium + CNF; Group 2: wood-mycelium particles + CNF).

Group	**Label**	**Materials**		
		Wood Particles (%)	Mycelium (%)	CNF (%)
Group 1	90W10M	90	10	0
	90W7.5M	90	7.5	2.5
	90W5M	90	5	5
	90W2.5M	90	2.5	7.5
	90W0M	90	0	10
		Wood-Mycelium Particles (%)		CNF (%)
Group 2	100WM	100		0
	97.5WM	97.5		2.5
	95WM	95		5
	92.5WM	92.5		7.5
	90WM	0		10

Table 6.2. The experimental design of lower-density hybrid composite manufacture.

Group	Label	Wood-Mycelium Particles (%)	CNF (%)	Density ($g \cdot cm^{-3}$)
Effect of Density Comparison	0.3	97.5	2.5	0.3
	0.4	97.5	2.5	0.4
	0.5	97.5	2.5	0.5
	0.6	97.5	2.5	0.6
Low-density Optimization	0.4-97.5WM	97.5	2.5	0.4
	0.4-95WM	95	5	0.4
	0.4-92.5WM	92.5	7.5	0.4
	0.4-90WM	90	10	0.4

Different components of the raw materials were mixed using a stand mixer with a paddle mixing blade, at speed 2 (KitchenAid, St. Joseph, MI, USA) for 2 mins. To make comparisons with the control formulation where CNFs were not used, equivalent amounts of water were added to the mixture. This was done to eliminate the effect of water on the properties of produced panels as CNF was a suspension in water and could not be used in dry form. Then the mixture was evenly distributed into a 120-mm square aluminum forming box. The formed mixture was first cold pressed using a hydraulic press (Dake Corporation, Grand Haven, MI) to remove approximately 50% of the water. The cold press pressure was around 400 kPa and the solid contents of the mats before and after cold press were approximately 16% and 38%, respectively. The dewatered mat was then hot pressed (Carver, INC., Wabash, IN) at 180 °C for 15 min to produce final hybrid panels.

6.2.3. Composite panel characterization

6.2.3.1. Material morphology

The nanostructure of CNF was viewed by transmission electron microscopy (TEM) (CM10 TEM, Philips, Amsterdam, Netherlands). Drops of 0.001 wt. % CNF suspensions were deposited on carbon-coated electron microscopy grids and negatively stained with 1% uranium acetate. The grids were dried in air and observed at an acceleration voltage of 80 kV. The morphology of the wood particles, wood-mycelium particles, pure mycelium and different combinations of the mixture were studied by a scanning

electron microscope (SEM) (Amray 1820, Amray Inc., New Bedford, MA) with an acceleration voltage of 10kV. The samples were placed on specimen mounts with double-sided carbon tape and grounded on all edges with conductive silver paint and sputter coated with 23 nm of gold-palladium.

6.2.3.2. Thermal stability analysis

The thermal stability evaluation of the raw materials was carried out under nitrogen gas on a TA Instruments TGA Q500 (TA Instruments, New Castle, DE) with a high resolution (Hi-Res) option from room temperature to 600 °C. In the Hi-Res approach, the heating rate is dynamically and continuously modified, ranging from 0.001 °C min^{-1} to the maximum heating rate (20 °C min^{-1}) in response to changes in the decomposition rate of the sample. The Hi-Res option is used to differentiate overlapping or close decomposition peaks. The resolution and sensitivity settings were 4.0 and 1.0 °C, respectively. The TGA results are shown as the variation of the sample mass (TG) or as a derivative weight loss (DTG) curve corresponding to the temperature.

6.2.3.3. Particle size distribution and dimensional analysis

The wood and wood-mycelium particles were well dispersed on a sheet of paper and the images were scanned by a Canon Document Feeder (DADF-AP1, Canon, Inc., Tokyo, Japan) with a resolution of 600 dpi. The original color images were first converted to black background using Photoshop software (Photoshop CC, Adobe Systems, Mountain View, CA, USA) and binary image using Image J software (Schneider et al., 2012) (ImageJ 1.48v, National Institutes of Health, USA). The basic geometrical attributes of the particles including length, width, area and perimeter were analyzed by ImageJ based on the best-fitting ellipse. Three shape factors were also calculated as aspect ratio, circularity and roundness (Rezaei et al., 2016). A minimum of 500 particles of each sample were analyzed.

6.2.3.4. Water absorption and thickness swelling

The water absorption and thickness swelling of different composites were measured according to ASTM D1037 (2012) (ASTM, 2012) with modifications using 3 × 3 cm specimens (8 replicates were used in each group). The specimens were immersed in distilled water and the weights and thicknesses were

measured after 2 and 24h. The water absorption and thickness swelling values were determined from the weight and thickness difference in relation to initial weight and thickness.

6.2.3.5. Mechanical testing

The modulus of rupture, the modulus of elasticity and the internal bond strength were determined according to ASTM D1037 (2012) (ASTM, 2012) with modifications using an Instron 5966 universal testing machine (Instron, Norwood, MA, USA) with a 10 kN load cell capacity. For the three-point bending test, rectangular specimens measuring 12 × 3 cm were tested using a span of 80 mm and a cross-head speed of 3 mm min^{-1}. For the internal bond strength tests, the dimensions of the specimens were 3 × 3 cm and the cross-head speed was 0.4 mm min^{-1}. Eight replicates were tested in each group.

6.2.4. Statistical analysis

The obtained data were analyzed using IBM SPSS Statistics Version 23 (IBM Corp., Armonk, NY, USA). Because the variables were different in the two groups of experiments, a one-way analysis of variance (ANOVA) was used to determine the differences between the group means for the two groups separately. A Duncan's Multiple Range Test (MRT) test was then performed to further assess the significance level of the mean values for each treatment level. All comparisons were made at 95% confidence level.

6.3. Results and Discussion

6.3.1. Characterizations of raw materials

The morphology images of the raw materials are shown in Figure 6.2. The surfaces of the original tracheids in the wood particles are very smooth (Figure 6.2A). After mycelium colonization, smooth cell walls are covered by a fibrous network of fungal hypha and the color of the wood particles turned darker (Figure 6.2B). At the initial stage of wood decay, the fungi hyphae penetrate wood, initiate colonization, and release enzymes (Zabel & Morrell, 2012). The brownness is a common change attributed to the synthesis of melanin at the early stage of wood decay (Lekounougou et al., 2008; Zabel & Morrell, 2012). As shown in Figure 6.2C, the aerial mycelium grown in a solid-state fermentation method has a porous structure composed of tubular hyphae. This structure was not apparent on the wood-mycelium particle

surfaces (Figure 6.2D). Under TEM, CNF appeared as thin elongated and branched fibers with multiple ramifications and sub-ramifications, which would easily form networks upon drying (Figure 6.2D) (Diop et al., 2017; Peng et al., 2012).

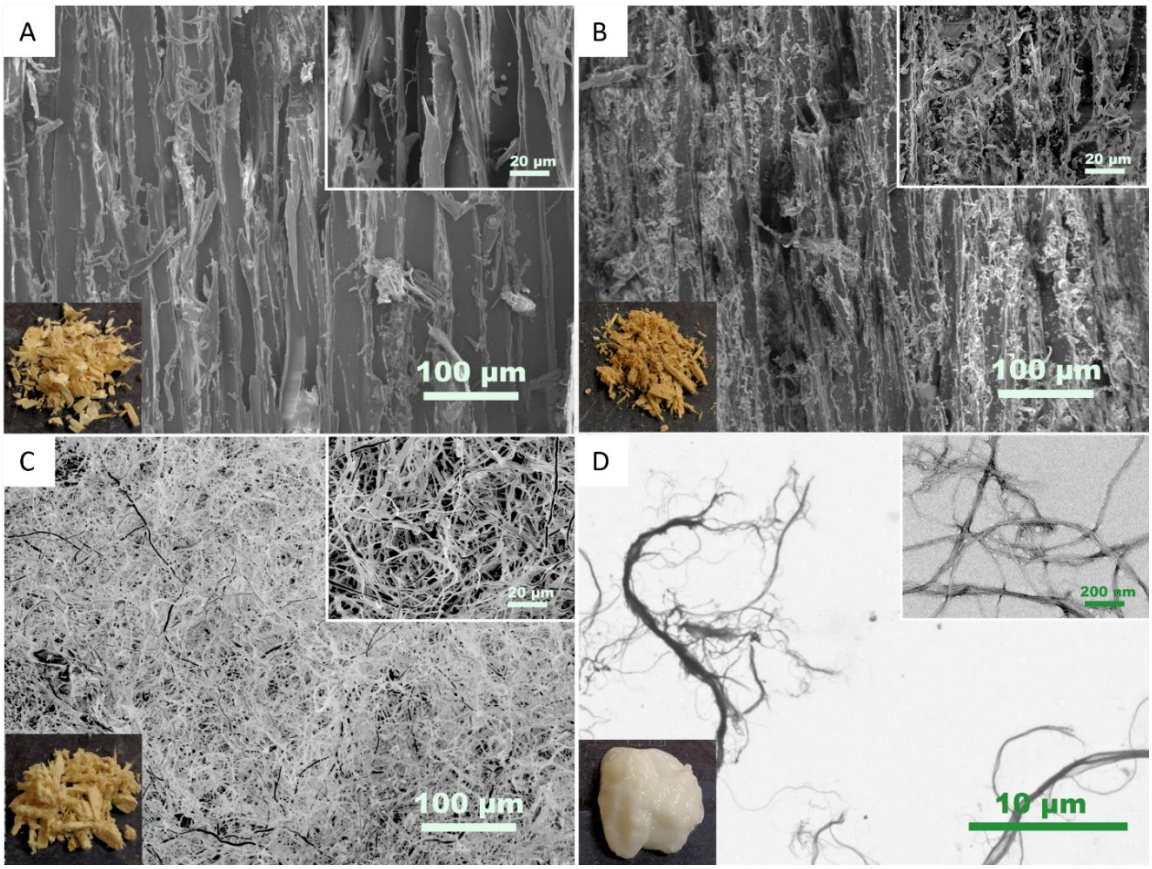

Figure 6.2. Morphology of raw materials: (A) wood particles, (B) wood-mycelium particles, (c) pure mycelium, and (d) CNF.

The thermal degradation profiles of raw materials reveal that most of the degradation occurred between 200 and 350 °C (Figure 6.3). Pure mycelium showed the lowest thermal stability and started to degrade at around 208°C (T_{on}). The two peaks appearing at 239 °C (T_{P1}) and 269 °C (T_{P2}) (Table 6.3) in the DTG curve match the reported degradation of carbohydrates and proteins, respectively, in the mycelium (Tănase et al., 2014). Both the TG and DTG curves of wood-mycelium particles appear similar to the curves of wood particles, showing that the weight percentage of mycelium in wood particles was very low. Compositional TGA analysis performed on mixtures of wood particles and mycelium (data not presented

here) showed that the weight percentage of mycelium in the wood particles was less than 10%. The degradation by fungi had very little influence on the thermal stability of wood particles. Compared with wood particles, which started to degrade at around 244 °C (T_{on}, or initial rise in 3b), with a maximum degradation temperature of 316°C (T_{P2}), the thermal degradation onset of CNF occurred at a higher temperature at 257°C (T_{on}), with one degradation peak at 301°C (T_{P2}). This increase in thermal stability (higher onset temperature in Figure 3b, indicated by arrow) is proposed to be caused by the removal of hemicellulose, lignin, pectin and other less stable components in wood (Dufresne, 2017).

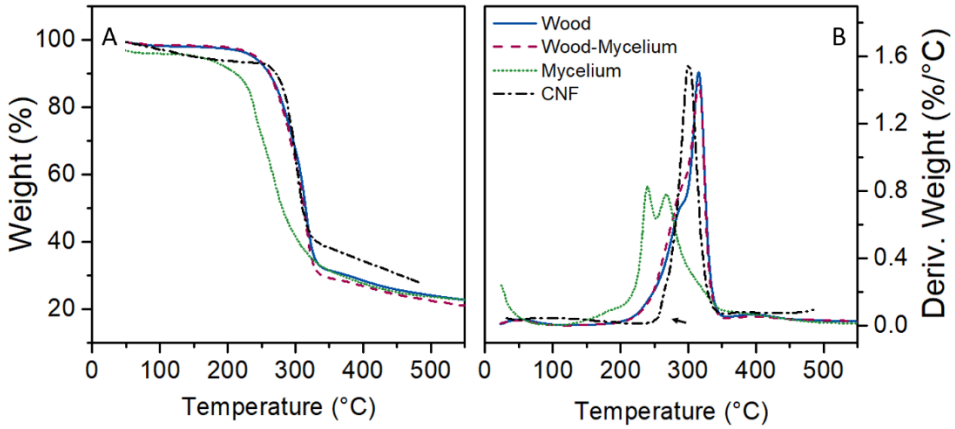

Figure 6.3. (A) TG and (B) DTG curves of composite raw materials.

Table 6.3. Onset and peak temperatures of thermal degradation for wood particles, wood-mycelium particles, pure mycelium and CNF obtained from DTG data (Figure 6.3B).

Materials	**[a]T_{on} (°C)**	**[b]T_{P1} (°C)**	**[b]T_{P2} (°C)**
Wood	243.8	286.2	316.0
Wood-Mycelium	241.9	283.0	315.1
Mycelium	207.9	239.0	268.9
CNF	257.2	-	301.0

[a] The onset temperature T_{on} was estimated by the intersection of the tangent lines in 4b.

[b] The degradation temperature T_{P1} and T_{P2} refer to the different peak temperatures observed on the DTG curves and are related to the different thermal degradation steps for each material.

All the wood and wood-mycelium particles used in this study were obtained after sieving. The mesh size was between 1.40 and 3.35 mm. However, particles normally pass through the sieves only based on their width (Rezaei et al., 2016). By image analysis, more information about the particles can be obtained and compared. Figure 6.4 and Table 6.4 show the relative length frequencies and other dimension and shape factors of wood and wood-mycelium particles, respectively. No significant difference was found in particle length distribution between wood and wood-mycelium particles, as expected (p-value>0.05) meaning that changes seen in physical and mechanical properties of panels were not affected by wood particle size.

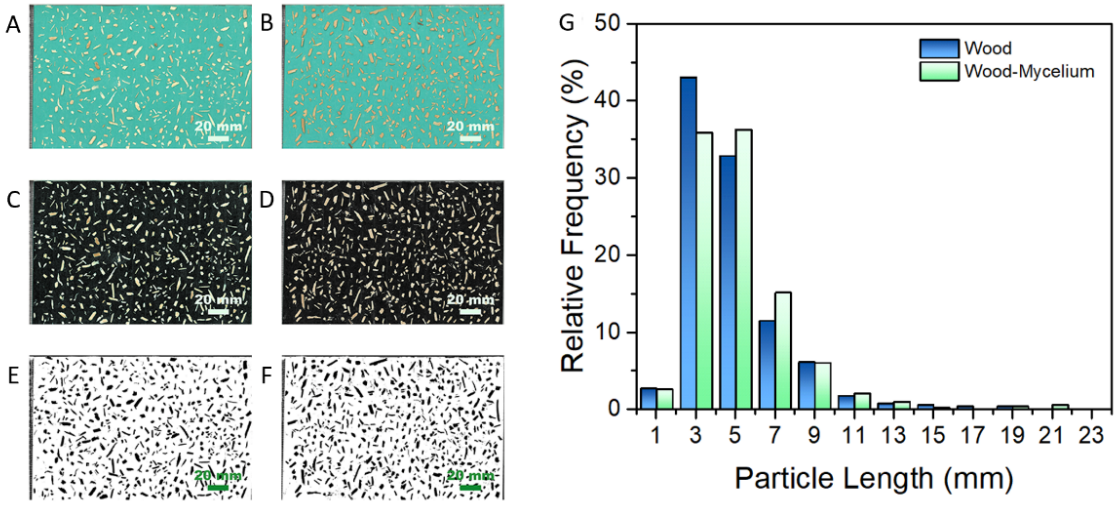

Figure 6.4. (A) (B) Original scanned, (C) (D) black background, and (E) (F) binary images of (A) (C) (E) wood, (B) (D) (F) wood-mycelium particles (left) and (G) relative length frequencies of wood and wood-mycelium particles (right).

Table 6.4. Dimensions and shape factors (width, length, aspect ratio, circularity and roundness) of wood and wood-mycelium particles (mean ± one standard deviation).

Parameters	Wood Particles	Wood-Mycelium Particles
Width (mm)	1.87 ± 0.77	1.97 ± 0.81
Length (mm)	4.79 ± 2.48	5.04 ± 2.65
Aspect Ratio	3.16 ± 5.62	3.11 ± 3.11
Circularity	0.46 ± 0.17	0.48 ± 0.17
Roundness	0.46 ± 0.22	0.46 ± 0.23

6.3.2. Comparison of the two wood-mycelium-CNF hybrid systems

Water absorption and thickness swelling are not limiting factors for indoor type composites such as particleboard. However, more dimensionally stable products are often preferred and these two properties can also shed some light on the quality of adhesion in the panel. Figure 6.5 shows the water absorption and thickness swelling results of the two groups. Both water absorption and thickness swelling values are very high in Group 1 (Figure 6.5A, C), revealing that there was not sufficient adhesion in the system. No data could be collected from the specimens with no CNF addition (90W10M) in Group 1 as the panel quickly fell apart after being immersed in water, which shows that the interactions between pure mycelium blended with wood particles are not water resistant. Conversely, specimens in Group 2 show much lower water absorption and thickness swelling values (Figure 6.5 B, D). The specimen 100WM with no CNF addition shows 158% water absorption and 70% thickness swelling after 24h, which is significantly lower than all the specimens in Group 1. At the initial stage of wood decay, fungal hyphae grow on wood cell walls and cover the particle surfaces (Figure 6.2A, B), which increases the surface interactions during the hot-pressing process. Enzymes typically produced by white-rot fungi can degrade lignin and produce radicals which might help improve the adhesive bonding (Barsberg & Thygesen, 1999; Li, 2003; Munk et al., 2017).

The many available hydroxyl groups on CNF form hydrogen bonds with wood, mycelium, and other CNF particles, which is one of the main adhesion mechanisms contributing to CNF bonded panels. The higher water absorption and thickness swelling of Group 1 samples with higher levels of CNF (Figure 6.5A, C) is attributed to the loss of hydrogen bonds between the wood/mycelium particles during water soaking. Group 2, however, shows a small positive (reducing) effect of CNF addition on water absorption and thickness swelling (Figure 6.5B, D)). Common letters on the columns in the figure indicate that the means of the parameters were not significantly different at 95% confidence level; therefore, the effect of adding CNF to the Group 2 samples on water absorption and thickness swelling was statistically significant (p-value < 0.05) only when 2.5% CNF was added. Further addition of CNF did not change these parameters significantly. A possible explanation is that the hydroxyl groups reacted with crosslinkers or radicals formed

during fungi-induced degradation and were fixed in the entire system (Widsten & Kandelbauer, 2008; Widsten et al., 2004).

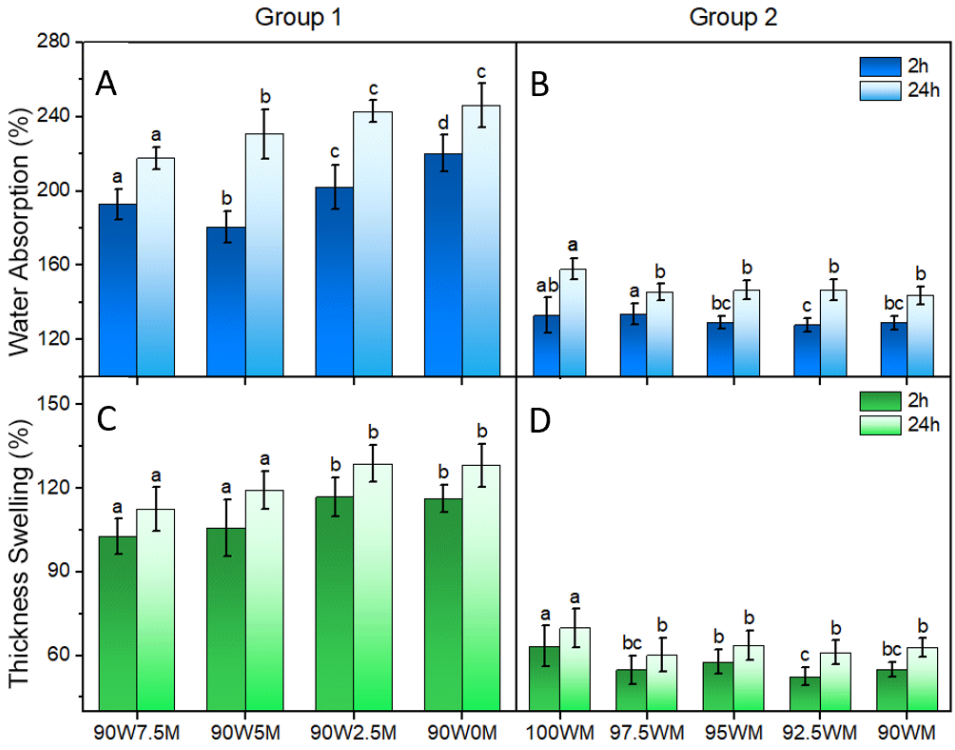

Figure 6.5. (A) (B) Water absorption and (C) (D) thickness swelling of (A) (C) Group 1 and (B) (D) Group 2. In each figure, columns with common letters are not significantly different at 95% confidence level (p-value>0.05).

Figure 6.6 shows the modulus of rupture and the modulus of elasticity results of Group 1 (A) and Group 2 (B). The modulus of rupture measures the ultimate load-carrying capacity while the modulus of elasticity measures the resistance to bending and reveals the stiffness of the sample (Shmulsky & Jones, 2011). These two parameters are widely used to evaluate the mechanical performance of panel products. With no CNF addition, both the modulus of rupture and the modulus of elasticity of Group 1 (90W10M) and Group 2 (100WM) are very low. Compared with 90W10M, 100WM shows higher modulus of rupture and the modulus of elasticity values indicating that treating wood particles with the mycelium positively affects CNF performance as binder. This could be because of wood composition changes caused by fungal degradation had positive effects on bonding and properties by providing more hydrogen bonding sites as

corroborated by thickness swelling data presented earlier. Water can easily abrupt hydrogen boding and the fact that thickness swelling data are in agreement with mechanical performance indicates the importance of hydrogen bonding in adhesion.

The addition of CNFs increased both the modulus of rupture and the modulus of elasticity in both Group 1 and Group 2 significantly (p-value < 0.05). However, there was no significant difference in the specimens of a series when the amount of CNF was higher than 5% in Group 1 and 2.5% in Group 2. This shows there may be an ultimate loading level of CNF on the surface of wood and mycelium enough for promoting adhesion beyond which no further improvement is observed (Theng et al., 2015).

Adhesion performance in wood-based panels is also quantified using the internal bond strength. The results of the internal bond strength tests are shown in Figure 6.7. With no CNF addition, the composites from both groups (90W10M and 100WM) were too weak to be measured in the internal bond strength test. The internal bond strength values reached 0.03 MPa and 0.06 MPa after adding 2.5% and 7.5% of CNF in Group 1, respectively. There was no significant difference between any of the CNF levels in Group 2, which was the same as the observation in the bending test.

The horizontal lines in both Figure 6.6 and Figure 6.7 indicate the required values for the particleboard grade LD-1 from the US particleboard performance standard, ANSI A208.1 (ANSI, 2016b). Composites made by wood-mycelium particles and CNF in Group 2 met the standard in both the modulus of rupture and the modulus of elasticity, but the values of the internal bond strength were lower than the standard value (0.1 MPa). Previous work showed that with 15% of CNF addition to southern pine wood particles, the internal bond strength value of the composite was around 0.4 MPa (Amini et al., 2017). The much lower the internal bond strength value in this study might be caused by the larger particle size of the raw material and less CNF used. Water absorption and thickness swelling are not included in ANSI A208.1 as particleboards are interior products not meant to be exposed to water therefore direct comparison with the standard is not possible. However, the significant reduction in these two parameters in Group 2 samples is very promising.

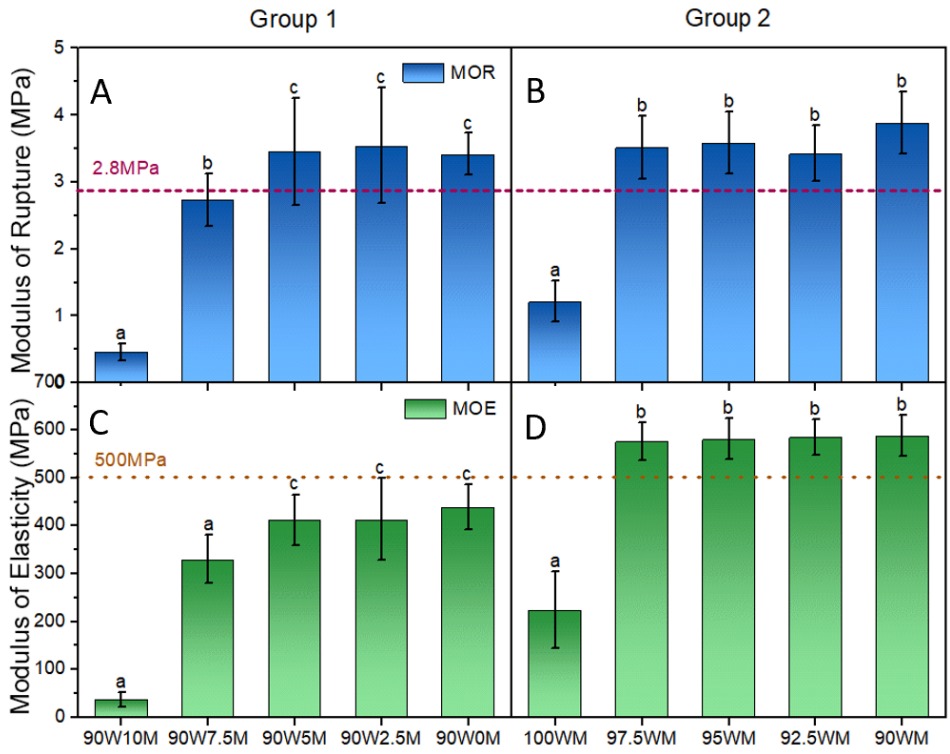

Figure 6.6. (A) (B) The modulus of rupture and the (C) (D) modulus of elasticity of (A) (C) Group 1 and (B) (D) Group 2. The horizontal lines indicate the minimum value of the modulus of rupture and the modulus of elasticity required to meet the ANSI A208.1 standard for LD-1grade (ANSI, 2016b). In each figure, columns with common letters are not significantly different at 95% confidence level (p-value>0.05).

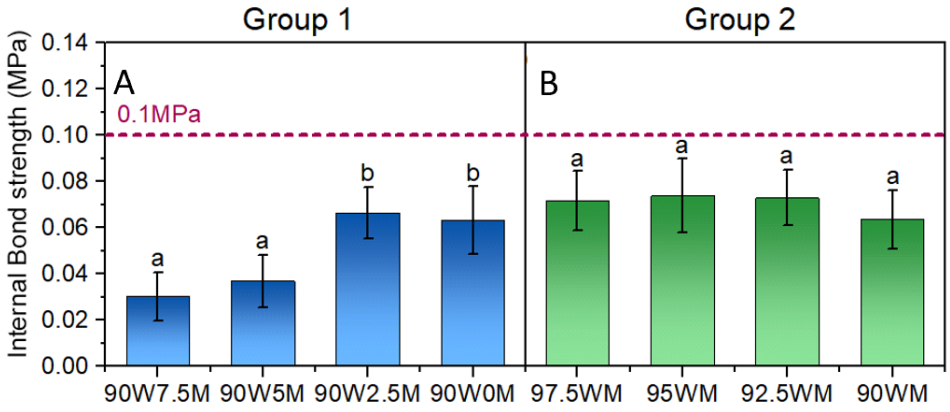

Figure 6.7. The internal bond strength of (A) Group 1 and (B) Group 2. The horizontal line indicates the minimum value of the internal bond strength required to meet the ANSI A208.1 standard for LD-1 grade

(ANSI, 2016b). In each figure, columns with common letters are not significantly different at 95% confidence level (p-value>0.05).

To further investigate the interactions among raw materials in different mixtures and explain the property difference between Group 1 and Group 2, various combinations of raw materials were mixed and dried and then observed by SEM (Figure 6.8). Simply mixing pure mycelium and wood particles together did not adequately distribute the mycelium particles (Figure 6.8 A, B). Some areas of the surfaces of wood particles were covered with mycelial hyphae, similar to Figure 6.2C, while other parts remained the same as untreated wood particles seen in Figure 6.2A. This uneven distribution of mycelium is likely to be at least partly responsible for the lower properties of the composites in Group 1. Figures 6.8 C, D show the morphology of wood-mycelium particles after mixing with 2.5% CNFs- where the original surfaces of the particles (Figure 6.2B) were well covered by a layer of CNF film and look much smoother. This structure looks similar to the structure of mixing pure wood particles with CNF (Figure 6.8 E, F). The fungal mycelium-covered surfaces of wood-mycelium particles have a positive effect on the deposition of CNs and the strong CNF-CNF interaction helped improve the modulus of rupture and the modulus of elasticity in both groups.

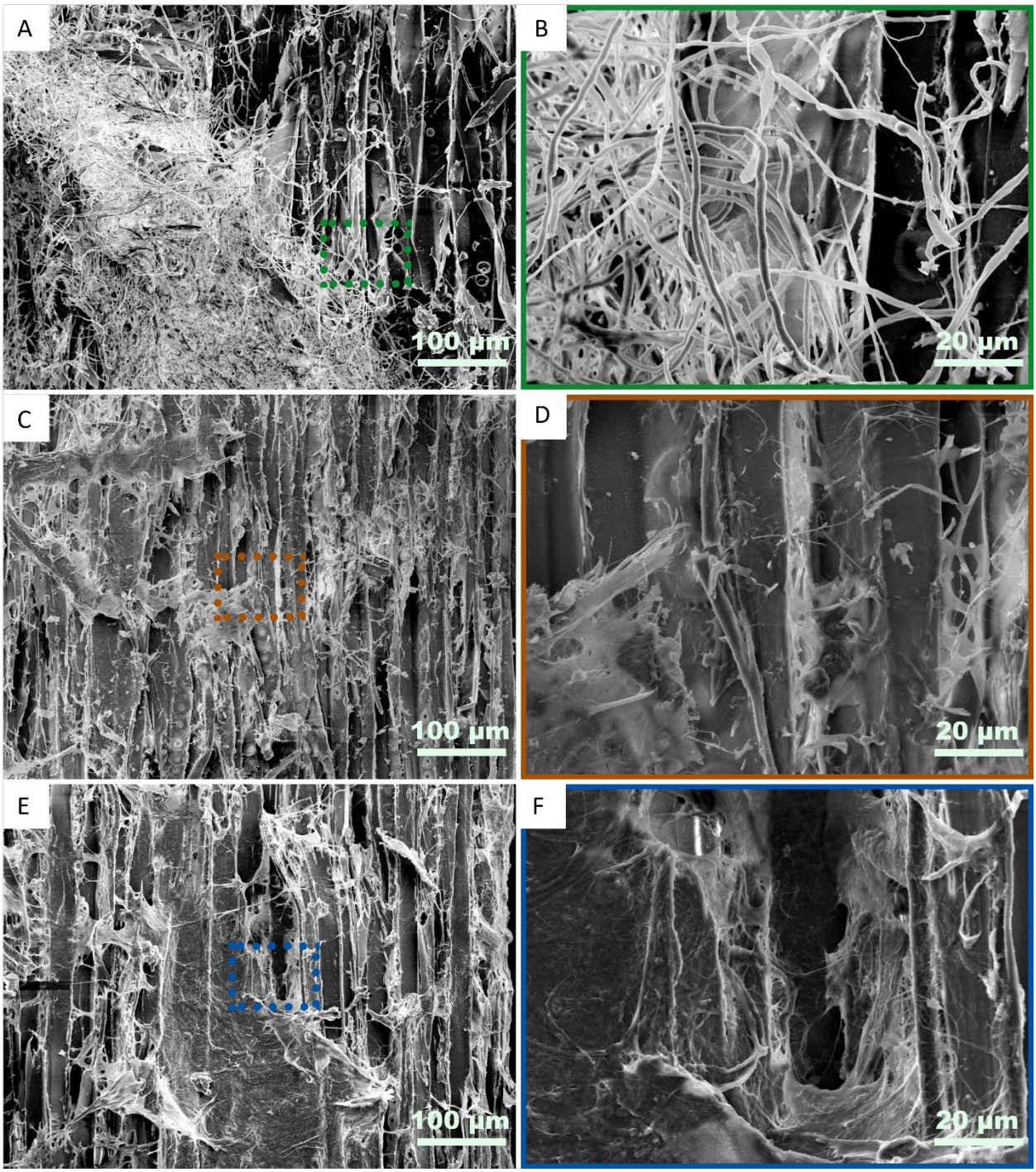

Figure 6.8. SEM images of different mixtures of raw materials with different magnifications, (A, C, E) 200 × and (B, D, F) 1000 ×. (A) (B): 90% Wood + 10% Mycelium; (C) (D): 90% Wood-Mycelium + 2.5% CNF; (E)(F): 90% Wood + 10% CNF.

There are many possible mechanisms to explain the performance of these two hybrid systems. The better properties achieved by Group 2 than Group 1 might be caused by, but may not be limited to the following reasons (Gardner & Tajvidi, 2016): 1) the better dispersion of mycelium thereby providing better adhesion, 2) the chemical changes of wood particles such as degradation of hemicellulose and lignin which may open more pores on the surface of wood cell wall, increase the surface energy and provide more functional groups for bonding and 3) the chemical differences in the structure of mycelium grown on different substrates. The SEM images clearly confirm that hypothesis 1 is reasonable but other possibilities might also be involved and are currently being studied by our research group. The CNF impressively improved the (dry) the modulus of rupture and the modulus of elasticity at low addition rates, which we attribute to its very good hydrogen bonding (Gardner & Tajvidi, 2016), but had little effect on wet properties of water absorption and thickness swelling .

6.3.3. Utilization of the hybrid system in lightweight composites

The experimental results in the former sections confirm that the wood-mycelium particles and CNF system (Group 2) is a viable way to achieve fully bio-based particleboard-like composites. Considering the special attention to lightweight composites in packaging, handling and transportation in recent years (Dziurka & Mirski, 2013; Monteiro et al., 2016), the utilization of this hybrid system in lightweight composites was further investigated. The ultimate goal was to produce light-weight composites with acceptable physical and mechanical properties using mycelium-treated wood particles.

The first step was to vary densities at the same CNF addition ration (2.5 wt.%). The water absorption, the thickness swelling, the modulus of rupture and the modulus of elasticity results of the hybrid composite with 2.5 wt.% CNF addition at different densities (Table 6.2) are shown in Figure 9. The 2.5% addition of CNF bonded the composites with different densities very well. The water absorption decreased with increasing composite density as a result of the decreasing the amount of voids and pores, whereas the thickness swelling, the modulus of rupture and the modulus of elasticity increased with density, as is typical (Amini et al., 2017; Leng et al., 2017).

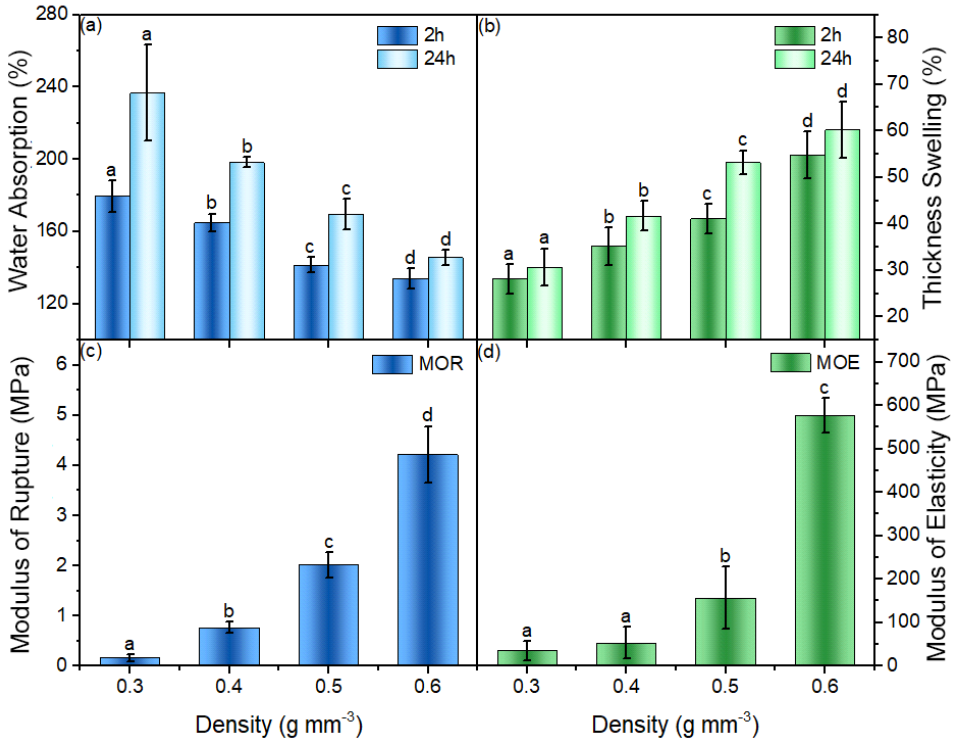

Figure 6.9. (A)Water absorption, (B)thickness swelling, (C) modulus of rupture and (D) modulus of elasticity of samples labeled "Effect of Density Comparison" group in Table 6.2. In each figure, columns with common letters are not significantly different at 95% confidence level (p-value > 0.05).

As 2.5% CNF was found to be the optimal level for the 0.6 g·cm^{-3} density composite system, it was interesting to see if it was the same in lower density systems. Therefore, the 0.4 g·cm^{-3} density system was chosen and the hybrid composites with 2.5%, 5%, 7.5%, 10% addition of CNF were manufactured (Table 6.2) to optimize physical and mechanical properties. As shown in Figure 10, the water absorption, the modulus of rupture and the modulus of elasticity were significantly higher (p-value<0.05) at 5% CNF loading than 2.5% in these panels at 0.4 g·cm^{-3}. With the decrease of density, the structure benefited from additional CNF available to enhance bonding.

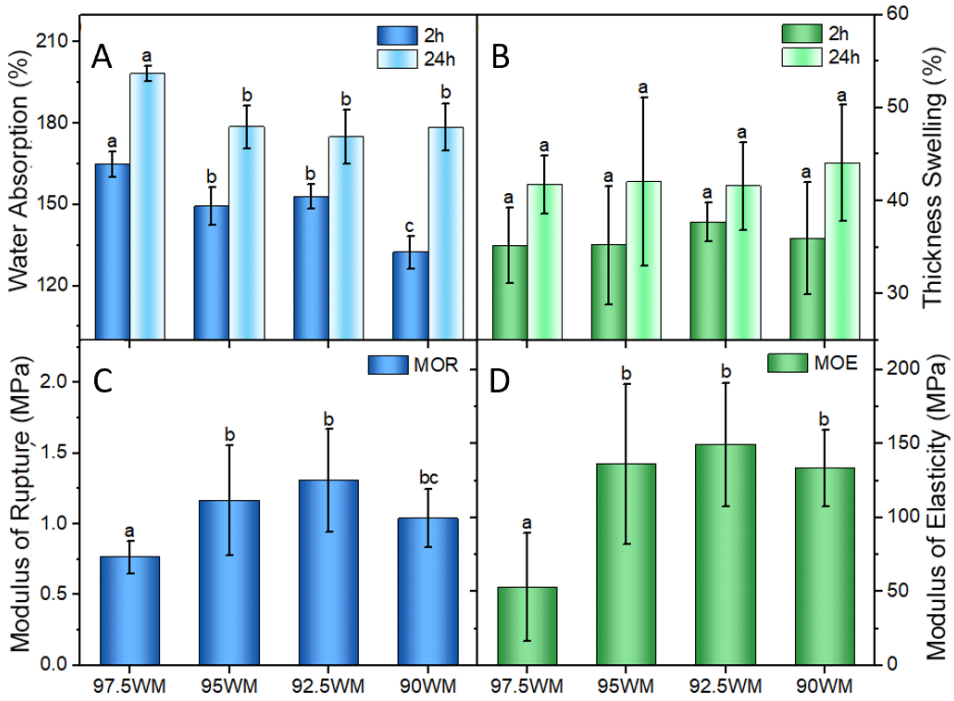

Figure 6.10. (A) Water absorption, (B) thickness swelling, (C) modulus of rupture and (D) modulus of elasticity of "Low-density Optimization" group in Table 6.2. In each figure, columns with common letters are not significantly different at 95% confidence level (p-value>0.05).

Overall, hybridization of CNF and mycelium as two fully bio-based adhesive systems proved very promising. Efficient dewatering and reduction of press cycle remain important issues key to the successful implementation of CNF as binder in wet-formed composite panels. Studies on the dewatering mechanism through contact dewatering are currently underway in our research group and preliminary efforts to reduce press cycle confirm the important role of initial dewatering. Another possibility especially for lower density panels is convection drying in an oven instead of conductive drying in a hot press or a combination of the two methods. The hybridization of CNF binder with fungal treatment of wood particles promises the possibility of cost reduction attributed to the lower amount of CNF required to achieve acceptable physical and mechanical properties. In our previous studies (Amini et al., 2017; Leng et al., 2017) where CNF was the sole binder to produce particleboard panels, at least 15 wt.% CNF was required to meet ANSI standard

minimum levels. Using mycelium treated wood particles the required CNF content was only 2.5% indicating the great potential of hybridizing the two binder systems.

6.4. Conclusion

This chapter investigated the hybrid systems of wood, mycelium and CNF in the production of fully bio-based composite panels. Two systems of applying fungal biomass were compared and growing mycelia on the wood resulted in better properties than physically mixing pure wood particles and mycelium. Growing mycelium on wood did not change particle dimensions and shape but well covered on the surface of the particles, which had positive effects on bonding. The added CNF formed a uniform film over the particles and improved the physical and mechanical properties of the composites at loadings up to 5% and 2.5%, respectively, for 0.4 $g \cdot cm^{-3}$ and 0.6 $g \cdot cm^{-3}$ composite panels. This system also works in lower density composite systems. Overall, this novel composite system showed good physical and mechanical properties and has potential to replace formaldehyde-based composites. Further improvement of the hybrid system, testing of other properties and other potential mechanisms are the focus of our current studies. Finally, the impressive better dimensional stability of composites produced from mycelium-treated wood was promising in terms of potential to produce outdoor-type composites using water-resistant resins.

CHAPTER 7

TUNABLE MYCELIUM SURFACE

7.1. Introduction

Natural surfaces exhibit a variety of structures and chemical compositions which influence their wettability and absorbability. Some useful functionalities which exist in plant- or animal-based materials include superhydrophobic surfaces with self-cleaning properties (Barthlott & Neinhuis, 1997; Guo & Liu, 2007; Neinhuis & Barthlott, 1997), superhydrophobic surfaces with high adhesive forces (Zheng et al., 2007), and patterned wetting for water collection (Hu et al., 2003; Zheng et al., 2010) , among others. Learning from nature, artificial surfaces have been developed by fabricating hierarchical structures and applying chemical modifications afterward. These mimicked surfaces normally have similar functions to those naturally found but when they exhibit properties not found naturally, the practice is labelled "biomimicking beyond nature" (Liu et al., 2012). Surfaces with tunable wettability are an example of such a type of artificial surfaces and have received broad scientific interest. Surface properties may be altered by diverse stimuli such as mechanical force, photo exposure, temperature change, pH change, electrical potential, electrolytes, and more (Guo & Guo, 2016; Stratakis et al., 2010; Xia et al., 2009).

In addition to artificial smart surfaces, naturally-existing biological systems can also exhibit the characteristics of self-healing and self-adjustment. For example, filamentous fungi can produce a type of surface amphiphilic protein called hydrophobin as structural components. Hydrophobin proteins have relatively low molecular weight (about 100 amino acid residues) and are extractable with formic acid or trifluoroacetic acid (Bidochka et al., 1995; Lo et al., 2014; Wessels et al., 1991). They have both hydrophilic and hydrophobic parts to help fungi escape the aqueous environment to spread their spores by the self-assembly function (Kershaw & Talbot, 1998; Linder et al., 2005). The self-assembly property of hydrophobins under different conditions and environments has been widely investigated on extracted and purified hydrophobin proteins (Aimanianda et al., 2009; Armenante et al., 2010; Lo et al., 2014; Longobardi et al., 2012; Scholtmeijer et al., 2009). Specifically, the class I hydrophobin Vmh2 (0.1-0.2 mg mL^{-1} in 60% ethanol) extracted from the mycelium of oyster mushroom (*Pleurotus ostreatus)* undergoes a reversible

conformational change from the helical structure to a disordered structure and reversible aggregation at a temperature of 80 °C (Longobardi et al., 2012). Class I hydrophobin SC3 from the fungus *Schizophyllum commune* adopts the amyloid state at the water-PTFE interface at high concentration (300 μg ml^{-1}) and prolonged incubation (16 h) (Scholtmeijer et al., 2009).

In recent years, fungal mycelium-based products have achieved increasing research interest and commercialization as novel sustainable materials to replace petroleum-based products. Specific products have been commercialized in textile, packaging, and construction applications (Appels et al., 2019; Attias et al., 2020; Sun et al., 2019). In this chapter, we aim to understand the surface property of a commercialized mycelium product. Specifically, we were interested to know if the surface of mycelium carries switchable wettability similar to the exacted hydrophobin protein. We also further investigated the tunability of surface wettability and discussed possible mechanisms and potential applications.

7.2. Experimental Section

7.2.1. Sample preparation

Ecovative Design, LLC, manufactured the pure mycelium sheet using a solid fermentation method, outlined elsewhere (Islam et al., 2017). The obtained mycelium samples were cut into 20 × 10 × 2 mm sheets and labeled "MFoam" for further analysis. The "MFoam" was pressed under 5 MPa/ 80 °C for 5 min into "MFilm" with a thickness of about 0.15 (± 0.02) mm.

We developed a facile water treatment method to change the wettability of the mycelium surface. To wet the mycelium surface, 100 μL of deionized water was applied on the surface of each mycelium film sample. A plastic blade was used to manually push water down with a horizontal back and forth motion into the mycelium structure until the entire mycelium film was fully saturated with water. The samples were dried and conditioned on the lab bench in open air (20 ± 1 °C and 15 ± 5 %RH) until no weight change was recorded. The resulting wetted/dried samples are labeled as "W/D MFilm".

To remove the surface hydrophobins of the MFilm, the samples were saturated with 99% formic acid at 4 °C for 24h according to previous reports (de Vries et al., 1993; Wessels et al., 1991), then washed with distilled water until the pH reached 7 and dried in lab condition until no weight change was observed.

7.2.2. Conditioning treatment

The W/D MFilms were conditioned for up to 13 days. The four conditions were: 50 °C and 80%RH; 50 °C and 3%RH; 20 °C and 80%RH; and 20 °C and 50%RH. At the end of the conditioning treatments, the samples were placed in the lab until no weight change was observed.

7.2.3. Scanning electron microscopy

The morphology of the mycelium surface was investigated by a scanning electron microscope (SEM) (Amray 1820, Amray Inc., New Bedford, MA, USA). The surface of the samples was coated with gold (3 nm) before observation at 10 kV acceleration voltage on various locations and at ×200 and ×2000 magnifications.

7.2.4. Contact angle and wetting time measurement

The contact angle analysis was carried out using a mobile contact angle analyzer (KRÜSS GmbH, MSA, Hamburg, Germany) and the corresponding software for this device. For each measurement, one 1μL drop of water was applied on a random area of the surface, and the time-series of contact angles were collected starting at on average 2.5 ± 0.5s after the start of the experiment until total absorption or evaporation. For all analyses, the initial contact angles were determined at 2.5 ± 0.5s by averaging left- and right-side angles of the droplets. For each sample, 5-15 measurements were carried out.

7.2.5. Light microscopy

A Nikon NIE microscope (Nikon, Japan) was used to image the samples and obtain z-stack images (bright-field). The objective lens was a Nikon Plan Fluor 40× PH2 DLL, with a numerical aperture (NA) of 0.75 and a depth-of-field of 0.98 μm.

7.2.6. Moisture content analysis

Thermogravimetric analysis was used to measure the moisture content of MFilm and W/D Mfilm under nitrogen gas on a TGA Q500 (TA Instruments, New Castle, DE). The TGA temperature was increased from room temperature to 110 °C at a rate of 20 °C/min, then held at 110 °C for 20 min. The moisture content was calculated based on the mass loss detected by the TGA.

7.2.7. TGA

The thermal stability evaluation of the materials was carried out under nitrogen gas on a TGA Q500 (TA Instruments, New Castle, DE) with a high resolution (Hi-Res) option to differentiate overlapping decomposition peaks. In the Hi-Res approach, the temperature range is from room temperature to 600 °C. The heating rate is dynamically and continuously modified, ranging from 0.001 °C min^{-1} to the maximum heating rate (20 °C min^{-1}) in response to changes in the decomposition rate of the sample. The resolution and sensitivity settings were 4.0 and 1.0 °C, respectively. The TGA results are shown as the variation of the sample mass (TG) or as a derivative weight loss (DTG) curve corresponding to the temperature.

7.2.8. ATR-FTIR

ATR–FTIR spectra of the surface were obtained using a Spectrum Two IR spectrometer (Perkin Elmer, Waltham, MA). All spectra were obtained in the range of 4000 to 500 cm^{-1}, accumulating 32 scans. The tested samples were all in room condition. To ensure the reproducibility of the obtained spectra, three replicate specimens were measured.

7.3. Results and Discussion

7.3.1. Surface wettability

Figure 1A shows the original mycelium foam (MFoam) produced by Ecovative Design, LLC (Green Island, NY). Visual inspection of the SEM image (Figure 1D) shows that the distribution of the hyphae is uniform. The 2 mm-thick MFoam was compressed to about 0.15 (± 0.02) mm (Figure 7.1B) in thickness. The compression is visible when comparing the MFoam with the MFilm at moderate (Figure 7.1D and 7.1E), and high (Figure 7.1G and 7.1H) magnification (×2000). The compression process maintains the hydrophobicity of the original foam. As shown in Figure 7.2A, there is no significant difference ($p > 0.05$) between the initial water contact angle of the original MFoam and the compressed MFilm (135 ± 4° vs. 130 ± 2°, respectively). The hydrophobic nature of filamentous fungi is well known and is attributed to assemblies of the surface-active protein, hydrophobin (Aimanianda et al., 2009; Bidochka et al., 1995; Gunning et al., 1998). Furthermore, as shown in Figure 7.2C and 7.2D, with the increase of the wetting time, the single water droplet on the surface of MFoam undergoes a typical three-

stage route: 1) reduced contact angle; 2) reduced contact line with small contact angle changes; a mixed mode of 1 and 2 (Park et al., 2012) and finally disappears after about 1600 s (Figure 7.2B, C, and D). This behavior is similar to the behavior of common hydrophobic or nearly hydrophobic surfaces (Park et al., 2012). There is also no detectable weight change after the water droplet disappears, indicating that the applied water droplet mostly evaporated without being absorbed into the porous structure. The compressed film showed a similar trend but with shorter wetting time (Figure 7.2B, C, and E). This behavior could be attributed to partial water penetration between the hyphae. We also performed the wetting test on a non-absorbing Teflon surface as a reference. The contact angle and wetting time were 102 ± 5° and 1127 ± 144 s, respectively. The wetting time (actually evaporation time) on the Teflon sheet was significantly less ($p < 0.05$) than MFilm and MFoam, which may be attributable to the larger surface area of the same drop volume on Teflon (Chandra et al., 1996).

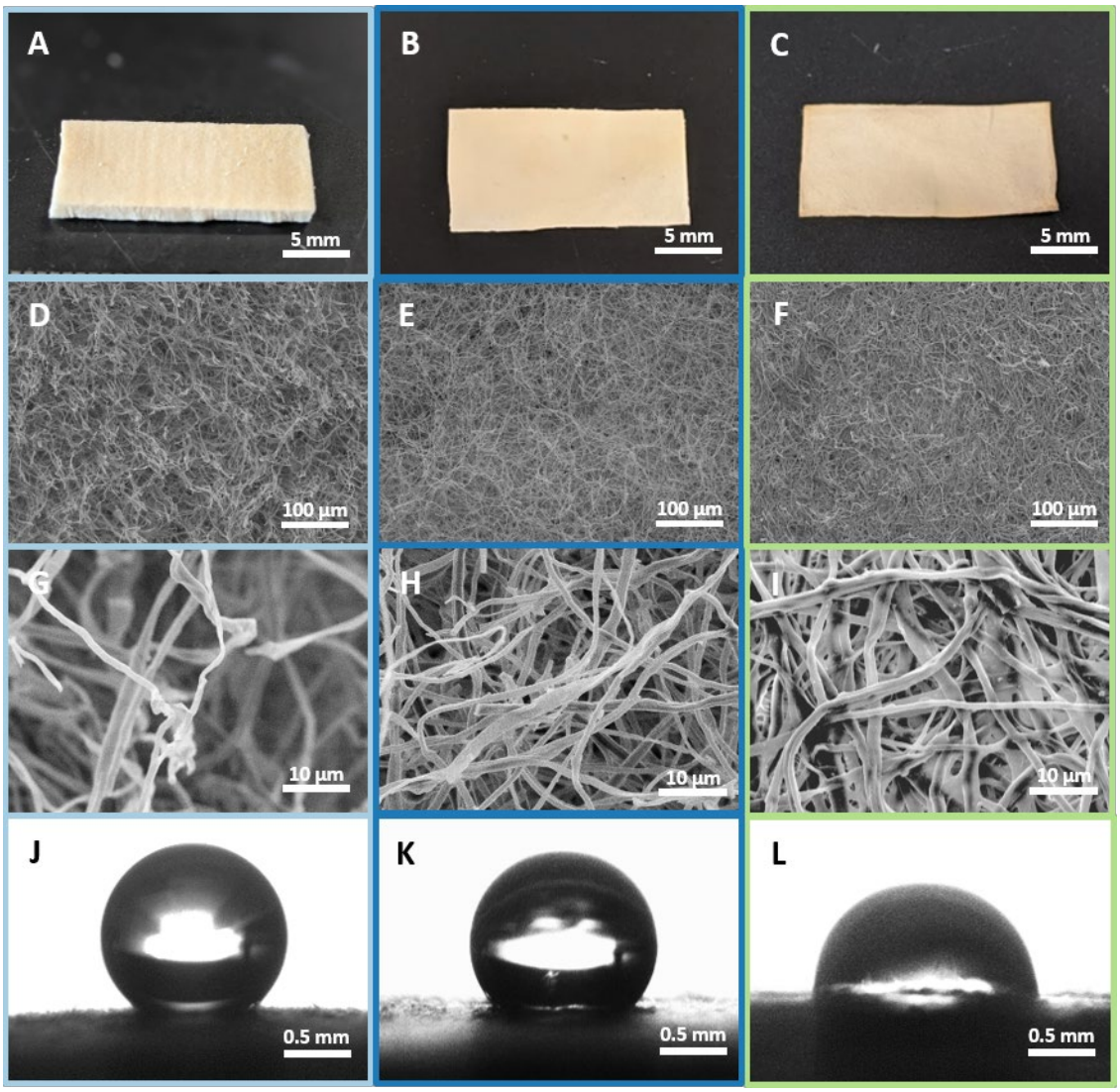

Figure 7.1. Morphology of MFoam (A, D, G), MFilm (B, E, H) and W/D MFilm (drying condition: 20 °C and 15 ± 5 %RH) (C, F, I). (A-C): Macroscale view. Scale bar: 5 mm. (D-F): SEM images of the microstructure. Scale bar: 100 µm. (G-I): SEM images of the microstructure. Scale bar: 10 µm. Initial contact angle image of MFoam (J), MFilm (K) and W/D MFilm (L). Scale bar: 0.5 mm.

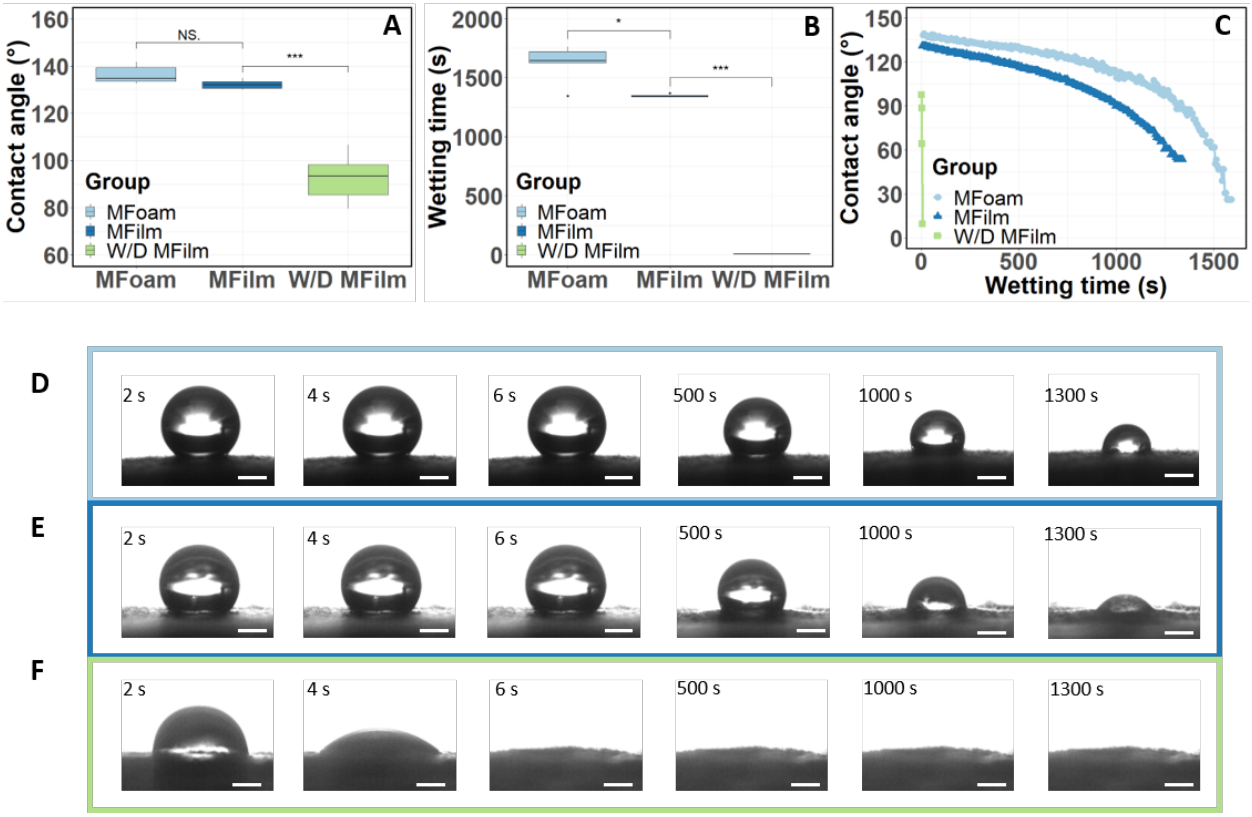

Figure 7.2. Wettability and absorption comparison of MFoam, MFilm and W/D MFilm (drying condition: 20 °C and 15 ± 5 %RH). (A): Initial contact angle (°). (B): Wetting time (s). (NS indicates $p > 0.05$; * indicates $p < 0.05$; *** indicates $p < 0.001$) (C): Change of contact angle with wetting time: MFoam (D), MFilm (E), W/D MFilm (F). Scale bar: 0.5 mm.

To further investigate the absorption behavior and the amphiphilicity of the mycelium surface, 100 µL (per 200 mm^2 area of mycelium) of water was applied to each MFilm sample and pressed into the surface to accelerate the absorption. The applied water was eventually absorbed, with water displacing internal air pockets evidenced by a change from white to a slightly translucent appearance. After drying at room temperature (20 ± 1 °C) and humidity (15 ± 5 %RH), a film with a more compacted surface was obtained (Figure 7.1C, F, I). The smaller opening area is caused by the apparent additional connectivity among hyphae (Figure 7.1F and I). The wettability of the wetted/dried mycelium film also changed significantly ($p < 0.001$) with the initial contact angle dropping to 93 ± 9° (Figure 7.2A) and the total wetting time reduced to less than 10 seconds (8 ± 2s) (Figure 7.2B, C, and F). This dramatic change of the wettability

and absorption of W/D MFilm could be caused by the change of the physical surface structure such as the reduced amount of air pockets and/or by the chemical surface components such as the reassembly of the surface hydrophobin proteins or a combination of these two factors.

7.3.2. MFilm vs. W/D MFilm

Comparing the SEM images of MFilm and W/D MFilm , shows that once the MFilm is wetted and re-dried (Figure 7.1C, F, I), the mat structure does not appear to alter, but there appears to be material bridging hyphae at many intersections (fillets), which would suggest additional bonding between hyphae (Figure 7.1H vs 7.1I). To further investigate the changes happening at different depths from the surface, we prepared a series of z-stack light microscopy images of MFoam, MFilm and W/D MFilm (Figure 7.3 A, B and C). In this figure, the numbers from 1 to 7 indicate the images taken from the first visible hypha on the surface down to 90 µm depth at 15 µm intervals. For MFoam and MFilm, the individual hyphae were clear and distinct up to Figure 7.3 A6 and B6, whereas for W/D MFilm, there was no distinct hyphae observed in Figure 7.3 C4. Therefore, the densification of the surface and the swelling of hyphae may attribute the change of wettability and surface hydrophobicity.

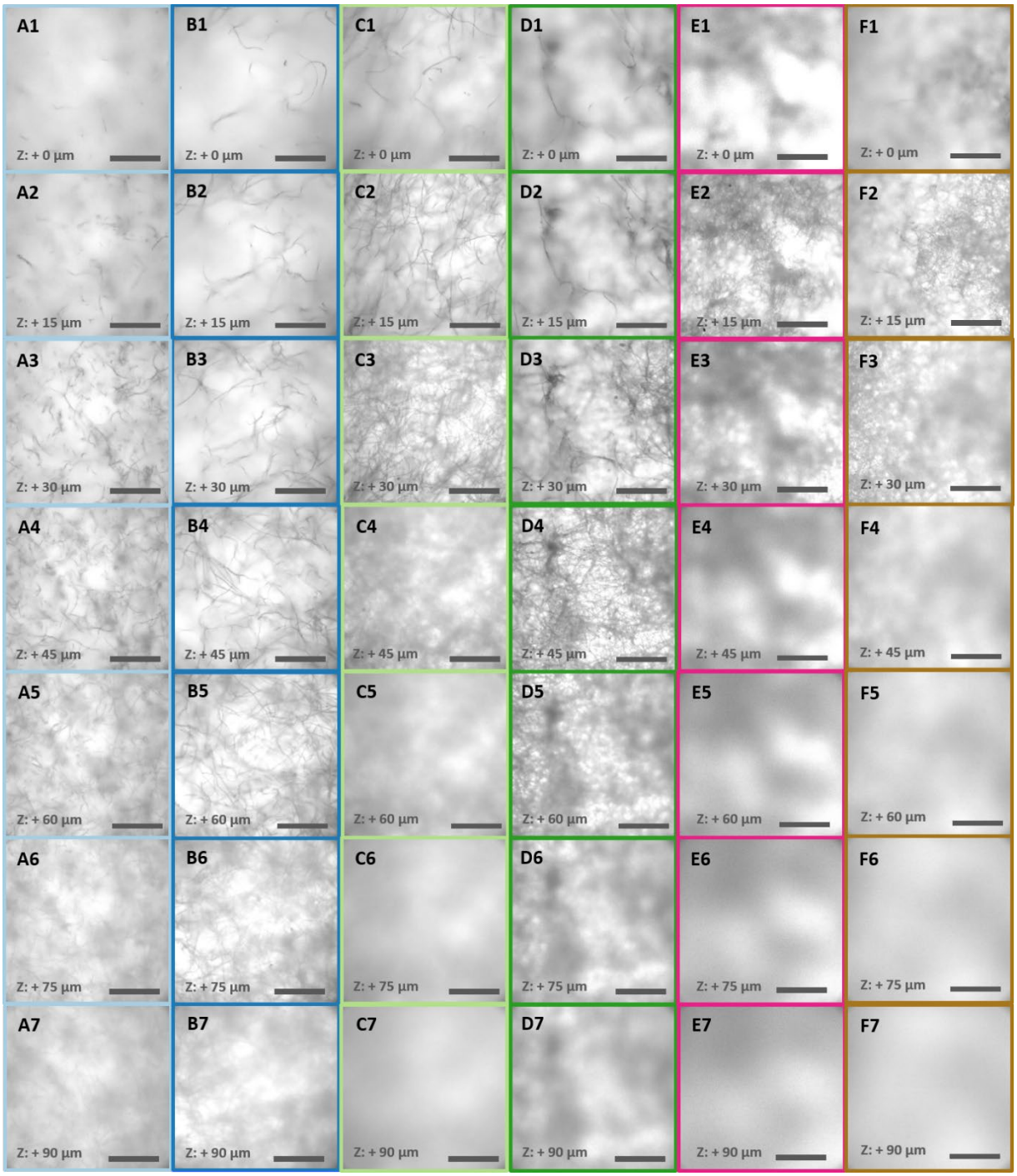

Figure 7.3. Z-stack images of (A) MFoam, (B) MFilm, (C) W/D MFilm (drying condition: 20 °C and 15 ± 5 %RH), (D) Acid treated MFilm, (E) W/D MFilm after conditioning (50 °C and 80%RH) for 15 days, (F) Acid-treated film after conditioning (50 °C and 80%RH) for 15 days. Scale bar: 100 µm.

Changes in surface morphology and arrangements of chemical components of W/D MFilm may also trap more water molecules in the structure and thus influence the wettability. To measure the potential small changes in moisture content, thermogravimetric analysis was applied on MFilm and W/D MFilm conditioned at the same room temperature and humidity (20 ± 1 °C and 15 ± 5 % RH). As shown in Table 1, the moisture content of both MFilm and W/D MFilm were both about 10% and there was no significant difference ($p > 0.05$) between the moisture contents of the two films.

Considering the fact that the total moisture content may not fully represent the mycelium surface, we also calculated the ratio of O-H and C-O groups on the surface spectra curve obtained from ATR-FTIR analysis. The OH/CO ratio of W/D MFilm was 0.02 (11%) higher than the ratio in the MFilm, indicating that there was a potential increase in available hydroxyl groups, which may contribute to the increased wetting.

Table 7.1. Moisture content (%) determined by thermogravimetric analysis and OH/CO ratio determined by ATR-FTIR of MFilm and W/D MFilm.

Groups	**MFilm**	**W/D MFilm**
Moisture content (%)	10.1 (± 2.31)	10.2 (± 0.97)
OH/CO ratio	0.18 (± 0.01)	0.20 (± 0.00)

7.3.3. Tunability of wetting/absorption

To evaluate potential surface chemistry changes influencing wettability, we further designed conditioning tests to understand if the surface wettability would change when the surface is exposed to higher temperature and/or humidity conditions. Comparisons of the wettability of the wetted/redried mycelium film exposed to different temperatures and relative humidity, as measured by the change in contact angle and total wetting time under lab conditions is presented in Figure 7.4. As shown in Figure 4A and 4B, temperature has a noticeable effect on both the contact angle and wetting time of the MFilm. The

two groups that were conditioned at 20 °C both showed a noticeably lower contact angle and wetting time (Figure 7.4A and 7.4B). When conditioning at high temperature (50 °C), the initial contact angle returned to > 120° after 3 days for high (80%) RH or 9 days at low (3%) RH and remained stable afterwards. However, for the two groups that were conditioned at room temperature, the contact angle only returned to ~110°. The wetting time showed a similar trend as well. At high humidity, the conditioning treatment performance was better, which might be explained by the plasticization effect of water on the material matrix allowing rearrangement of amphiphilic hydrophobin molecules back to their original pre-wetting condition. Figure 7.4D, E and F show the surface morphology of the wetted mycelium film after being conditioned for 15 days under 50 °C and 80%RH, 50 °C and 3%RH and 20 °C and 50%RH, respectively. Compared with Figure 1I, the swelling of hyphae remains similar in both groups. The distance between different layers of hyphae is not clear in the SEM images, but from the z-stack images shown in Figure 7.3C and E, there are no noticeable changes in the z-distance of the W/D MFilm before and after conditioning. Additionally, although the high-temperature conditioning was able to reverse the wettability of the mycelium surface, wetting/absorption time (Figure 7.3B) was still 10 times faster than the original mycelium films (Figure 7.2B), which could be explained by the increase of the surface in contact with the water droplet.

To test the tunability of the MFilm surface properties, the wetting, drying, and conditioning processes (3 days in total) were repeated for five cycles. The changes in contact angles are shown in Figure 4C, confirming the consistent switching of wettability over five cycles. It can be seen that regardless of conditioning treatment applied, the high initial contact angles can be restored by conditioning even after five cycles of wetting/redrying/conditioning.

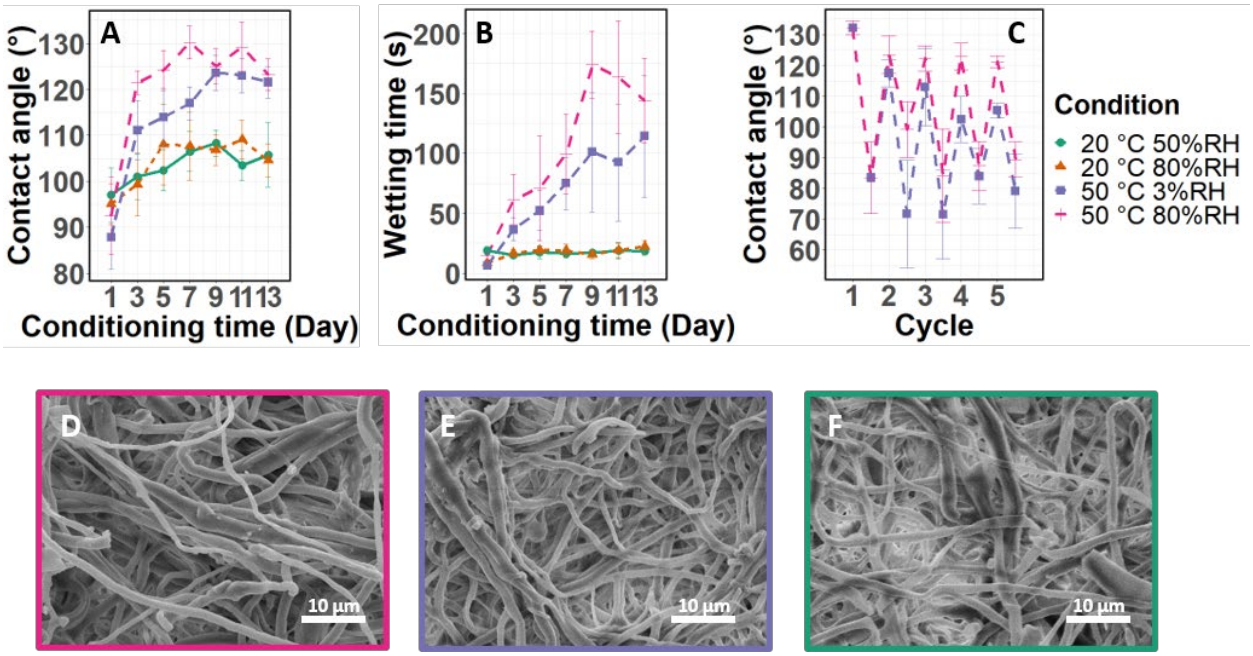

Figure 7.4. Changes in W/D MFilm (A) contact angle and (B) wetting/absorption time, with conditioning time. Window (C) shows the switch of wettability after multiple wetting, drying, and conditioning cycles; SEM images of W/D MFilm after conditioning for 13 days at (D) 50 °C and 80%RH, (E) 50 °C and 3%RH, and (F) 20 °C and 50%RH are also presented. Scale bar: 10 µm.

7.3.4. The role of hydrophobins

To further confirm that hydrophobins were indeed the cause of the observed switchable hydrophobicity, we treated the MFilm with formic acid to extract the hydrophobin proteins. We used very low temperature (4 °C) to minimize changes to other structural components. The wettability of the MFilm before and after formic acid treatment were compared and shown in Figure 7.5A and 7.5B. Formic acid-washed W/D MFilms lost their ability to become hydrophobic again after conditioning (Figure 7.5B), a result consistent with the proposed hydrophobin mechanism of switchable hydrophobicity. Figure 7.5C shows the SEM image of acid treated MFilm. The morphology is quite similar compared with that of the W/D film. The z-stack image series suggests that densification is slightly lower than that of the W/D MFilm but more than the MFilm (Figure 7.3D) and that there is not much difference in z-distance of acid-treated film after conditioning compared with the W/D film (Figure 7.3F).

TGA and ATR-FTIR were carried out on the untreated and acid treated MFilms to reveal if there are corresponding changes of the chemical component. In the ATR-FTIR curves shown in Figure 7.5F, the amide I (1644 cm^{-1}) and amide II (1540 cm^{-1}) peaks, which are attributed to C=O stretching and N-H bending (Lecellier et al., 2014) do not show a marked difference compared to the untreated MFilm. The peak at 1340 and 1250 cm^{-1} as amide III region attributed to C-N stretching and N-H bending decreased remarkably, which may relate to the partial removal of surface hydrophobins. The peak at 1716 cm^{-1} representing C=O stretching, showed up in the acid treated sample, which may have been caused by the residual formic acid in the structure (Zhang et al., 2010). The peak at 1155 cm^{-1} corresponding to the stretching of C-O is much higher in acid-treated samples than in the untreated sample; this may indicate more exposed polysaccharides. This could also be confirmed by the presence of the peak at 930 cm^{-1} which represents the vibration of C-O-C bridge (Fernando et al., 2017).

The Hi-Res option of TGA is often used to differentiate overlapping or close decomposition peaks. As shown in the DTG curve (Figure 7.5E), two peaks appearing at 231 and 250 °C were separated in the curve of untreated MFilm whereas there was only one peak shown in the acid treated MFilm. The disappearance of one peak indicates that the amount of one component in the MFilm has notably decreasing after acid treatment. In the TG curve (Figure 7.5D), the acid treated MFilm showed less residue after 600 °C, which may have been caused by the release of acidic species catalyzing the dehydration of carbohydrates to produce more thermally stable char (Alongi et al., 2014).

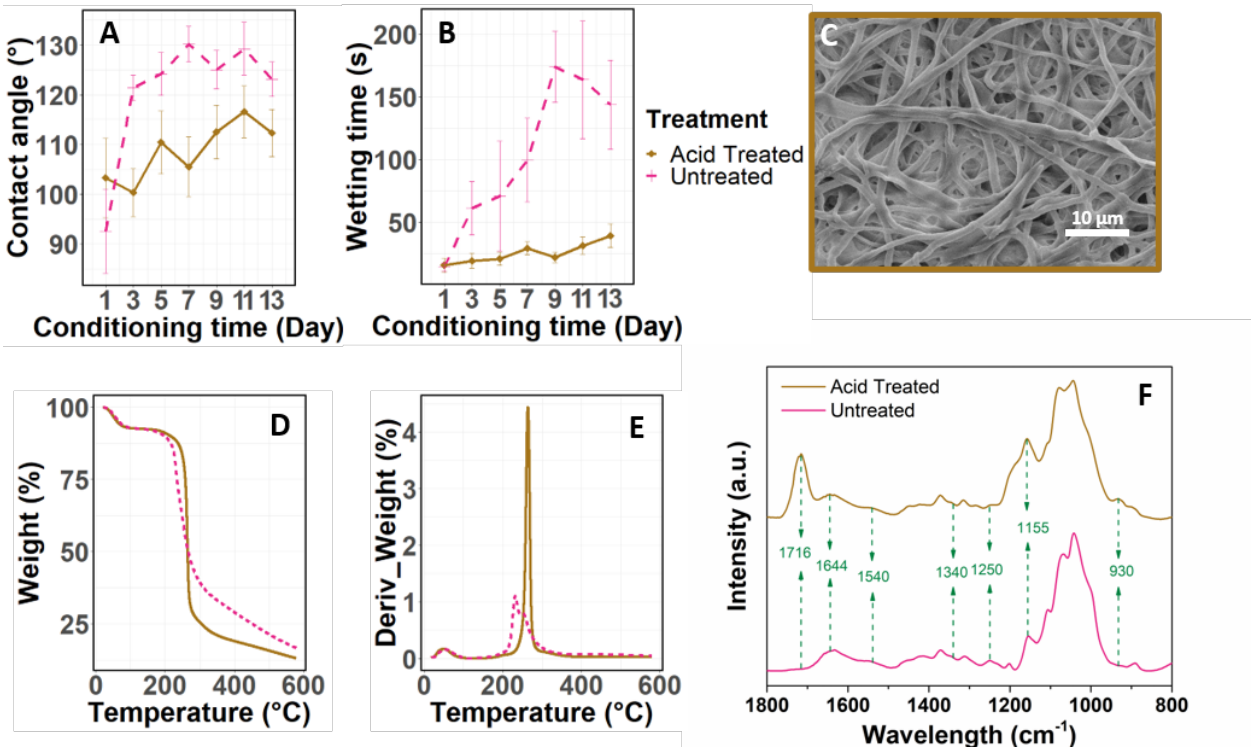

Figure 7.5. Influence of (A) acid treatment on the contact angle and (B) wetting time after conditioning at 50 °C and 80%RH C: SEM image of acid-treated film surface. Scale bar: 10 µm. (D) TG, (E) DTG and (F) FTIR curves of untreated and acid-treated MFilm.

7.3.5. Potential applications

The switchable wetting properties of this commercially available natural material has the potential to be used in many applied areas. Figure 7.6 shows two possible applications. The first application is patterning on MFilm (Figure 7.6A). In this example, the background of the letters was masked by an adhesive tape where the areas covered by letters were treated with water. The wettability of the area of the letters changed from hydrophobic to hydrophilic by applying water (Figure 7.6A1) and room temperature drying (Figure 7.6A2). When a water-based dye is applied to the surface, the original pattern appears (Figure 7.6A3).

Figure 7.6B reveals the potential utilization of the MFilm in microfluidic-related applications. After treating the designed channel with water and letting it dry at room temperature, the channel becomes hydrophilic while other background areas remain hydrophobic. The applied drop of water then moves back

and forth across the film following the channel. One issue for this application is that once the surface becomes hydrophilic, it also becomes absorbing. In this example, the water drop was partially absorbed and lost its original volume once it passed through the channel. Further modification and designs are needed to overcome this issue.

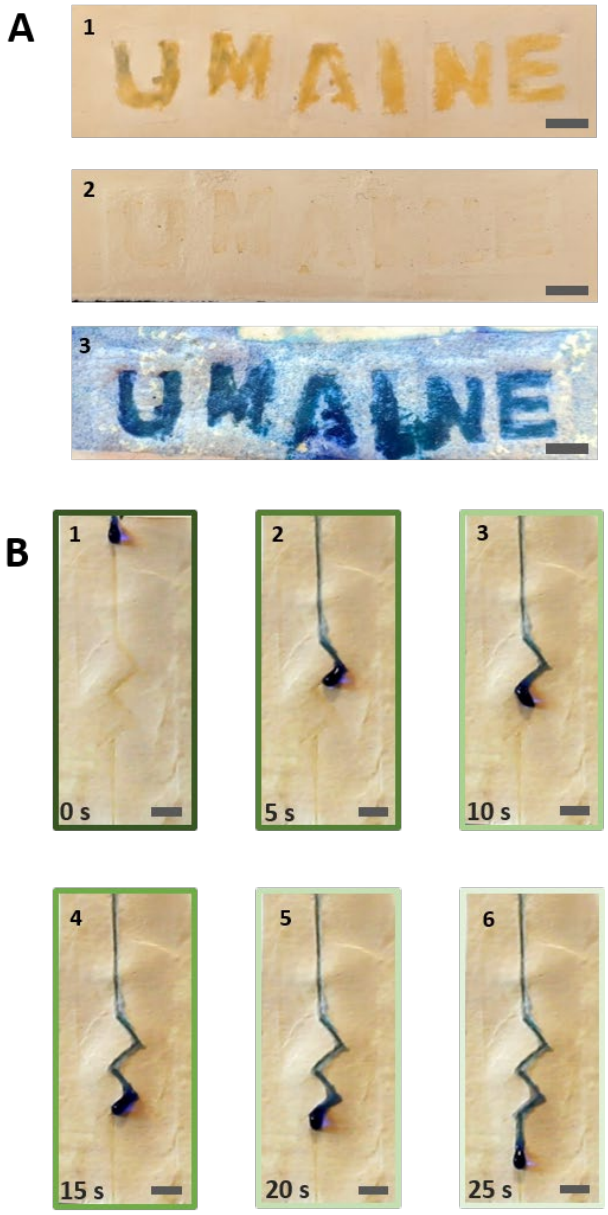

Figure 7.6. (A): Patterning process of MFilm. The area not covered by UMAINE letters was masked by an adhesive tape before water treatment. (B): Potential microfluidic channel application. Scale bar: 5 mm.

Apart from potential applications, considering the similarities of the hydrophobicity of aerial mycelium of different species of basidiomycete fungi, we also conducted similar tests on the mycelium of a known fungal species (*Trametes versicolor*) grown in the lab. We obtained very similar results of the switchable wetting properties (shown in Table 7.2, Figure 7.7 and Figure 7.8). Therefore, we can expect that this tunable wettability may be common within the basidiomycete family and more fungal species can be investigated in future to identify appropriate species or strains of fungus for specific applications.

Table 7.2. Contact angle and moisture content comparison of *T.vers* MFilm and *T.vers* W/D MFilm

	***T.vers* MFilm**	***T.vers* W/D MFilm**
Contact angle (°)	126.4 (±5.6)	94.1 (±12.7)
Moisture content (%)	9.98 (±1.27)	9.84 (± 0.59)

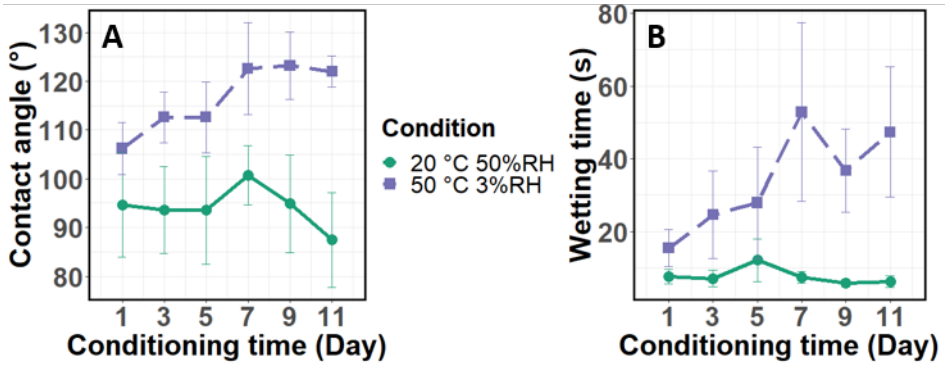

Figure 7.7. Change of (A) contact angle and (B) wetting time with conditioning time for T.vers W/D MFilm.

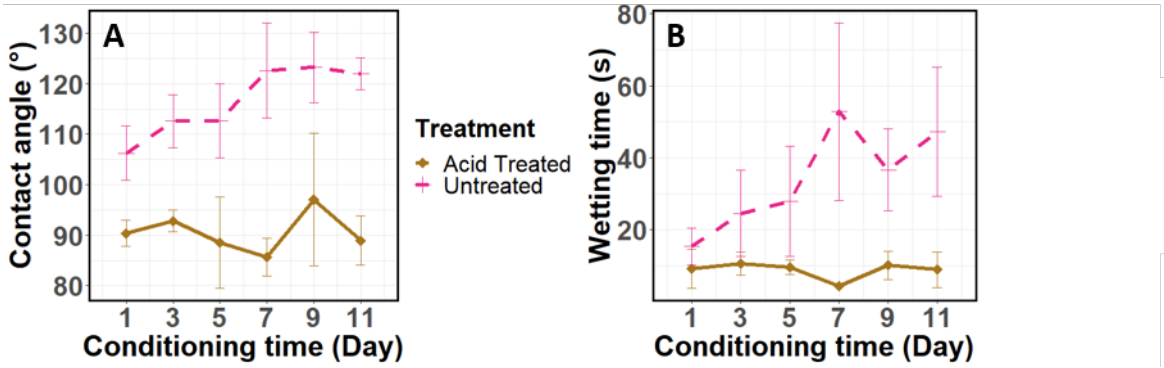

Figure 7.8. Influence of acid treatment on the contact angle (A) and wetting/absorption time (B) of *T.vers* W/D MFilm after different conditioning times (50 °C and 3%RH).

7.4 Conclusions

We have demonstrated a simple method to alter surface properties of a commercially available mycelium material that can be used to produce all-natural surfaces with reversible wettability. Surfaces can be made hydrophilic by forced wetting or prolonged water exposure, and hydrophobic by exposure to temperatures up to 50° C. The re-arrangement of amphiphilic protein hydrophobin was identified as the potential mechanism behind the behavior. Our findings suggest a possible low-cost and all-natural resource for multiple applications in different fields, such as microfluidics, smart coatings and self-cleaning surfaces.

CHAPTER 8

CONCLUSIONS

In this dissertation, the principal adhesion mechanisms involved in the production of mycelium bio-composites were investigated and further explored.

On the fundamental part, the functionality of surface mycelium for wood bonding was thoroughly investigated in **Chapter 3**. The results showed that the surface mycelium layer could also be utilized as a stand-alone adhesive to bond untreated wood. The bottom surface of the mycelium was found to be denser, flatter, more hydrophilic, and provided stronger bonding than the top surface. The details of the interface bonding were further investigated in **Chapter 4**. The water-soluble components, which mainly contain proteins and carbohydrates, were revealed as the essential adhesion factor for mycelium bonding through hydrogen bonds, Van de Waals interactions and limited covalent bonds through Maillard reaction. Lower temperatures have also been confirmed to be sufficient. **Chapter 5** studied the bonding mechanism at the low and high-density 3D composite systems and found different contribution strategies of fungal mycelium. For low-density as-grown foam structures, fungal mycelium only worked as a binder, the lignocellulosic substrate material played an essential role in sound absorption and thermal insulation properties, and the denser mycelium structure had a negative effect on them. In a higher-density hot-pressed panel system, fungal mycelium contributed to bonding and reinforced the bio-composite by filling the gaps. In summary, hydrogen bonds and Van der Waals interactions provide the majority of adhesion in the system based on the low wet strength. We found some evidence of covalent bonds forming at both wood-wood interface and wood-mycelium interface based on chemical characterizations through XPS, FTIR and NMR, but they are not enough to provide sufficient wet strength. Mechanical interlocking does not promote the bonding at wood-wood interface but in the 3D wood-mycelium composite structure, the mycelium was interlocked between wood particles, which provide sufficient bonding for the system.

The unique adhesion properties of mycelium were also explored based on their unique properties. **Chapter 6** demonstrated a hybrid system of wood, mycelium and CNF. The added CNF formed a uniform film over the particles and improved the physical and mechanical properties of the composites at different

density levels. **Chapter 7** demonstrated a simple method to alter surface properties of a commercially available mycelium material that can be used to produce all-natural surfaces with reversible wettability, and suggest a possible low-cost and all-natural resource for multiple applications in different fields, such as microfluidics, smart coatings and self-cleaning surfaces.

Overall, this dissertation contributes to the scientific knowledge of the adhesion mechanism of a newly developed bonding material and system and also provides potential improvement strategies and development directions. As mycelium-based novel materials had only been invented in the most recent twenty years, there is a broad industry with many potentials for people to explore. Finding the best application area that benefits from the advantages of this material might be the premier approach.

REFERENCES

Abhijith, R., Ashok, A., & Rejeesh, C. R. (2018). Sustainable packaging applications from mycelium to substitute polystyrene: a review. *Materials Today: Proceedings*, *5*(1), 2139-2145. https://doi.org/10.1016/j.matpr.2017.09.211

Ahmed, A., Narayanan, R. A., & Veni, A. R. (2020). Influence of carbon source complexity on porosity, water retention and extracellular matrix composition of Neurospora discreta biofilms. *Journal of Applied Microbiology*, *128*(4), 1099-1108. https://doi.org/10.1111/jam.14539

Aimanianda, V., Bayry, J., Bozza, S., Kniemeyer, O., Perruccio, K., Elluru, S. R., . . . Latge, J. P. (2009). Surface hydrophobin prevents immune recognition of airborne fungal spores. *Nature*, *460*(7259), 1117-1121. https://doi.org/10.1038/nature08264

Alongi, J., Carletto, R. A., Bosco, F., Carosio, F., Di Blasio, A., Cuttica, F., . . . Malucelli, G. (2014). Caseins and hydrophobins as novel green flame retardants for cotton fabrics. *Polymer Degradation and Stability*, *99*, 111-117. https://doi.org/10.1016/j.polymdegradstab.2013.11.016

Álvarez, C., Rojano, B., Almaza, O., Rojas, O. J., & Gañán, P. (2010). Self-Bonding Boards From Plantain Fiber Bundles After Enzymatic Treatment: Adhesion Improvement of Lignocellulosic Products by Enzymatic Pre-Treatment [journal article]. *Journal of Polymers and the Environment*, *19*(1), 182-188. https://doi.org/10.1007/s10924-010-0260-6

Amini, E., Tajvidi, M., Gardner, D. J., & Bousfield, D. W. (2017). Utilization of Cellulose Nanofibrils as a Binder for Particleboard Manufacture. *BioResources*, *12*(2), 4093-4110.

ANSI. (2016a). Medium Density Fiberboard (MDF) for Interior Applications. In (Vol. ANSI A208.2). Leesburg, VA: Composite Panel Association.

ANSI. (2016b). Particleboard. In (Vol. ANSI A208.1). Leesburg, VA: Composite Panel Association.

Antinori, M. E., Ceseracciu, L., Mancini, G., Heredia-Guerrero, J. A., & Athanassiou, A. (2020). Fine-Tuning of Physicochemical Properties and Growth Dynamics of Mycelium-Based Materials. *ACS Applied Bio Materials*, *3*(2), 1044-1051. https://doi.org/10.1021/acsabm.9b01031

Appels, F. V., Camere, S., Montalti, M., Karana, E., Jansen, K. M., Dijksterhuis, J., . . . Design. (2019). Fabrication factors influencing mechanical, moisture-and water-related properties of mycelium-based composites. *Materials and Design*, *161*, 64-71.

Appels, F. V. W., Dijksterhuis, J., Lukasiewicz, C. E., Jansen, K. M. B., Wosten, H. A. B., & Krijgsheld, P. (2018). Hydrophobin gene deletion and environmental growth conditions impact mechanical properties of mycelium by affecting the density of the material. *Scientific Reports*, *8*(1), 4703. https://doi.org/10.1038/s41598-018-23171-2

Arévalo, R., & Peijs, T. (2016). Binderless all-cellulose fibreboard from microfibrillated lignocellulosic natural fibres. *Composites Part A Applied Science and Manufacturing*, *83*, 38-46. http://www.sciencedirect.com/science/article/pii/S1359835X15004376

Armenante, A., Longobardi, S., Rea, I., De Stefano, L., Giocondo, M., Silipo, A., . . . Giardina, P. (2010). The Pleurotus ostreatus hydrophobin Vmh2 and its interaction with glucans. *Glycobiology*, *20*(5), 594-602. https://doi.org/10.1093/glycob/cwq009

Asina, F. N. U., Brzonova, I., Kozliak, E., Kubátová, A., & Ji, Y. (2017). Microbial treatment of industrial lignin: Successes, problems and challenges [Review]. *Renewable and Sustainable Energy Reviews*, *77*, 1179-1205. https://doi.org/10.1016/j.rser.2017.03.098

ASTM. (2012). Standard Test Methods for Evaluating Properties of Wood-Base Fiber and Particle Panel Materials. In. West Conshohocken, PA: ASTM International.

ASTM. (2017a). Standard Test Method for Measuring Compressive Properties of Thermal Insulations. In: ASTM International.

ASTM. (2017b). Standard test method for steady-state thermal transmission properties by means of the heat flow meter apparatus. In: ASTM International.

ASTM. (2019). Standard Test Method for Impedance and Absorption of acoustical Materials Using a Tube, Two Microphones and a Digital Frequency Analysis. In.

Attias, N., Danai, O., Abitbol, T., Tarazi, E., Ezov, N., Pereman, I., & Grobman, Y. J. (2020). Mycelium bio-composites in industrial design and architecture: Comparative review and experimental analysis. *Journal of Cleaner Production*, *246*, 119037. https://doi.org/10.1016/j.jclepro.2019.119037

Bajoul Kakahi, F., Ly, S., Tarayre, C., Deschaume, O., Bartic, C., Wagner, P., . . . Delvigne, F. (2019). Modulation of fungal biofilm physiology and secondary product formation based on physico-chemical surface properties. *Bioprocess Biosyst Eng*, *42*(12), 1935-1946. https://doi.org/10.1007/s00449-019-02187-6

Bajwa, D. S., Holt, G. A., Bajwa, S. G., Duke, S. E., & McIntyre, G. (2017). Enhancement of termite (Reticulitermes flavipes L.) resistance in mycelium reinforced biofiber-composites. *Industrial Crops and Products*, *107*, 420-426. https://doi.org/10.1016/j.indcrop.2017.06.032

Bari, E., Daniel, G., Yilgor, N., Kim, J. S., Tajick-Ghanbary, M. A., Singh, A. P., & Ribera, J. (2020). Comparison of the Decay Behavior of Two White-Rot Fungi in Relation to Wood Type and Exposure Conditions. *Microorganisms*, *8*(12), 1931. https://doi.org/10.3390/microorganisms8121931

Bari, E., Taghiyari, H. R., Naji, H. R., Schmidt, O., Ohno, K. M., Clausen, C. A., & Bakar, E. S. (2016). Assessing the destructive behaviors of two white-rot fungi on beech wood. *International Biodeterioration & Biodegradation*, *114*, 129-140. https://doi.org/10.1016/j.ibiod.2016.06.010

Barsberg, S., & Thygesen, L. G. (1999). Spectroscopic properties of oxidation species generated in the lignin of wood fibers by a laccase catalyzed treatment: electronic hole state migration and stabilization in the lignin matrix. *Biochimica et Biophysica Acta*, *1472*(3), 625-642. https://doi.org/10.1016/s0304-4165(99)00192-0

Barthlott, W., & Neinhuis, C. (1997). Purity of the sacred lotus, or escape from contamination in biological surfaces. *Planta*, *202*(1), 1-8. https://doi.org/10.1007/s004250050096

Basu, G., Datta, M., Sengupta, S., Nath, D., & Debnath, S. (2021). Jute Felt for Noise Reduction: Understanding Effect of Pore Size Distribution. *Journal of Natural Fibers*, 1-15. https://doi.org/10.1080/15440478.2021.1921663

Belleville, B., Koumba-Yoya, G., & Stevanovic, T. (2018). Effect of Wood Welding Process on Chemical Constituents of Australian Eucalyptus. *Journal of Wood Chemistry and Technology*, *39*(1), 43-56. https://doi.org/10.1080/02773813.2018.1494745

Belleville, B., Stevanovic, T., Cloutier, A., Pizzi, A., Prado, M., Erakovic, S., . . . Royer, M. (2013). An investigation of thermochemical changes in Canadian hardwood species during wood welding [journal article]. *European Journal of Wood and Wood Products*, *71*(2), 245-257. https://doi.org/10.1007/s00107-013-0671-x

Bhatt, I. M., Pramod, S., Koyani, R. D., & Rajput, K. S. (2016). Histological changes in the cell wall structure during wood decay byTrametes hirsutaandTrametes versicolorin neem (Azadirachta IndicaA. Juss). *Journal of Sustainable Forestry*, *35*(8), 578-590. https://doi.org/10.1080/10549811.2016.1236277

Bidochka, M. J., St Leger, R. J., Joshi, L., & Roberts, D. W. (1995). The rodlet layer from aerial and submerged conidia of the entomopathogenic fungus Beauveria bassiana contains hydrophobin. *Mycological Research*, *99*(4), 403-406. https://doi.org/10.1016/s0953-7562(09)80637-0

Brazdausks, P., Tupciauskas, R., Andzs, M., Rizhikovs, J., Puke, M., Paze, A., . . . Vedernikovs, N. (2015). Preliminary study of the biorefinery concept to obtain furfural and binder-less panels from hemp (Cannabis Sativa L.) shives. In S. Valtere (Ed.), *International Scientific Conference Environmental and Climate Technologies, Conect 2014* (Vol. 72, pp. 34-41). Elsevier Science Bv. https://doi.org/10.1016/j.egypro.2015.06.006

Bruck, J. (2017). Current and future needs of the wood based furniture industry. *Proceedings of International Conference on Wood Adhesives*.

Carlile, M. J. (1995). The Success of the Hypha and Mycelium. In N. A. R. Gow & G. M. Gadd (Eds.), *The Growing Fungus* (pp. 3-19). Springer Netherlands. https://doi.org/10.1007/978-0-585-27576-5_1

Chandra, S., di Marzo, M., Qiao, Y. M., & Tartarini, P. (1996). Effect of liquid-solid contact angle on droplet evaporation. *Fire Safety Journal*, *27*(2), 141-158. https://doi.org/10.1016/s0379-7112(96)00040-9

Chaturvedi, V., & Verma, P. (2013). An overview of key pretreatment processes employed for bioconversion of lignocellulosic biomass into biofuels and value added products. *3 Biotech*, *3*(5), 415-431. https://doi.org/10.1007/s13205-013-0167-8

Chen, Y., St.Ange, K., Lin, L., Liu, X., Zhang, X., & Linhardt, R. J. (2017). Quantitative analysis of the major linkage region tetrasaccharides in heparin. *Carbohydrate Polymers*, *157*, 244-250. https://doi.org/https://doi.org/10.1016/j.carbpol.2016.09.081

Cheng, H., & He, Z. (2017). Wood adhesives containing proteins and carbohydrates. In *Bio-Based Wood Adhesives: Preparation, Characterization* (pp. 140-155). CRC Press.

Cristescu, C., & Karlsson, O. (2013). Changes in content of furfurals and phenols in self-bonded laminated boards. *BioResources*, *8*(3), 4056-4071.

de Paula, R. G., Antonieto, A. C. C., Ribeiro, L. F. C., Srivastava, N., O'Donovan, A., Mishra, P. K., . . . Silva, R. N. (2019). Engineered microbial host selection for value-added bioproducts from

lignocellulose. *Biotechnology Advances*, *37*(6), 107347, Article 107347. https://doi.org/10.1016/j.biotechadv.2019.02.003

de Vries, O. M. H., Fekkes, M. P., Wösten, H. A. B., & Wessels, J. G. H. (1993). Insoluble hydrophobin complexes in the walls of Schizophyllum commune and other filamentous fungi. *Archives of Microbiology*, *159*(4), 330-335. https://doi.org/10.1007/bf00290915

Delmotte, L., Ganne-Chedeville, C., Leban, J. M., Pizzi, A., & Pichelin, F. (2008). CP-MAS 13C NMR and FT-IR investigation of the degradation reactions of polymer constituents in wood welding. *Polymer Degradation and Stability*, *93*(2), 406-412. https://doi.org/10.1016/j.polymdegradstab.2007.11.020

Diop, C. I. K., Tajvidi, M., Bilodeau, M. A., Bousfield, D. W., & Hunt, J. F. (2017). Isolation of lignocellulose nanofibrils (LCNF) and application as adhesive replacement in wood composites: example of fiberboard [journal article]. *Cellulose*, *24*(7), 3037-3050. https://doi.org/10.1007/s10570-017-1320-z

Dolan, J. A., Sathitsuksanoh, N., Rodriguez, K., Simmons, B. A., Frazier, C. E., & Renneckar, S. (2015). Biocomposite adhesion without added resin: understanding the chemistry of the direct conversion of wood into adhesives. *Rsc Advances*, *5*(82), 67267-67276. https://doi.org/10.1039/c5ra09676f

Dufresne, A. (2017). *Nanocellulose: from nature to high performance tailored materials*. Walter de Gruyter GmbH & Co KG.

Duvnjak, D., Pantić, M., Pavlović, V., Nedović, V., Lević, S., Matijašević, D., . . . Nikšić, M. (2016). Advances in batch culture fermented Coriolus versicolor medicinal mushroom for the production of antibacterial compounds. *Innovative Food Science & Emerging Technologies*, *34*, 1-8. https://doi.org/10.1016/j.ifset.2015.12.028

Dziurka, D., & Mirski, R. (2013). Lightweight boards from wood and rape straw particles. *Drewno*, *56*(190), 19-31. https://doi.org/10.12841/wood.1644-3985.051.02

Ecovative. (2017). https://ecovativedesign.com/myco-board

Ecovative. (2018). https://s3-us-west-2.amazonaws.com/ecovative-website-production/documents/EcovativeDesignSpecSheet_1.06.pdf

Elsacker, E., Vandelook, S., Van Wylick, A., Ruytinx, J., De Laet, L., & Peeters, E. (2020). A comprehensive framework for the production of mycelium-based lignocellulosic composites. *Science of the Total Environment*, *725*, 138431. https://doi.org/10.1016/j.scitotenv.2020.138431

Engelund, E. T., Thygesen, L. G., Svensson, S., & Hill, C. A. S. (2012). A critical discussion of the physics of wood–water interactions. *Wood Science and Technology*, *47*(1), 141-161. https://doi.org/10.1007/s00226-012-0514-7

EPA. (2017). Formaldehyde Emission Standards for Composite Wood Products EPA-HQ-OPPT-2016-0461. In. Washington DC.

Euring, M. (2008). *Einsatz von Mediatoren bei der enzymatischen Aktivierung der fasereigenen Bindekräfte zur Herstellung von enzymgebundenen, bindemittelfreien Holzwerkstoffen* Niedersächsische Staats-und Universitätsbibliothek Göttingen].

Euring, M., Kirsch, A., Schneider, P., & Kharazipour, A. (2016). Lignin-laccasemediator-systems (LLMS) for the production of binderless medium density fiberboards (MDF). *Journal of Materials Science Research*, *5*(2), 7. https://doi.org/http://dx.doi.org/10.5539/jmsr.v5n2p7

Euring, M., Ruhl, M., Ritter, N., Kues, U., & Kharazipour, A. (2011). Laccase mediator systems for eco-friendly production of medium-density fiberboard (MDF) on a pilot scale: physicochemical analysis of the reaction mechanism. *Biotechnol J*, *6*(10), 1253-1261. https://doi.org/10.1002/biot.201100119

Euring, M., Trojanowski, J., Horstmann, M., & Kharazipour, A. (2011). Studies of enzymatic oxidation of TMP-fibers and lignin model compounds by a Laccase–Mediator-System using different 14C and 13C techniques. *Wood Science and Technology*, *46*(4), 699-708. https://doi.org/10.1007/s00226-011-0439-6

Euring, M., Trojanowski, J., & Kharazipour, A. (2013). Laccase-Mediator Catalyzed Modification of Wood Fibers: Studies on the Reaction Mechanism and Making of Medium-Density Fiberboard. *Forest Products Journal*, *63*(1-2), 54-60. https://doi.org/10.13073/fpj-d-12-00075

Fackler, K., Gradinger, C., Schmutzer, M., Tavzes, C., Burgert, I., Schwanninger, M., . . . Messner, K. (2007). Biotechnological wood modification with selective white-rot fungi and its molecular mechanisms [Review]. *Food Technology and Biotechnology*, *45*(3), 269-276. <Go to ISI>://WOS:000249369700006

Fackler, K., Schmutzer, M., Manoch, L., Schwanninger, M., Hinterstoisser, B., Ters, T., . . . Gradinger, C. (2007). Evaluation of the selectivity of white rot isolates using near infrared spectroscopic techniques. *Enzyme and Microbial Technology*, *41*(6-7), 881-887. https://doi.org/10.1016/j.enzmictec.2007.07.016

Fackler, K., Schwanninger, M., Gradinger, C., Hinterstoisser, B., & Messner, K. (2007). Qualitative and quantitative changes of beech wood degraded by wood-rotting basidiomycetes monitored by Fourier transform infrared spectroscopic methods and multivariate data analysis. *FEMS Microbiology Letters*, *271*(2), 162-169. https://doi.org/10.1111/j.1574-6968.2007.00712.x

Fackler, K., Stevanic, J. S., Ters, T., Hinterstoisser, B., Schwanninger, M., & Salmén, L. (2011). FT-IR imaging microscopy to localise and characterise simultaneous and selective white-rot decay within spruce wood cells. *Holzforschung*, *65*(3), 411-420. https://doi.org/10.1515/hf.2011.048

FAO. (2020, Wednesday, December 30, 2020). *Global production and trade in forest products in 2019*. Food and Agriculture Organization of the United Nations.

Felby, C., Hassingboe, J., & Lund, M. (2002). Pilot-scale production of fiberboards made by laccase oxidized wood fibers: board properties and evidence for cross-linking of lignin. *Enzyme and Microbial Technology*, *31*(6), 736-741. https://doi.org/10.1016/s0141-0229(02)00111-4

Felby, C., Pedersen, L. S., & Nielsen, B. R. (1997). Enhanced auto adhesion of wood fibers using phenol oxidases. *Holzforschung-International Journal of the Biology, Chemistry, Physics and Technology of Wood*, *51*(3), 281-286. https://doi.org/https://doi.org/10.1515/hfsg.1997.51.3.281

Felby, C., Thygesen, L. G., Sanadi, A., & Barsberg, S. (2004). Native lignin for bonding of fiber boards—evaluation of bonding mechanisms in boards made from laccase-treated fibers of beech (Fagus

sylvatica). *Industrial Crops and Products*, *20*(2), 181-189. https://doi.org/10.1016/j.indcrop.2004.04.020

Ferdosian, F., Pan, Z., Gao, G., & Zhao, B. (2017). Bio-Based Adhesives and Evaluation for Wood Composites Application [Review]. *Polymers (Basel)*, *9*(2), 29, Article 70. https://doi.org/10.3390/polym9020070

Fernando, I., Sanjeewa, K., Samarakoon, K. W., Lee, W. W., Kim, H.-S., Kim, E.-A., . . . De Silva, E. (2017). FTIR characterization and antioxidant activity of water soluble crude polysaccharides of Sri Lankan marine algae. *Algae*, *32*(1), 75-86.

Gardner, D., & Tajvidi, M. (2016). Hydrogen bonding in wood-based materials: an update. *Wood and Fiber Science*, *48*(4), 234-244. https://doi.org/https://doi.org/10.4490/algae.2017.32.12.1

Gardner, D. J., Blumentritt, M., Wang, L., & Yildirim, N. (2014). Adhesion theories in wood adhesive bonding. *Reviews of Adhesion and Adhesives*, *2*(2), 127-172. https://doi.org/https://doi.org/10.7569/RAA.2014.097304

Ghasemi, S., Tajvidi, M., Bousfield, D. W., Gardner, D. J., & Gramlich, W. M. (2017). Dry-Spun Neat Cellulose Nanofibril Filaments: Influence of Drying Temperature and Nanofibril Structure on Filament Properties [Article]. *Polymers (Basel)*, *9*(9), 13, Article 392. https://doi.org/10.3390/polym9090392

Girometta, C., Dondi, D., Baiguera, R. M., Bracco, F., Branciforti, D. S., Buratti, S., . . . Savino, E. (2020). Characterization of mycelia from wood-decay species by TGA and IR spectroscopy. *Cellulose*, *27*(11), 6133-6148. https://doi.org/10.1007/s10570-020-03208-4

Girometta, C., Picco, A. M., Baiguera, R. M., Dondi, D., Babbini, S., Cartabia, M., . . . Savino, E. (2019). Physico-Mechanical and Thermodynamic Properties of Mycelium-Based Biocomposites: A Review. *Sustainability*, *11*(1), 281. https://doi.org/https://doi.org/10.3390/su11010281

Gorshkova, R. P., Isakov, V. V., Nazarenko, E. L., Ovodov, Y. S., Guryanova, S. V., & Dmitriev, B. A. (1993). Structure of the O-specific polysaccharide of the lipopolysaccharide from Yersinia kristensenii O:25.35. *Carbohydrate Research*, *241*, 201-208. https://doi.org/https://doi.org/10.1016/0008-6215(93)80106-O

Gow, N. A. R., Latge, J. P., & Munro, C. A. (2017). The Fungal Cell Wall: Structure, Biosynthesis, and Function [Article]. *Microbiol Spectr*, *5*(3), 25, Article Unsp funk-0035-2016. https://doi.org/10.1128/microbiolspec.FUNK-0035-2016

Grønli, M. G., Várhegyi, G., & Di Blasi, C. (2002). Thermogravimetric Analysis and Devolatilization Kinetics of Wood. *Industrial & Engineering Chemistry Research*, *41*(17), 4201-4208. https://doi.org/10.1021/ie0201157

Gunning, A. P., De Groot, P. W. J., Visser, J., & Morris, V. J. (1998). Atomic Force Microscopy of a Hydrophobin Protein from the Edible MushroomAgaricus bisporus. *Journal of Colloid and Interface Science*, *201*(2), 118-126. https://doi.org/10.1006/jcis.1998.5405

Guo, F., & Guo, Z. (2016). Inspired smart materials with external stimuli responsive wettability: a review [10.1039/C6RA04079A]. *Rsc Advances*, *6*(43), 36623-36641. https://doi.org/10.1039/c6ra04079a

Guo, Z., & Liu, W. (2007). Biomimic from the superhydrophobic plant leaves in nature: Binary structure and unitary structure. *Plant Science*, *172*(6), 1103-1112. https://doi.org/10.1016/j.plantsci.2007.03.005

Hakkou, M., Pétrissans, M., Zoulalian, A., & Gérardin, P. (2005). Investigation of wood wettability changes during heat treatment on the basis of chemical analysis. *Polymer Degradation and Stability*, *89*(1), 1-5. https://doi.org/10.1016/j.polymdegradstab.2004.10.017

Haneef, M., Ceseracciu, L., Canale, C., Bayer, I. S., Heredia-Guerrero, J. A., & Athanassiou, A. (2017). Advanced Materials From Fungal Mycelium: Fabrication and Tuning of Physical Properties. *Scientific Reports*, *7*, 41292. https://doi.org/10.1038/srep41292

He, Z. (2017). *Bio-based wood adhesives: preparation, characterization, and testing*. CRC Press.

Hemmilä, V., Adamopoulos, S., Karlsson, O., & Kumar, A. (2017). Development of sustainable bio-adhesives for engineered wood panels - A Review [Review]. *Rsc Advances*, *7*(61), 38604-38630. <Go to ISI>://WOS:000407442000059
http://pubs.rsc.org/en/content/articlepdf/2017/ra/c7ra06598a

Herrera, R., Erdocia, X., Labidi, J., & Llano-Ponte, R. (2015). Chemical analysis of industrial-scale hydrothermal wood degraded by wood-rotting basidiomycetes and its action mechanisms. *Polymer Degradation and Stability*, *117*, 37-45. https://doi.org/10.1016/j.polymdegradstab.2015.03.013

Hofer, A., Hauer, S., Kroll, P., Fricke, J., & Herwig, C. (2018). In-depth characterization of the raw material corn steep liquor and its bioavailability in bioprocesses of Penicillium chrysogenum. *Process Biochemistry*, *70*, 20-28. https://doi.org/10.1016/j.procbio.2018.04.008

Hostikka, S., & Matala, A. (2017). Pyrolysis Model for Predicting the Heat Release Rate of Birch Wood. *Combustion Science and Technology*, *189*(8), 1373-1393. https://doi.org/10.1080/00102202.2017.1295959

Hu, D. L., Chan, B., & Bush, J. W. (2003). The hydrodynamics of water strider locomotion. *Nature*, *424*(6949), 663-666. https://doi.org/10.1038/nature01793

Hubbe, M. A., Pizzi, A., Zhang, H., & Halis, R. (2017). Critical Links Governing Performance of Self-binding and Natural Binders for Hot-pressed Reconstituted Lignocellulosic Board without Added Formaldehyde: A Review. *BioResources*, *13*(1), 2049-2115.

Hunt, C. G., Frihart, C. R., Dunky, M., & Rohumaa, A. (2018). Understanding Wood Bonds–Going Beyond What Meets the Eye: A Critical Review. *Reviews of Adhesion and Adhesives*, *6*(4), 369-440. https://doi.org/10.7569/raa.2018.097312

Ioannou, A. (2017). Study of maillard reactions with coupled chromatographic and spectroscopic techniques. In: Τμήμα Επιστήμης και Τεχνολογίας Περιβάλλοντος, Σχολή Γεωτεχνικών Επιστημών και Διαχείρισης Περιβάλλοντος, Τεχνολογικό Πανεπιστήμιο Κύπρου.

Ioannou, A., & Varotsis, C. (2017). Modifications of hemoglobin and myoglobin by Maillard reaction products (MRPs). *PloS one*, *12*(11), e0188095. https://doi.org/10.1371/journal.pone.0188095

Islam, M., Tudryn, G., Bucinell, R., Schadler, L., & Picu, R. (2018). Mechanical behavior of mycelium-based particulate composites. *Journal of Materials Science*, 1-12. https://doi.org/https://doi.org/10.1007/s10853-018-2797-z

Islam, M. R., Tudryn, G., Bucinell, R., Schadler, L., & Picu, R. C. (2017). Morphology and mechanics of fungal mycelium. *Scientific Reports*, *7*(1), 13070. https://doi.org/10.1038/s41598-017-13295-2

Jakes, J. E., Hunt, C. G., Zelinka, S. L., Ciesielski, P. N., & Plaza, N. Z. (2019). Effects of Moisture on Diffusion in Unmodified Wood Cell Walls: A Phenomenological Polymer Science Approach. *10*(12), 1084. https://www.mdpi.com/1999-4907/10/12/1084

Janusz, G., Pawlik, A., Sulej, J., Swiderska-Burek, U., Jarosz-Wilkolazka, A., & Paszczynski, A. (2017). Lignin degradation: microorganisms, enzymes involved, genomes analysis and evolution. *FEMS Microbiology Review*, *41*(6), 941-962. https://doi.org/10.1093/femsre/fux049

Johnson, D. A., Paradis, M. A., Bilodeau, M., Crossley, B., Foulger, M., & Gelinas, P. (2016). Effects of cellulosic nanofibrils on papermaking properties of fine papers [Article]. *Tappi Journal*, *15*(6), 395-402. <Go to ISI>://WOS:000380267900006

Jones, M., Bhat, T., & John, S. (2018). Inherent species characteristic influence and growth performance assessment for mycelium composite applications. *Advanced Materials Letters*, *9*(1), 71-80.

Jones, M., Bhat, T., Kandare, E., Thomas, A., Joseph, P., Dekiwadia, C., . . . Wang, C. H. (2018). Thermal Degradation and Fire Properties of Fungal Mycelium and Mycelium - Biomass Composite Materials. *Scientific Reports*, *8*(1), 17583. https://doi.org/10.1038/s41598-018-36032-9

Jones, M., Mautner, A., Luenco, S., Bismarck, A., & John, S. (2020). Engineered mycelium composite construction materials from fungal biorefineries: A critical review. *Materials & Design*, *187*, 108397. https://doi.org/10.1016/j.matdes.2019.108397

Jones, M. P., Lawrie, A. C., Huynh, T. T., Morrison, P. D., Mautner, A., Bismarck, A., & John, S. (2019). Agricultural by-product suitability for the production of chitinous composites and nanofibers utilising Trametes versicolor and Polyporus brumalis mycelial growth. *Process Biochemistry*, *80*, 95-102. https://doi.org/10.1016/j.procbio.2019.01.018

Julia, B. M., Belén, A. M., Georgina, B., & Beatriz, F. (2016). Potential use of soybean hulls and waste paper as supports in SSF for cellulase production by Aspergillus niger [Article]. *Biocatalysis and Agricultural Biotechnology*, *6*, 1-8. https://doi.org/10.1016/j.bcab.2016.02.003

Kershaw, M. J., & Talbot, N. J. (1998). Hydrophobins and repellents: proteins with fundamental roles in fungal morphogenesis. *Fungal Genet Biol*, *23*(1), 18-33. https://doi.org/10.1006/fgbi.1997.1022

Kharazipour, A., Bergmann, K., Nonninger, K., & Huttermann, A. (1998). Properties of fibre boards obtained by activation of the middle lamella lignin of wood fibres with peroxidase and H_2O_2 before conventional pressing. *Journal of Adhesion Science and Technology*, *12*(10), 1045-1053. https://doi.org/https://doi.org/10.1163/156856198X00713

Kharazipour, A., Huettermann, A., & Luedemann, H. D. (1997). Enzymatic activation of wood fibres as a means for the production of wood composites. *Journal of Adhesion Science and Technology*, *11*(3), 419-427. https://doi.org/10.1163/156856197x00796

Khoo, S. C., Peng, W. X., Yang, Y., Ge, S. B., Soon, C. F., Ma, N. L., & Sonne, C. (2020). Development of formaldehyde-free bio-board produced from mushroom mycelium and substrate waste. *Journal of Hazardous materials*, *400*, 123296. https://doi.org/10.1016/j.jhazmat.2020.123296

Kirsch, A., Ostendorf, K., Kharazipour, A., & Euring, M. (2016). Phenolics as Mediators to Accelerate the Enzymatically Initialized Oxidation of Laccase-Mediator-Systems for the Production of Medium Density Fiberboards. *BioResources*, *11*(3), 7091-7101. https://doi.org/10.15376/biores.11.3.7091-7101

Komal, A., Venkatesh, C., & Pradeep, V. (2018). Fungal laccase discovered but yet undiscovered. *Bioresources and Bioprocessing*, *5*(4). https://doi.org/https://doi.org/10.1186/s40643-018-0190-z

Kumar, R., Mago, G., Balan, V., & Wyman, C. E. (2009). Physical and chemical characterizations of corn stover and poplar solids resulting from leading pretreatment technologies. *Bioresource Technology*, *100*(17), 3948-3962. https://doi.org/10.1016/j.biortech.2009.01.075

Landry, V., & Blanchet, P. (2012). Surface preparation of wood for application of waterborne coatings. *Forest Products Journal*, *62*(1), 39-45. https://doi.org/https://doi.org/10.13073/FPJ-D-10-00011.1

Lecellier, A., Mounier, J., Gaydou, V., Castrec, L., Barbier, G., Ablain, W., . . . Sockalingum, G. D. (2014). Differentiation and identification of filamentous fungi by high-throughput FTIR spectroscopic analysis of mycelia. *Int J Food Microbiol*, *168-169*, 32-41. https://doi.org/10.1016/j.ijfoodmicro.2013.10.011

Lekounougou, S., Mounguengui, S., Dumarçay, S., Rose, C., Courty, P. E., Garbaye, J., . . . Gelhaye, E. (2008). Initial stages of Fagus sylvatica wood colonization by the white-rot basidiomycete Trametes versicolor: Enzymatic characterization. *International Biodeterioration and Biodegradation*, *61*(4), 287-293. https://doi.org/https://doi.org/10.1016/j.ibiod.2016.10.004

Leng, W., Hunt, J. F., & Tajvidi, M. (2017). Effects of Density, Cellulose Nanofibrils Addition Ratio, Pressing Method, and Particle Size on the Bending Properties of Wet-formed Particleboard. *BioResources*, *12*(3), 4986-5000.

Lew, R. R. (2011). How does a hypha grow? The biophysics of pressurized growth in fungi [Article]. *Nat Rev Microbiol*, *9*(7), 509-518. https://doi.org/10.1038/nrmicro2591

Li, K. (2003). The role of enzymes and mediators in white-rot fungal degradation of lignocellulose. In *Wood deterioration and preservation*. ACS Publications.

Li, N., Mao, W., Liu, X., Wang, S., Xia, Z., Cao, S., . . . Liu, S. (2016). Sequence analysis of the pyruvylated galactan sulfate-derived oligosaccharides by negative-ion electrospray tandem mass spectrometry. *Carbohydrate Research*, *433*, 80-88. https://doi.org/https://doi.org/10.1016/j.carres.2016.07.018

Linder, M. B., Szilvay, G. R., Nakari-Setala, T., & Penttila, M. E. (2005). Hydrophobins: the protein-amphiphiles of filamentous fungi. *FEMS Microbiology Review*, *29*(5), 877-896. https://doi.org/10.1016/j.femsre.2005.01.004

Liu, R., Li, X., Long, L., Sheng, Y., Xu, J., & Wang, Y. (2020). Improvement of mechanical properties of mycelium/cotton stalk composites by water immersion. *Composite Interfaces*, 1-14. https://doi.org/10.1080/09276440.2020.1716573

Liu, R., Long, L., Sheng, Y., Xu, J., Qiu, H., Li, X., . . . Wu, H. (2019). Preparation of a kind of novel sustainable mycelium/cotton stalk composites and effects of pressing temperature on the properties. *Industrial Crops and Products*, *141*, 111732. https://doi.org/10.1016/j.indcrop.2019.111732

Liu, X., Liang, Y., Zhou, F., & Liu, W. (2012). Extreme wettability and tunable adhesion: biomimicking beyond nature? [10.1039/C1SM07003G]. *Soft Matter*, *8*(7), 2070-2086. https://doi.org/10.1039/c1sm07003g

Lo, V. C., Ren, Q., Pham, C. L., Morris, V. K., Kwan, A. H., & Sunde, M. (2014). Fungal Hydrophobin Proteins Produce Self-Assembling Protein Films with Diverse Structure and Chemical Stability. *Nanomaterials (Basel)*, *4*(3), 827-843. https://doi.org/10.3390/nano4030827

Lokko, M.-l. J. (2016). *Invention, design and performance of coconut agrowaste fiberboards for ecologically efficacious buildings* Rensselaer Polytechnic Institute].

Longobardi, S., Picone, D., Ercole, C., Spadaccini, R., De Stefano, L., Rea, I., & Giardina, P. (2012). Environmental conditions modulate the switch among different states of the hydrophobin Vmh2 from Pleurotus ostreatus. *Biomacromolecules*, *13*(3), 743-750. https://doi.org/10.1021/bm201663f

Mantanis, G. I., Athanassiadou, E. T., Barbu, M. C., & Wijnendaele, K. (2017). Adhesive systems used in the European particleboard, MDF and OSB industries. *Wood Material Science & Engineering*, *13*(2), 104-116. https://doi.org/10.1080/17480272.2017.1396622

Mantanis, G. I., Athanassiadou, E. T., Barbu, M. C., & Wijnendaele, K. (2018). Adhesive systems used in the European particleboard, MDF and OSB industries. *Wood Material Science & Engineering*, *13*(2), 104-116. https://doi.org/https://doi.org/10.1080/17480272.2017.1396622

Maurya, D. P., Singla, A., & Negi, S. (2015). An overview of key pretreatment processes for biological conversion of lignocellulosic biomass to bioethanol. *3 Biotech*, *5*(5), 597-609. https://doi.org/10.1007/s13205-015-0279-4

Meyer, V., Basenko, E. Y., Benz, J. P., Braus, G. H., Caddick, M. X., Csukai, M., . . . Wosten, H. A. B. (2020). Growing a circular economy with fungal biotechnology: a white paper. *Fungal Biol Biotechnol*, *7*(1), 5. https://doi.org/10.1186/s40694-020-00095-z

Mishra, V., Jana, A. K., Jana, M. M., & Gupta, A. (2017). Improvement of selective lignin degradation in fungal pretreatment of sweet sorghum bagasse using synergistic CuSO4-syringic acid supplements. *Journal of Environment Management*, *193*, 558-566. https://doi.org/10.1016/j.jenvman.2017.02.057

MOGU. (2019). *Mogu floor preview book 2019*.

Mohebby, B. (2005). Attenuated total reflection infrared spectroscopy of white-rot decayed beech wood. *International Biodeterioration & Biodegradation*, *55*(4), 247-251. https://doi.org/10.1016/j.ibiod.2005.01.003

Monteiro, S., Martins, J., Magalhaes, F. D., & Carvalho, L. (2016). Low Density Wood-Based Particleboards Bonded with Foamable Sour Cassava Starch: Preliminary Studies. *Polymers (Basel)*, *8*(10), Article 354. https://doi.org/10.3390/polym8100354

Munk, L., Andersen, M. L., & Meyer, A. S. (2017). Direct rate assessment of laccase catalysed radical formation in lignin by electron paramagnetic resonance spectroscopy. *Enzyme and Microbial Technology*, *106*, 88-96. https://doi.org/10.1016/j.enzmictec.2017.07.006

Nadir, N., Ismail, N. L., & Hussain, A. S. (2019). Fungal Pretreatment of Lignocellulosic Materials. In *Biomass for Bioenergy-Recent Trends and Future Challenges*. IntechOpen.

Narayanaswamy, N., Dheeran, P., Verma, S., & Kumar, S. (2013). Biological Pretreatment of Lignocellulosic Biomass for Enzymatic Saccharification. In Z. Fang (Ed.), *Pretreatment Techniques for Biofuels and Biorefineries* (pp. 3-34). Springer Berlin Heidelberg. https://doi.org/10.1007/978-3-642-32735-3_1

Nasir, M., Gupta, A., Beg, M. D. H., Chua, G. K., & Asim, M. (2014). Laccase application in medium density fibreboard to prepare a bio-composite. *Rsc Advances*, *4*(22), 11520-11527. https://doi.org/10.1039/C3RA40593A

Nasir, M., Khali, D., Jawaid, M., Tahir, P., Siakeng, R., Asim, M., & Khan, T. (2019). Recent development in binderless fiber-board fabrication from agricultural residues: A review. *Construction and Building Materials*, *211*, 502-516. https://doi.org/https://doi.org/10.1016/j.conbuildmat.2019.03.279

Nasir, M., Sulaiman, O., Hashim, R., Hossain, K., Gupta, A., & Asim, M. (2015). Rubberwood fiber treatment by laccase enzyme and its application in medium density fiberboard. *Journal of Pure and Applied Microbiology*, *9*(3), 2095-2101.

Naumann, A. (2009). A novel procedure for strain classification of fungal mycelium by cluster and artificial neural network analysis of Fourier transform infrared (FTIR) spectra [10.1039/B821286D]. *Analyst*, *134*(6), 1215-1223. https://doi.org/10.1039/b821286d

Nazari, B., Kumar, V., Bousfield, D. W., & Toivakka, M. (2016). Rheology of cellulose nanofibers suspensions: boundary driven flow. *Journal of Rheology*, *60*(6), 1151-1159. https://doi.org/https://doi.org/10.1122/1.4960336

Neinhuis, C., & Barthlott, W. (1997). Characterization and Distribution of Water-repellent, Self-cleaning Plant Surfaces. *Annals of Botany*, *79*(6), 667-677. https://doi.org/10.1006/anbo.1997.0400 %J Annals of Botany

Nooshkam, M., & Madadlou, A. (2016). Maillard conjugation of lactulose with potentially bioactive peptides. *Food Chemistry*, *192*, 831-836. https://doi.org/10.1016/j.foodchem.2015.07.094

Pandey, K. K., & Pitman, A. J. (2003). FTIR studies of the changes in wood chemistry following decay by brown-rot and white-rot fungi. *International Biodeterioration & Biodegradation*, *52*(3), 151-160. https://doi.org/10.1016/s0964-8305(03)00052-0

Park, J. K., Ryu, J., Koo, B. C., Lee, S., & Kang, K. H. (2012). How the change of contact angle occurs for an evaporating droplet: effect of impurity and attached water films [10.1039/C2SM26559A]. *Soft Matter*, *8*(47), 11889-11896. https://doi.org/10.1039/c2sm26559a

Pelaez-Samaniego, M. R., Yadama, V., Lowell, E., & Espinoza-Herrera, R. (2013). A review of wood thermal pretreatments to improve wood composite properties [Review]. *Wood Science and Technology*, *47*(6), 1285-1319. https://doi.org/10.1007/s00226-013-0574-3

Peleg, Y., Barak, A., Scrutton, M. C., & Goldberg, I. (1989). Malic acid accumulation by Aspergillus flavus. *Applied Microbiology and Biotechnology*, *30*(2), 176-183. https://doi.org/10.1007/BF00264008

Pelletier, M. G., Holt, G. A., Wanjura, J. D., Bayer, E., & McIntyre, G. (2013). An evaluation study of mycelium based acoustic absorbers grown on agricultural by-product substrates. *Industrial Crops and Products*, *51*, 480-485. https://doi.org/https://doi.org/10.1016/j.indcrop.2013.09.008

Pelletier, M. G., Holt, G. A., Wanjura, J. D., Greetham, L., McIntyre, G., Bayer, E., & Kaplan-Bie, J. (2019). Acoustic evaluation of mycological biopolymer, an all-natural closed cell foam alternative. *Industrial Crops and Products*, *139*, 111533. https://doi.org/10.1016/j.indcrop.2019.111533

Pelletier, M. G., Holt, G. A., Wanjura, J. D., Lara, A. J., Tapia-Carillo, A., McIntyre, G., & Bayer, E. (2017). An evaluation study of pressure-compressed acoustic absorbers grown on agricultural by-products. *Industrial Crops and Products*, *95*, 342-347. https://doi.org/10.1016/j.indcrop.2016.10.042

Peng, Y., Gardner, D. J., & Han, Y. (2012). Drying cellulose nanofibrils: in search of a suitable method [journal article]. *Cellulose*, *19*(1), 91-102. https://doi.org/10.1007/s10570-011-9630-z

Pérez, E. M. S., Ávalos, M., Babiano, R., Cintas, P., Light, M. E., Jiménez, J. L., . . . Sancho, A. (2010). Schiff bases from d-glucosamine and aliphatic ketones. *Carbohydrate Research*, *345*(1), 23-32. https://doi.org/https://doi.org/10.1016/j.carres.2009.08.032

Perna, V., Agger, J. W., Andersen, M. L., Holck, J., & Meyer, A. S. (2019). Laccase Induced Lignin Radical Formation Kinetics Evaluated by Electron Paramagnetic Resonance Spectroscopy. *ACS Sustainable Chemistry & Engineering*, *7*(12), 10425-10434. https://doi.org/10.1021/acssuschemeng.9b00723

Pintiaux, T., Viet, D., Vandenbossche, V., Rigal, L., & Rouilly, A. (2015). Binderless materials obtained by thermo-compressive processing of lignocellulosic fibers: a comprehensive review. *BioResources*, *10*(1), 1915-1963.

Pizzi, A. (2006). Recent developments in eco-efficient bio-based adhesives for wood bonding: opportunities and issues. *Journal of Adhesion Science and Technology*, *20*(8), 829-846. https://doi.org/https://doi.org/10.1163/156856106777638635

Pramod, P. S., Shah, R., & Jayakannan, M. (2015). Dual stimuli polysaccharide nanovesicles for conjugated and physically loaded doxorubicin delivery in breast cancer cells [10.1039/C5NR00799B]. *Nanoscale*, *7*(15), 6636-6652. https://doi.org/10.1039/C5NR00799B

Rajak, R. C., & Banerjee, R. (2016). Enzyme mediated biomass pretreatment and hydrolysis: a biotechnological venture towards bioethanol production. *Rsc Advances*, *6*(66), 61301-61311. https://doi.org/https://doi.org/10.1039/C6RA09541K

Rana, R., Langenfeld-Heyser, R., Finkeldey, R., & Polle, A. (2009). FTIR spectroscopy, chemical and histochemical characterisation of wood and lignin of five tropical timber wood species of the family of Dipterocarpaceae. *Wood Science and Technology*, *44*(2), 225-242. https://doi.org/10.1007/s00226-009-0281-2

Rezaei, H., Lim, C. J., Lau, A., & Sokhansanj, S. (2016). Size, shape and flow characterization of ground wood chip and ground wood pellet particles. *Powder Technology*, *301*, 737-746. http://www.sciencedirect.com/science/article/pii/S0032591016304090

Rowell, R. M. (1992). *Opportunities for lignocellulosic materials and composites* (Vol. 476). American Chemical Society. https://doi.org/10.1021/bk-1992-0476

Saha, P., Chowdhury, S., Roy, D., Adhikari, B., Kim, J. K., & Thomas, S. (2015). A brief review on the chemical modifications of lignocellulosic fibers for durable engineering composites. *Polymer Bulletin*, *73*(2), 587-620. https://doi.org/10.1007/s00289-015-1489-y

Sammer, D., Krause, K., Gube, M., Wagner, K., & Kothe, E. (2016). Hydrophobins in the Life Cycle of the Ectomycorrhizal Basidiomycete Tricholoma vaccinum. *PloS one*, *11*(12), e0167773, Article e0167773. https://doi.org/10.1371/journal.pone.0167773

Sauerwein, M., Karana, E., & Rognoli, V. (2017). Revived Beauty: Research into Aesthetic Appreciation of Materials to Valorise Materials from Waste. *Sustainability*, *9*(4), 529.

Schimpf, U., & Schulz, R. (2016). Industrial by-products from white-rot fungi production. Part I: Generation of enzyme preparations and chemical, protein biochemical and molecular biological characterization. *Process Biochemistry*, *51*(12), 2034-2046. https://doi.org/10.1016/j.procbio.2016.08.032

Schneider, C. A., Rasband, W. S., & Eliceiri, K. W. (2012). NIH Image to ImageJ: 25 years of image analysis. *Nat Methods*, *9*(7), 671-675. https://doi.org/10.1038/nmeth.2089

Scholtmeijer, K., de Vocht, M. L., Rink, R., Robillard, G. T., & Wosten, H. A. (2009). Assembly of the fungal SC3 hydrophobin into functional amyloid fibrils depends on its concentration and is promoted by cell wall polysaccharides. *Journal of Biological Chemistry*, *284*(39), 26309-26314. https://doi.org/10.1074/jbc.M109.005553

Shakir, M. A., Azahari, B., Yusup, Y., Firdaus Yhaya, M., Salehabadi, A., & Ahmad, M. I. (2020). Preparation and Characterization of Mycelium as a Bio-Matrix in Fabrication of Bio-Composite. *J. Adv. Res. Fluid Mech. Therm. Sci. J.*, *65*, 253-263.

Shi, Y., Zhu, K., Dai, Y., Zhang, C., & Jia, H. (2020). Evolution and stabilization of environmental persistent free radicals during the decomposition of lignin by laccase. *Chemosphere*, *248*, 125931. https://doi.org/10.1016/j.chemosphere.2020.125931

Shirkavand, E., Baroutian, S., Gapes, D. J., & Young, B. R. (2016). Combination of fungal and physicochemical processes for lignocellulosic biomass pretreatment–A review. *Renewable and Sustainable Energy Reviews*, *54*, 217-234. https://doi.org/https://doi.org/10.1016/j.rser.2015.10.003

Shmulsky, R., & Jones, P. D. (2011). *Forest products and wood science*. John Wiley & Sons.

Sinn, G., Reiterer, A., & Stanzl-Tschegg, S. E. (2001). Surface analysis of different wood species using X-ray photoelectron spectroscopy (XPS). *Journal of Materials Science*, *36*(19), 4673-4680. https://doi.org/10.1023/a:1017954300015

Sisti, L., Kalia, S., Totaro, G., Vannini, M., Negroni, A., Zanaroli, G., & Celli, A. (2018). Enzymatically treated curaua fibers in poly(butylene succinate)-based biocomposites. *Journal of Environmental Chemical Engineering*, *6*(4), 4452-4458. https://doi.org/10.1016/j.jece.2018.06.066

Slagman, S., Zuilhof, H., & Franssen, M. C. R. (2018). Laccase-Mediated Grafting on Biopolymers and Synthetic Polymers: A Critical Review. *Chembiochem*, *19*(4), 288-311. https://doi.org/10.1002/cbic.201700518

Song, W., Zhang, K., Chen, Z., Hong, G., Lin, J., Hao, C., & Zhang, S. (2018). Effect of Xylanase–Laccase Synergistic Pretreatment on Physical–Mechanical Properties of Environment-Friendly Self-bonded Bamboo Particleboards [journal article]. *Journal of Polymers and the Environment*, *26*(10), 4019-4033. https://doi.org/10.1007/s10924-018-1275-7

Steudler, S., & Bley, T. (2015). Better One-Eyed than Blind—Challenges and Opportunities of Biomass Measurement During Solid-State Fermentation of Basidiomycetes. In R. Krull & T. Bley (Eds.), *Filaments in Bioprocesses* (pp. 223-252). Springer International Publishing. https://doi.org/10.1007/10_2014_300

Stratakis, E., Mateescu, A., Barberoglou, M., Vamvakaki, M., Fotakis, C., & Anastasiadis, S. H. (2010). From superhydrophobicity and water repellency to superhydrophilicity: smart polymer-functionalized surfaces [10.1039/C003294H]. *Chem Commun (Camb)*, *46*(23), 4136-4138. https://doi.org/10.1039/c003294h

Suchsland, O., & Woodson, G. E. (1987). *Fiberboard manufacturing practices in the United States*. US Dept. of Agriculture, Forest Service.

Sugai-Guérios, M. H., Balmant, W., Furigo, A., Krieger, N., & Mitchell, D. A. (2015). Modeling the Growth of Filamentous Fungi at the Particle Scale in Solid-State Fermentation Systems. In R. Krull & T. Bley (Eds.), *Filaments in Bioprocesses* (pp. 171-221). Springer International Publishing. https://doi.org/10.1007/10_2014_299

Sun, W., Tajvidi, M., Howell, C., & Hunt, C. G. (2020). Functionality of Surface Mycelium Interfaces in Wood Bonding. *ACS Appl Mater Interfaces*, *12*(51), 57431-57440. https://doi.org/10.1021/acsami.0c18165

Sun, W., Tajvidi, M., Hunt, C. G., McIntyre, G., & Gardner, D. J. (2019). Fully bio-based hybrid composites made of wood, fungal mycelium and cellulose nanofibrils. *Scientific Reports*, *9*(1), 1-12. https://doi.org/https://doi.org/10.1038/s41598-019-40442-8

Tajvidi, M., Gardner, D. J., & Bousfield, D. W. (2016). Cellulose Nanomaterials as Binders: Laminate and Particulate Systems. *Journal of Renewable Materials*, *4*(5), 365-376. https://doi.org/10.7569/JRM.2016.634103

Tănase, C., Odochian, L., Balaeş, T., Lisă, G., Gherca, D., & Pui, A. (2014). Study of thermal behaviour of some edible mushrooms [journal article]. *Journal of Thermal Analysis and Calorimetry*, *115*(1), 947-953. http://dx.doi.org/10.1007/s10973-013-3335-5

Theng, D., Arbat, G., Delgado-Aguilar, M., Vilaseca, F., Ngo, B., & Mutjé, P. (2015). All-lignocellulosic fiberboard from corn biomass and cellulose nanofibers. *Industrial Crops and Products*, *76*, 166-173. http://www.sciencedirect.com/science/article/pii/S0926669015302119

Tian, X.-f., Fang, Z., & Guo, F. (2012). Impact and prospective of fungal pre-treatment of lignocellulosic biomass for enzymatic hydrolysis. *Biofuels, Bioproducts and Biorefining*, *6*(3), 335-350. https://doi.org/10.1002/bbb.346

Tudryn, G. J. (2014). A Formaldehyde-Free, Sustainable Alternative. *RADTECH REPORT*(2), 40-45.

Tuller, M., Or, D., & Dudley, L. M. (1999). Adsorption and capillary condensation in porous media: Liquid retention and interfacial configurations in angular pores. *Water Resources Research*, *35*(7), 1949-1964. https://doi.org/10.1029/1999wr900098

Tye, Y. Y., Lee, K. T., Wan Abdullah, W. N., & Leh, C. P. (2016). The world availability of non-wood lignocellulosic biomass for the production of cellulosic ethanol and potential pretreatments for the enhancement of enzymatic saccharification. *Renewable and Sustainable Energy Reviews*, *60*, 155-172. https://doi.org/10.1016/j.rser.2016.01.072

Unbehaun, H., Dittler, B., Kühne, G., & Wagenführ, A. (2000). Investigation into the biotechnological modification of wood and its application in the wood-based material industry. *Acta Biotechnologica*, *20*(3-4), 305-312. https://doi.org/10.1002/abio.370200311

Vachoud, L., Chen, T., Payne, G. F., & Vazquez-Duhalt, R. (2001). Peroxidase catalyzed grafting of gallate esters onto the polysaccharide chitosan. *Enzyme and Microbial Technology*, *29*(6), 380-385. https://doi.org/https://doi.org/10.1016/S0141-0229(01)00404-5

van Kuijk, S. J. A., Sonnenberg, A. S. M., Baars, J. J. P., Hendriks, W. H., & Cone, J. W. (2015). Fungal treated lignocellulosic biomass as ruminant feed ingredient: a review. *Biotechnology Advances*, *33*(1), 191-202. https://doi.org/10.1016/j.biotechadv.2014.10.014

Wan, C., & Li, Y. (2012). Fungal pretreatment of lignocellulosic biomass. *Biotechnology Advances*, *30*(6), 1447-1457. https://doi.org/10.1016/j.biotechadv.2012.03.003

Wang, W., Zhu, Y., Cao, J., & Sun, W. (2015). Correlation between dynamic wetting behavior and chemical components of thermally modified wood. *Applied Surface Science*, *324*, 332-338. https://doi.org/10.1016/j.apsusc.2014.10.139

Watanabe, T., Ohashi, Y., Tanabe, T., Honda, Y., & Messner, K. (2007). Lignin Biodegradation by Selective White Rot Fungus and Its Potential Use in Wood Biomass Conversion. In D. S. Argyropoulos (Ed.), *Materials, Chemicals, and Energy from Forest Biomass* (Vol. 954, pp. 409-421). https://doi.org/10.1021/bk-2007-0954.fw001

Wesenberg, D., Kyriakides, I., & Agathos, S. N. (2003). White-rot fungi and their enzymes for the treatment of industrial dye effluents. *Biotechnology Advances*, *22*(1-2), 161-187. https://doi.org/10.1016/j.biotechadv.2003.08.011

Wessels, J., De Vries, O., Asgeirsdottir, S. A., & Schuren, F. (1991). Hydrophobin Genes Involved in Formation of Aerial Hyphae and Fruit Bodies in Schizophyllum. *Plant Cell*, *3*(8), 793-799. https://doi.org/10.1105/tpc.3.8.793

Widsten, P. (2002). *Oxidative activation of wood fibers for the manufacture of MDF* Helsinki Univeristy of Technology]. Espoo, Finland.

Widsten, P., & Kandelbauer, A. (2008). Adhesion improvement of lignocellulosic products by enzymatic pre-treatment. *Biotechnology Advances*, *26*(4), 379-386. https://doi.org/10.1016/j.biotechadv.2008.04.003

Widsten, P., Laine, J. E., Tuominen, S., & Qvintus-Leino, P. (2003). Effect of high defibration temperature on the properties of medium-density fiberboard (MDF) made from laccase-treated hardwood fibers. *Journal of Adhesion Science and Technology*, *17*(1), 67-78. https://doi.org/10.1163/15685610360472448

Widsten, P., Tuominen, S., Qvintus-Leino, P., & Laine, J. E. (2004). The influence of high defibration temperature on the properties of medium-density fiberboard (MDF) made from laccase-treated softwood fibers. *Wood Science and Technology*, *38*(7), 521-528. https://doi.org/10.1007/s00226-003-0206-4

Wilcox, W. W. (1978). Review of literature on the effects of early stages of decay on wood strength. *Wood Fiber Science*, *9*(4), 252-257.

Wu, J., Chen, C., Zhang, H., Xia, L., Huang, Y., Huang, H., . . . Zhang, T. (2020). Eco-friendly fiberboard production without binder using poplar wood shavings bio-pretreated by white rot fungi Coriolus versicolor. *Construction and Building Materials*, *236*, 117620. https://doi.org/10.1016/j.conbuildmat.2019.117620

Wu, J., Zhang, X., Liu, J., Xiong, M., Lu, X., Fan, H., . . . Zhang, X. (2016). Medium density fibreboard production by hot pressing without adhesive using Triarrhena saccharifloraresidue bio-pretreated by white-rot fungus Coriolus versicolor. *Journal of Applied Microbiology*, *121*(2), 415-421. https://doi.org/ https://doi.org/10.1111/jam.13148

Wu, J., Zhang, X., Wan, J., Ma, F., Tang, Y., & Zhang, X. (2011). Production of fiberboard using corn stalk pretreated with white-rot fungus Trametes hirsute by hot pressing without adhesive [Article]. *Bioresource Technology*, *102*(24), 11258-11261. https://doi.org/10.1016/j.biortech.2011.09.097

Xia, F., Zhu, Y., Feng, L., & Jiang, L. (2009). Smart responsive surfaces switching reversibly between super-hydrophobicity and super-hydrophilicity [10.1039/B803951H]. *Soft Matter*, *5*(2), 275-281. https://doi.org/10.1039/b803951h

Xiao, X., Hou, Y., Du, J., Liu, Y., Liu, Y., Dong, L., . . . Luo, G. (2012). Determination of main categories of components in corn steep liquor by near-infrared spectroscopy and partial least-squares regression. *Journal of Agricultural and Food Chemistry*, *60*(32), 7830-7835. https://doi.org/10.1021/jf3012823

Xie, C., Gong, W., Yang, Q., Zhu, Z., Yan, L., Hu, Z., & Peng, Y. (2017). White-rot fungi pretreatment combined with alkaline/oxidative pretreatment to improve enzymatic saccharification of industrial hemp. *Bioresource Technology*, *243*, 188-195. https://doi.org/10.1016/j.biortech.2017.06.077

Xu, G., Wang, L., Liu, J., & Wu, J. (2013). FTIR and XPS analysis of the changes in bamboo chemical structure decayed by white-rot and brown-rot fungi. *Applied Surface Science*, *280*, 799-805. https://doi.org/10.1016/j.apsusc.2013.05.065

Yang, T., Hu, L., Xiong, X., Petrů, M., Noman, M. T., Mishra, R., & Militký, J. (2020). Sound Absorption Properties of Natural Fibers: A Review. *Sustainability*, *12*(20), 8477. https://doi.org/https://doi.org/10.3390/su12208477

Yang, Z., Song, W., Cao, Y., Wang, C., Hu, X., Yang, Y., & Zhang, S. (2017). The Effect of Laccase Pretreatment Conditions on the Mechanical Properties of Binderless Fiberboards with Wheat Straw. *BioResources*, *12*(2), 3707-3719. https://doi.org/10.15376/biores.12.2.3707-3719

Zabel, R. A., & Morrell, J. J. (2012). *Wood microbiology: decay and its prevention*. Academic press.

Zabel, R. A., & Morrell, J. J. (2020a). Changes in the strength and physical properties of wood caused by decay fungi. In R. A. Zabel & J. J. Morrell (Eds.), *Wood Microbiology* (pp. 271-291). Academic Press. https://doi.org/10.1016/b978-0-12-819465-2.00010-3

Zabel, R. A., & Morrell, J. J. (2020b). Fungal metabolism in relation to wood decay. In R. A. Zabel & J. J. Morrell (Eds.), *Wood Microbiology* (pp. 129-148). Academic Press. https://doi.org/10.1016/b978-0-12-819465-2.00005-x

Zha, F., Yang, Z., Rao, J., & Chen, B. (2019). Gum Arabic-Mediated Synthesis of Glyco-pea Protein Hydrolysate via Maillard Reaction Improves Solubility, Flavor Profile, and Functionality of Plant Protein. *Journal of Agricultural and Food Chemistry*, *67*(36), 10195-10206. https://doi.org/10.1021/acs.jafc.9b04099

Zhai, M., Guo, L., Zhang, Y., Dong, P., Qi, G., & Huang, Y. (2016). Kinetic Parameters of Biomass Pyrolysis by TGA. *BioResources*, *11*(4), 8548-8557. https://ojs.cnr.ncsu.edu/index.php/BioRes/article/view/10061

Zhang, D., Zhang, A., & Xue, L. (2015). A review of preparation of binderless fiberboards and its self-bonding mechanism [journal article]. *Wood Science and Technology*, *49*(4), 661-679. https://doi.org/10.1007/s00226-015-0728-6

Zhang, M., Qi, W., Liu, R., Su, R., Wu, S., & He, Z. (2010). Fractionating lignocellulose by formic acid: Characterization of major components. *Biomass and Bioenergy*, *34*(4), 525-532. https://doi.org/10.1016/j.biombioe.2009.12.018

Zhang, X., Yu, H., Huang, H., & Liu, Y. (2007). Evaluation of biological pretreatment with white rot fungi for the enzymatic hydrolysis of bamboo culms. *International Biodeterioration & Biodegradation*, *60*(3), 159-164. https://doi.org/10.1016/j.ibiod.2007.02.003

Zhao, Z., Huang, C., Wu, D., Chen, Z., Zhu, N., Gui, C., . . . Yong, Q. (2020). Utilization of enzymatic hydrolysate from corn stover as a precursor to synthesize an eco-friendly plywood adhesive. *Industrial Crops and Products*, *152*, 112501. https://doi.org/https://doi.org/10.1016/j.indcrop.2020.112501

Zheng, Y., Bai, H., Huang, Z., Tian, X., Nie, F. Q., Zhao, Y., . . . Jiang, L. (2010). Directional water collection on wetted spider silk. *Nature*, *463*(7281), 640-643. https://doi.org/10.1038/nature08729

Zheng, Y., Gao, X., & Jiang, L. (2007). Directional adhesion of superhydrophobic butterfly wings [10.1039/B612667G]. *Soft Matter*, *3*(2), 178-182. https://doi.org/10.1039/b612667g

Zhu, X., Han, S., Liu, Y., & Chen, G. (2017). Effects of laccase incubated from white rot fungi on the mechanical properties of fiberboard [journal article]. *Journal of Forestry Research*, *28*(6), 1293-1300. https://doi.org/10.1007/s11676-017-0398-3

BIOGRAPHY OF THE AUTHOR

Wenjing Sun was born and raised in Yizheng, Jiangsu, China. She attended Beijing Forestry University and graduated in 2013 with a Bachelor's degree in Wood Science and Engineering and a Master's degree in Wood Science and Technology in 2016. She came to Maine and started PhD in Forest Resources graduate program at the University of Maine in the spring of 2017. Wenjing is a candidate for the Doctor of Philosophy degree in Forest Resources: Bioproducts Engineering from the University of Maine in August 2021.